# Study of cellular mechanisms of inflammation and the involvement of mast cells in disease

A DISSERTATION
SUBMITTED TO THE FACULTY OF
UNIVERSITY OF MINNESOTA
BY

Benjamin Michael Manning

IN PARTIAL FULFILLMENT OF THE REQUIREMENTS
FOR THE DEGREE OF
DOCTOR OF PHILOSOPHY

Christy L Haynes, Advisor

July, 2013

**Acknowledgements**

There are many people who have contributed to this work and are owed my sincere gratitude. First and foremost, I'm very thankful for the support of my advisor, Prof. Christy Haynes, and for her dedicated mentorship throughout my graduate career. I'm lucky to have had the opportunity to work under her guidance. I look forward to watching the Haynes group continue to evolve and produce exciting new research under her leadership.

I'm also incredibly grateful for the other members of the Haynes research group, past and present, for their support over the past five years. The opportunity to work in an environment full of wonderful, fun, and encouraging colleagues has been invaluable. Former members Nate Wittenberg, Bryce Marquis, Shencheng Ge, Kyle Bantz, Sara Love, Yu-Shen Lin, Melissa Maurer-Jones, and Secil Koseoglu were all exceedingly helpful and an invaluable resource in the early years of my graduate career. Bryce, Shencheng, Melissa, Sara, and Secil, along with Audrey Meyer, all contributed to preliminary experiments that lead to the research summarized in Chapter 2 of this dissertation. All the current members of the Haynes group have continued to create a positive and productive work environment. Audrey Meyer, Donghyuk Kim and Sarah Gruba have been especially helpful in the generation of research ideas, as collaborators the lab, and in the interpretation of data.

I have been fortunate in my graduate work to benefit from a fruitful collaboration with Prof. Kalpna Gupta of the Department of Medicine here at the University of Minnesota. Working with the Gupta group generated very interesting research, some of which is summarized in Chapters 2 and 3 of this dissertation. Prof. Gupta has also been very supportive of my progress through graduate school as a mentor. I am grateful for her willingness to talk through research ideas and put up with my occasional pursuit of tangential research interests. Several members of the Gupta research group, including Julia Nguyen, Derek Vang, and Dr. Lucille Vincent, contributed to this work through assistance with cell isolation procedures as part of the aforementioned collaborations.

It is difficult to overstate my appreciation for my family and friends and their continuous support, without which it's hard to imagine completing this work. My parents, siblings, extended family, and friends have all provided a network of support that has allowed me to maintain focus and perspective, and find rejuvenation when I've needed it most.

Finally, I'm forever grateful for my wife, Allison; for her endless patience and unwavering encouragement, for keeping me grounded, and for being my best friend throughout.

## Dedication

For my Dad – who has always enthusiastically shared his own curiosity and appreciation for the natural world

**Abstract**

The principal motivation of this dissertation is to expand the utility of single-cell microelectrochemical methods, specifically carbon-fiber microelectrode amperometry (CFMA), beyond the study of fundamental cellular biophysics and toward applications investigating the cellular signaling networks in inflammation. From an analytical perspective, the inflammatory response presents several technical challenges. The inherent complexity of the immune system makes unraveling the pathogenesis of inflammatory disease a particularly challenging endeavor. An ability to detect and monitor immune cell signaling, at low, physiologically relevant concentrations and in the presence of a complex biological matrix is critical. Furthermore, although the use of bulk in vitro assays are essential for any research in biological systems, the capacity to study important cellular signaling processes at the single cell-level carries several added advantages. For these reasons, CFMA has substantial potential as a unique tool for the study of immune cell signaling. Mast cells, in particular, are an ideal model for this research because 1) they're found in most connective tissues and mucosal surfaces throughout the body, 2) they posses a broad capacity to regulate the immune response and are thought to take part in the progression of many inflammatory diseases, and 3) they release electroactive serotonin, along many other preformed immune-active mediators, via exocytosis which can be monitored by CFMA. The first part of this dissertation consists of several examples wherein CFMA is used to study mast cell degranulation in response to an altered in vivo inflammatory microenvironment, such as

the chronic inflammation associated with sickle hemoglobin expression (Chapter 2), chronic in vivo morphine exposure (Chapter 2), and the effects of the endogenous opioid receptor system (Chapter 3). These chapters are followed by research that highlights the advantages of CFMA for the direct comparison of different mast cell stimulation conditions, including a study of chemokine-induced mast cell degranulation to explore the critical interactions between mast cells and airway smooth muscle in asthma (Chapter 4) as well as neuropeptide-induced mast cell degranulation to characterize mast cell function in neurogenic inflammation (Chapter 5). Collectively, this work presents CFMA as a promising technique for the study of cellular signaling in inflammatory disease.

## Table of Contents

## List of Tables

### Chapter 1



### Chapter 6

## List of Figures

### Chapter 1



### Chapter 2

**Chapter 3**



**Chapter 4**



**Chapter 5**

## List of Abbreviations

| | |
|---|---|
| ˚C | Degrees Celsius |
| AAALAC | Association for Assessment and Accreditation of Laboratory Animal Care |
| Ag/AgCl | Silver-silver chloride |
| Anti-TNP | Anti-trinitrophenol |
| ASM | Airways smooth muscle |
| BCS | Bovine calf serum |
| BERK | Transgenic mouse homozygous for human sickle hemoglobin |
| C1q | Complement component 1q |
| C3a | Complement component 3a |
| C5a | Complement component 5a |
| CCR1 | C-C motif chemokine receptor 1 |
| CCR3 | C-C motif chemokine receptor 3 |
| CFMA | Carbon-fiber microelectrode amperometry |
| CRAC | Calcium release-activated calcium |
| CXCL10 | C-X-C motif cytokine receptor ligand 10 |
| CXCR3 | C-X-C motif cytokine receptor 3 |
| DMEM | Dulbecco's modified eagle medium |
| DORKO | Delta opioid receptor knockout |
| FcγRI | Immunoglobulin-gamma receptor I |
| FcγRII | Immunoglobulin-gamma receptor II |
| FcγRIII | Immunoglobulin-gamma receptor III |
| FcεRI | Immunoglobulin-epsilon receptor I |
| FSCV | Fast-scan cyclic voltammetry |
| Hb | Hemoglobin |
| HbA-BERK | Transgenic mouse homozygous for human normal hemoglobin |
| hBERK1 | Transgenic mouse hemizygous for human sickle hemoglobin |
| HPLC | High performance liquid chromatography |
| Hz | Hertz |
| IACUC | Institutional Animal Care and Use Committee |
| Ig | Immunoglobulin |
| IgE | Immunoglobulin class E |
| IgG | Immunoglobulin class G |
| KCl | Potassium chloride |
| KORKO | Kappa opioid receptor knockout |
| MC | Mast cell |
| MHC | Major histocompatibility complex |
| mL | Milliliter |
| mM | Millimolar |

| | |
|---|---|
| MORKO | Mu opioid receptor knockout |
| MS | Morphine sulfate |
| mV | Millivolt |
| nA | Nanoampere |
| NGF | Nerve growth factor |
| NK | Neurokinin |
| pA | Picoampere |
| PBS | Phosphate buffered saline |
| PLC-γ | Phospholipase C-gamma |
| Q | Peak area/charge |
| $Q_{foot}$ | Pre-spike foot area/charge |
| RANTES | Regulated on activation, normal T-cell expressed and secreted |
| SCD | Sickle cell disease |
| SNAP | Synaptosome-associated protein |
| SNARE | Soluble N-ethyl-maleimide-sensitive factor-attachment protein receptor |
| $t_{1/2}$ | Peak half-width |
| $T_C$ | Cytotoxic T-cell |
| TCR | T-cell receptor |
| $t_{foot}$ | Duration of pre-spike foot |
| $T_H$ | Helper T-cell |
| $T_H1$ | Helper T-cell type 1 |
| $T_H2$ | Helper T-cell type 2 |
| TKO | Triple knockout |
| TLR | Toll-like receptor |
| TNF-α | Tumor necrosis factor-alpha |
| TNP-OVA | Trinitrophenol-modified ovalbumin |
| $T_{reg}$ | T-regulatory cell |
| Tris | Tris(hyroxymethyl)aminomethane |
| $t_{rise}$ | Peak rise-time |
| VAMP | Vesicle-associated membrane protein |
| VEGF | Vascular endothelial growth factor |
| WT | Wild type |
| βA | Normal hemoglobin subunit β |
| βS | Sickle hemoglobin subunit β |
| µL | Microliter |
| µm | Micrometer |

# Chapter 1

## Introduction to single cell monitoring of mast cell degranulation using carbon-fiber microelectrode amperometry and its applications for the study of inflammation

In part from:

Kim, D., Koseoglu, S., Manning, B. M., Meyer, A. F., and Haynes, C. L. *Anal. Chem.* 2011, 83, 7242-7249

## 1.1 Introduction

Unraveling the highly interconnected nature of complex biological systems is fundamental to a wide range of modern research questions. At the heart of any coordinated biological network is cell-cell communication, and researching the means by which different cell types communicate is an essential prerequisite to fully understanding many aspects of biology. One major mechanism of cell signaling is the regulated release of chemical messengers from preformed vesicles in the cytoplasm. The process of transporting these vesicles to the exterior of the cell and the subsequent release of vesicular contents via membrane fusion is known as exocytosis. In recent decades, carbon-fiber microelectrodes have become increasingly useful for the measurement and study of exocytosis in a variety of biological contexts.

### 1.1.1 Electrochemical approaches to studying cellular signaling

The use of carbon as an electrode material was first popularized by Ralph Adams in the 1950s.[1] Since its inception, carbon has been a popular choice for electrochemical applications, as carbon electrodes demonstrate a wide working potential window, stable background currents, low noise, and high sensitivity. The development of carbon electrodes with active surfaces on the scale of several microns introduces additional advantages. For voltammetry experiments, microelectrodes offer the ability to observe diffusion-limited currents at high scan rates and thus provide very fast time resolution.[2] The small surface area of microelectrodes enables the use of high scan rates with

relatively low background currents. Because of the small number of molecules that must be detected at the single cell level, however, most electrochemical measurements made with carbon microelectrodes produce currents in the nanoampere or picoampere range, depending on the method used.[2] These current levels require electrodes that are both sensitive and exhibit low levels of noise, and carbon microelectrodes meet both of these criteria. Conveniently, using microelectrodes requires only a two-electrode system, as such low currents render the use of an auxiliary electrode unnecessary. Perhaps most importantly, microelectrodes provide much greater spatial resolution, and thus permit electrochemical measurements to be made from single cells.[3] Although other forms of carbon can also be used, carbon-fiber microelectrodes are often favored because they can be fabricated in large quantities and are relatively inexpensive.

R. Mark Wightman and coworkers first demonstrated the utility of carbon-fiber microelectrodes for the detection of exocytosis from single cells in 1990.[4] Carbon-fiber microelectrodes of different geometries are used depending on the intended application; for single-cell electrochemical techniques, beveled and polished disc microelectrodes are most widely used. While Wightman's initial demonstration explored exocytosis from chromaffin cells, the cells responsible for the release of adrenaline, exocytosis is highly conserved across several cell types including neurons, chromaffin cells, platelets, and a variety of immune cells such as mast cells and macrophages. Accordingly, microelectrochemistry techniques are uniquely suited to reveal critical mechanistic

details about exocytosis in these cell types, providing new insight into the fundamental behavior of normal and dysfunctional secretory cells.

### 1.1.2 Exocytosis

In order to study the physiological impact of mast cell signaling, it is critical to have a working knowledge of exocytosis at a fundamental level. Single-cell electrochemistry methods have proven very effective for the study of this cellular process. The basic function of exocytosis is comprised of several distinct sub-mechanisms that operate in an organized manner to facilitate the secretion of vesicular contents from the cell (Figure 1.1). A detailed description of the fundamentals of exocytosis that can be monitored using electrochemical techniques appears later is this chapter.

In the presence of an appropriate stimulus, intracellular signaling first initiates the rearrangement of preformed vesicles within the cell. The result of this process is the transport and trafficking of vesicles from cytoplasmic sites to the cell membrane in preparation for fusion. Once a vesicle has been transported to a position immediately proximal to the plasma membrane, specialized proteins embedded in both the vesicle and cell membranes interact through a docking mechanism, securing the vesicle for fusion. Fusion is the last sub-mechanism of exocytosis, and is considered distinct from vesicle docking both because of its dependence on separate molecular machinery as well as its sensitivity to cytosolic calcium. The initial stimulus and subsequent intracellular

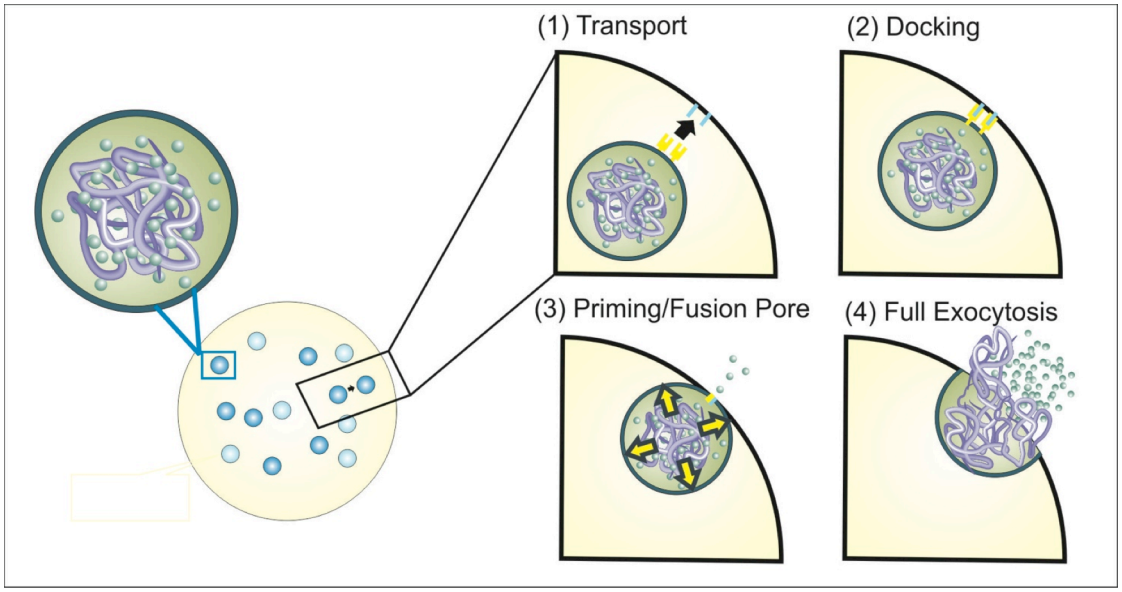


**Figure 1.1 Steps of exocytosis**
Exocytosis of preformed cytosolic secretory vesicles requires several distinct submechanisms. Individual vesicles contain many preformed, biologically active mediators and are supported by a biopolymer matrix (top left). Following an external stimulus, vesicles are 1) transported from cytoplasmic sites to the cell membrane, where they 2) dock with specialized protein machinery. An increase in cytosolic calcium concentration triggers 3) the formation of a fusion pore which is usually followed rapidly by 4) the full exocytosis event where a large portion of the vesicular cargo is released to the extracellular space.

signaling cascade results in an increase in cytosolic calcium ion concentration, causing the fusion of the two membranes, creating a small opening between the interior of the vesicle and the exterior of the cell called the fusion pore.[5,6] Once the fusion pore is formed, small amounts of the vesicular contents are able to leak to the exterior of the cell. In general, this phase of exocytosis is followed rapidly by fusion pore expansion, resulting in the release of a large portion of the vesicle's contents. Sub-millisecond resolution microelectrochemical methods are uniquely suited to distinguish between the separate contributions of individual sub-mechanisms of cellular exocytosis.

## 1.2 Single-cell electrochemistry

Electrochemical methods using carbon-fiber microelectrodes are the gold standard for studying single cell exocytosis. Carbon-fiber microelectrode amperometry (CFMA) and fast-scan cyclic voltammetry (FSCV) are the most widely used, as these methods allow the direct measurement of secreted molecules without damaging cells or interfering with endocytosis, which is a common issue in capacitance-based measurement methods such as patch-clamp techniques.[7] Although, the focus of this dissertation is centered on the use of CFMA for the study of mast cell degranulation, FSCV is a very useful technique in many applications, particularly the identification of secreted species because of the ability to identify standard oxidation/reduction potentials. Because FSCV is complementary to CFMA and has played an important role in the characterization of single cell exocytosis, a brief description of this technique is included here.

In FSCV, individual voltammograms are obtained by repeated application of triangular waveform scans through a range of potentials at regular intervals.[2,8-15] Any electroactive species that can be oxidized/reduced in the potential window are therefore monitored simultaneously. For each scan, the amplitude of the current signal depends on the number of analyte molecules diffusing to the electrode surface.[2] As the scan rate is hundreds of volts per second, a large background current occurs during the measurement.[11,15] This background current is relatively stable for carbon-fiber microelectrodes and can be subtracted from later scans.[11] In single cell exocytosis studies, voltammograms obtained

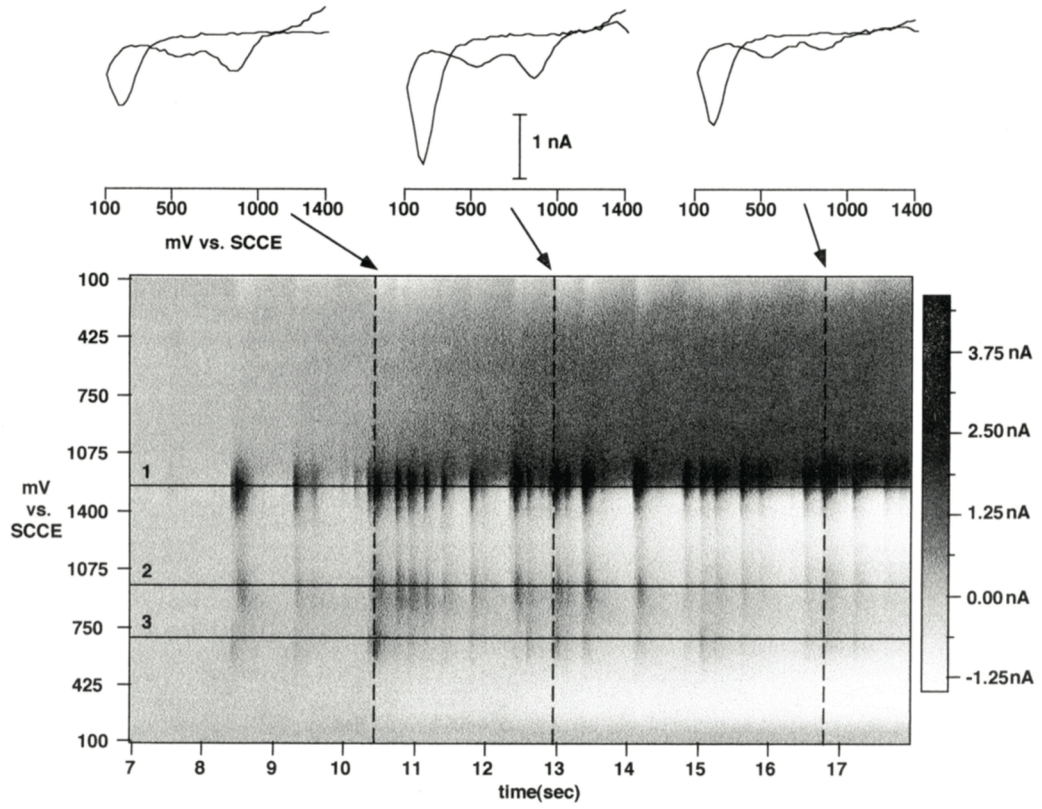


**Figure 1.2 FSCV used to demonstrate the co-localized release of histamine and serotonin from rat peritoneal mast cells**
Stacked FSCV voltammograms (three representative examples shown at top) presented as a gradient plot, demonstrate the oxidation of histamine at roughly +1250 mV (horizontal lines 1 and 2) and serotonin at about +650 mV (horizontal line 3) versus a saturated calomel reference electrode. Reprinted with permission from Pihel, K et al. (1995) Anal. Chem. 67(24), 4514-4521. Copyright 1995 American Chemical Society.

before stimulation of the cell are subtracted from voltammograms containing information related to the local chemical change after stimulation.[2] This method provides chemical identification of oxidized/reduced species and also can be used to monitor multiple

electroactive species simultaneously based on their oxidation potential.[12,14] Accordingly, FSCV is most commonly used to identify molecules secreted from a cell. Figure 1.2 shows the use of FSCV by Pihel and coworkers to demonstrate the co-localization of histamine and serotonin in mast cell granules. However, the temporal resolution of single cell FSCV measurements is generally no greater than the 100 millisecond level,[15,16] limiting insight into the real-time kinetics of exocytosis; as a result, having identified the molecules of interest, CFMA is commonly employed as a complimentary technique for in-depth exocytosis kinetics studies, and is the focus of the research in this dissertation.

### 1.2.1 Carbon-fiber microelectrode amperometry

In CFMA experiments, in contrast to FSCV, a constant potential sufficient to oxidize or reduce the chemical messenger of interest is supplied at the tip of the carbon-fiber microelectrode.[3,7,17,18] Current at the electrode tip is then monitored as a function of time (Figure 1.3c). Oxidative current from the analyte at a positive potential is monitored while detection of reductive current at a negative potential can be troublesome due to the interference from oxygen. Upon stimulation of a single cell, exocytotic behavior of the cell is revealed as current spikes (peaks) that represent vesicles of chemical messenger molecules stored in a quantal fashion, meaning that the concentration in each vesicle is approximately the same.[13,19,20] Each peak in current represents one vesicle; however, it is also possible, though statistically improbable, to simultaneously detect multiple vesicles. As electron transfer is faster than diffusion of chemical messengers to the electrode surface, redox reactions occurring at the electrode are limited by diffusion of chemical

messengers.[3,19] This allows the CFMA method to achieve sub-millisecond temporal resolution and enables real-time monitoring of exocytotic events. In an amperometric trace, each spike has a fast rising and slower decaying phase due to the convolution effects of diffusion and dissociation of chemical messenger molecules, commonly from a dynamic intragranular biopolymeric matrix scaffold.[17] Analysis of various peak characteristics reveals several aspects of exocytosis such as vesicle release kinetics and membrane properties.[3,17] A more detailed discussion of CFMA instrumentation and the information gained from CFMA data appears sections 1.2.3 and 1.2.4 of this chapter.

### 1.2.2 Challenges of CFMA

With regard to sensitivity and selectivity, the chemical messengers that are most commonly analyzed using CFMA have an adsorption affinity for the carbon surface. As more adsorption of analyte onto the electrode surface occurs, measured current increases at the cost of temporal resolution.[8,10,21] Surface coatings of the carbon electrode have been used to increase selectivity and sensitivity of the measurement for specific chemical messengers but these methods add another layer for analyte to diffuse through, sacrificing temporal resolution. Selectivity of CFMA is defined by the electrochemistry of secreted molecular species. Although only a limited number of biological molecules are electroactive at sufficiently low potentials to be observed, the small number of observable species minimizes the complexity of the biological matrix. The dimensions of the microelectrode can also significantly affect the measurement. During CFMA experiments, the use of small diameter microelectrodes significantly reduces the number

of superimposed spikes in a trace but it also reduces the total number of events detected.[22] In summary, there are the expected trade-offs between sensitivity, selectivity, and resolution, but adjusting the parameters mentioned above facilitates optimal outcomes.

### 1.2.3 Experimental procedures and setup

The experimental setup for single-cell CFMA measurements is conceptually simple. Carbon-fiber microelectrodes (Figure 1.3a) are typically fabricated in-house, and fabrication methods can vary slightly by laboratory. Generally, a single carbon fiber with roughly 5-10 μm diameter is aspirated into a glass capillary, which is then pulled using a capillary puller that applies thermal and magnetic fields. Using a microscope, the extruded carbon-fiber is cut to within 50 μm of the insulating glass layer. The carbon-fiber is next sealed in the capillary using epoxy resin for insulation and cured at high temperatures (100-1500 ˚C). Prior to electrochemistry experiments, cured electrodes are polished at 45° using a micropipette polisher and stored tip-down in isopropyl alcohol to remove any surface contaminants.

The instrumental setup for CFMA (Figure 1.3b) includes a working electrode (the microelectrode) and a reference electrode (often a Ag/AgCl electrode). Both the microelectrode and the reference electrode are connected to the potentiostat that controls the voltage between electrodes. Because currents derived from the contents of single vesicles are quite small (nA to pA level), a low-noise measuring device or patch-clamp amplifier is employed between the microelectrode and the potentiostat. The cells of

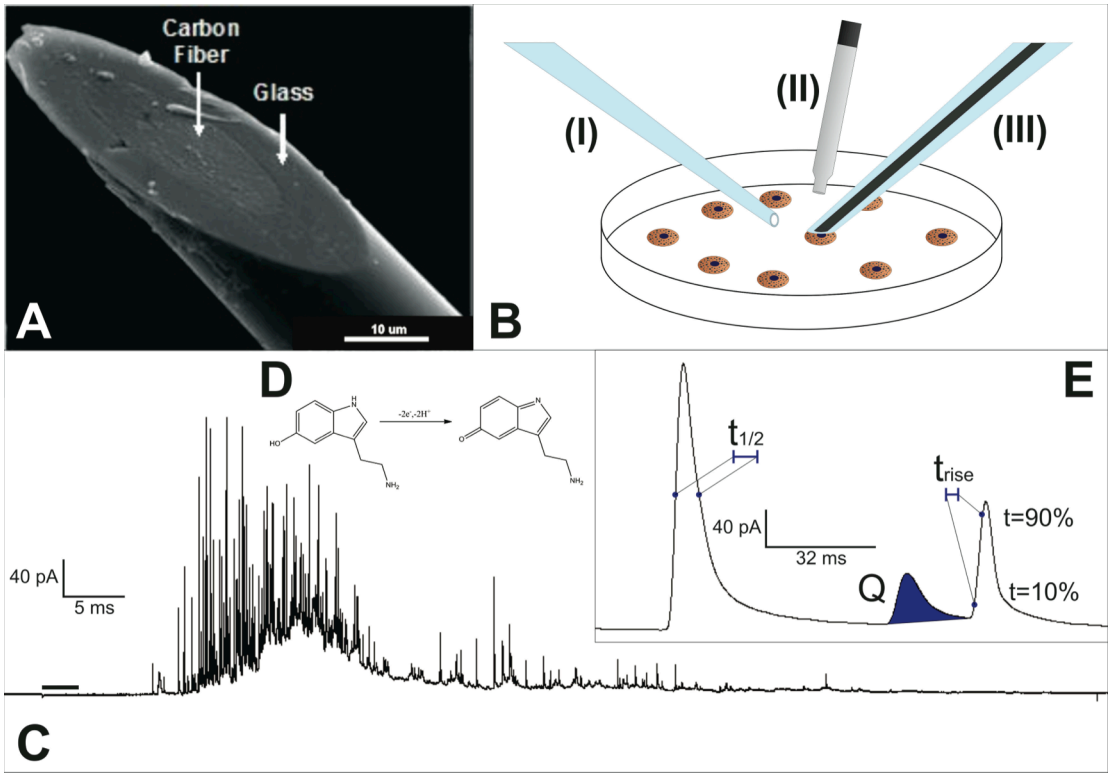


**Figure 1.3 Carbon-fiber microelectrode amperometry experimental setup and data analysis**
Carbon-fiber microelectrodes (A) are polished to a 45˚ angle to produce an active surface of roughly 10 µm in diameter. The CFMA experimental setup (B) includes (I) a pulled glass stimulating pipette, (II) a Ag/AgCl reference electrode, and (III) the carbon-fiber microelectrode set to an oxidizing potential and placed in contact with a single cell (for this work, a single mast cell). Amperometric traces (C) are collected as current detected over time as electroactive molecules (in this case serotonin) are released to the exterior of the cell and oxidized (D) at the surface of the microelectrode. Individual current spikes (peaks) are then analyzed (E) for several peak parameters including peak area (Q), peak half-width ($t_{1/2}$), peak rise-time ($t_{rise}$) and peak frequency/number.

interest are cultured in a Petri dish and are placed in a culture dish warmer to maintain physiological temperature. An inverted microscope is used to visualize cells and position

the carbon-fiber microelectrode. For cell stimulation, a pulled capillary containing a stimulating solution is connected to a pressure-driven flow controller and positioned near the cell of interest. Positioning of the carbon-fiber microelectrode (adjacent to the single cell) and stimulating pipette is accomplished using piezoelectric micromanipulators.

### 1.2.4 CFMA data analysis

Because this dissertation focuses on the application of CFMA for the study of mast cell exocytosis, serotonin is of particular interest as it is released from mast cell granules and is easily oxidized at +700 mV versus a Ag/AgCl reference electrode. After obtaining amperometric traces from individual mast cells (Figure 1.3c), analysis of the resulting data first requires identifying peaks (current spikes) and the corresponding baseline current. Usually, the root-mean-square current noise is measured before cell stimulation, and the peak detection threshold is set using a multiple of the measured noise.[23] In the case of overlapping or abnormally shaped peaks, individual peaks are manually selected. Following baseline determination and peak selection, each trace is analyzed for individual peak parameters (Figure 1.3e) to characterize and quantify the observed single-cell exocytosis process. The area underneath individual peaks (Q), full-width at half maximum ($t_{1/2}$), peak rise-time ($t_{rise}$), and the frequency or number of peaks in a trace are used in the research herein to describe each cell's exocytotic behavior (Figure 1.3).

Q is a measure of charge, and thus represents the number of electrons transferred per release event. Because the oxidation of serotonin is a two-electron process, the area of an

individual peak can be converted, using Faraday's law, to the number of serotonin molecules released per granule.[13] Peak frequency/number is calculated as the number of release events detected over the total release time and corresponds to the efficiency of the overall granule transport, docking and fusion mechanisms. Together, total Q and peak frequency/number can be combined to reveal the amount of serotonin released per cell (taking into account that the microelectrode covers only ~10% of the cell surface area and assuming equal secretion from all regions of the cell).

In addition to peak area and frequency/number, peak rise-time ($t_{rise}$) and half-width ($t_{1/2}$) values are monitored as a measure of the serotonin release kinetics from each granule fusion event. $T_{rise}$ is calculated as the time between 10% and 90% of the full peak height on the rising phase of each current peak. $T_{rise}$ reflects the amount of serotonin not directly associated with the chondroitin sulfate biopolymer matrix. Upon fusion, this 'free' serotonin diffuses to the electrode surface more rapidly than the bulk of the intragranular serotonin that interacts strongly with the negatively charged matrix. $T_{rise}$ is heavily influenced by the dilation of the initially formed fusion pore (Between the granular and the plasma membranes) to the maximally fused state. $T_{1/2}$, the width of the peak at half its full height, is a measure of the rate by which the biopolymer matrix expands and unfolds, releasing the remaining matrix-associated serotonin. Together, $t_{1/2}$ and $t_{rise}$ reflect the biophysical forces that determine the peak shape (sharp leading edge followed by a slower decay) typical of exocytotic release events.[3,17,22,24] Together, these parameters are

reliably used to quantify the exocytotic processes of single cells under various experimental circumstances.[17,23,25]

In certain contexts, a flux of redox-active chemical messengers before full exocytosis results in a characteristic pre-spike feature known as a pre-spike foot.[17,23] Pre-spike foot features, which were first investigated by Chow and co-workers[26] are diverse in magnitude, duration, and shape, yielding information about the dynamic nature of the fusion site. Analysis of pre-spike foot features often includes consideration of the number of spikes preceded by a foot event, charge within the foot portion of the feature ($Q_{foot}$), and duration of the foot before full exocytosis occurs ($t_{foot}$) relative to the corresponding value for the full exocytosis spike since, for a given condition, the portion of the messengers released through the fusion pore should be the similar.[27]

Analysis of CFMA data varies depending on the experimental aims and the particular context in which it is applied. The research central to this dissertation is largely focused on determining the biological significance of an altered cellular response, as well as leveraging the high degree of detail characteristic of CFMA data to provide additional insight into the regulatory processes that govern the observed changes in cellular function. To achieve this, peak area and peak frequency/number are generally used to assess the greater impact on total secretion, and are then considered in combination with

kinetic parameters ($t_{1/2}$ and $t_{rise}$) to propose reasonable cellular and biophysical mechanisms that account for the measured change in secretory function.

### 1.2.5 Use of CFMA to monitor exocytosis across different cell types

As many cell types release electroactive chemical messengers through exocytosis of cytoplasmic vesicles, FSCV and CFMA have been very effective tools used to monitor these important biological processes. The first effort in monitoring single cell exocytosis was performed using stimulated single bovine chromaffin cells, confirming that epinephrine and norepinephrine are co-stored and released during chromaffin cell exocytosis.[4,5] Norepinephrine and epinephrine have been similarly detected from murine and rat adrenal medullary cells.[28] Kennedy and colleagues detected peptide exocytosis from rat melanotrophs, and used both CFMA and FSCV to probe the exocytosis of these cells, finding the oxidation of alpha-melanocyte stimulating hormone was the primary source of the amperometric spikes.

Both dopaminergic and serotonergic neurons have been isolated and examined using CFMA. Zhou and Misler isolated cervical ganglia from rats, cultured individual dopaminergic and serotonergic neurons, and used CFMA to record amperometric traces.[29] Sulzer and co-workers detected dopamine exocytosis from cultured midbrain neurons of rat pups.[30,31] Dopamine has also been detected from retinal amacrine cells, which are dopaminergic neurons located in the retina, by Wightman and colleagues.[32]

Serotonergic leech neurons, called Retzius cells, have also been isolated and examined with carbon-fiber microelectrode techniques.[33,34]

Hematopoietic cells of the immune system have also been studied. Haynes and co-workers characterized the secretion of serotonin and histamine from the δ-granules of platelets, anuclear circulating cell type with critically important roles in blood clot formation and hemostasis, using FSCV.[35] By maintaining the potential of the electrode below the oxidation potential of histamine, they were able to use CFMA to explore the biophysical properties of platelet exocytosis with the well-understood serotonin redox reaction both in rabbit and human platelets.[27,36]

Finally, and most relevant for this dissertation, both FSCV and CFMA have been used to characterize the secretory function of mast cells. As is detailed later in this chapter, mast cells are a tissue-bound granulated cell found in most connective tissues. Importantly, these cells have a complex function in the immune system, providing a line of defense against parasitic organisms but also playing a primary role as mediators of the allergic response. Millar and co-workers used FSCV to detect exocytosis from single mast cells and identified the secreted substance as serotonin.[37] De Toledo, et al. were subsequently able to use amperometry as well as FSCV to probe mast cell exocytosis and determined the amount of serotonin secreted was $1.24 \times 10^6$ zmol/vesicle.[38] As mentioned above, Wightman and co-workers later employed FSCV and CFMA to determine that histamine

and serotonin are co-stored in mast cell granules, using features unique to the voltammograms of each species to discriminate between the two compounds (Figure 1.2).[39]

As the research field of single-cell electrochemistry has matured, the range of cell types and secreted analytes that can be detected has expanded, increasing the opportunities to broaden the application of these techniques. Following a natural progression, CFMA and FSCV have been increasingly used to explore the fundamentals of exocytosis and characterize the biophysical mechanisms that regulate this highly conserved cellular process.

### 1.2.6 Applications of CFMA for the study of exocytosis

Beyond the utility of fundamental characterization and quantitative detection of chemical messengers released from the vesicles of single cells, carbon-fiber microelectrodes have been extensively used to probe the biophysical phenomena of exocytosis including chemical messenger storage and release mechanisms, fusion pore formation, and intragranular matrix swelling. For example, in combination with single cell electron microscopy, CFMA studies have revealed that the concentration of chemical messengers within vesicles, across cell types, is 0.5-1.0 M, which is much higher than previously thought possible.[40] Several additional discoveries, outlined below, have also been made using single-cell electrochemical techniques.

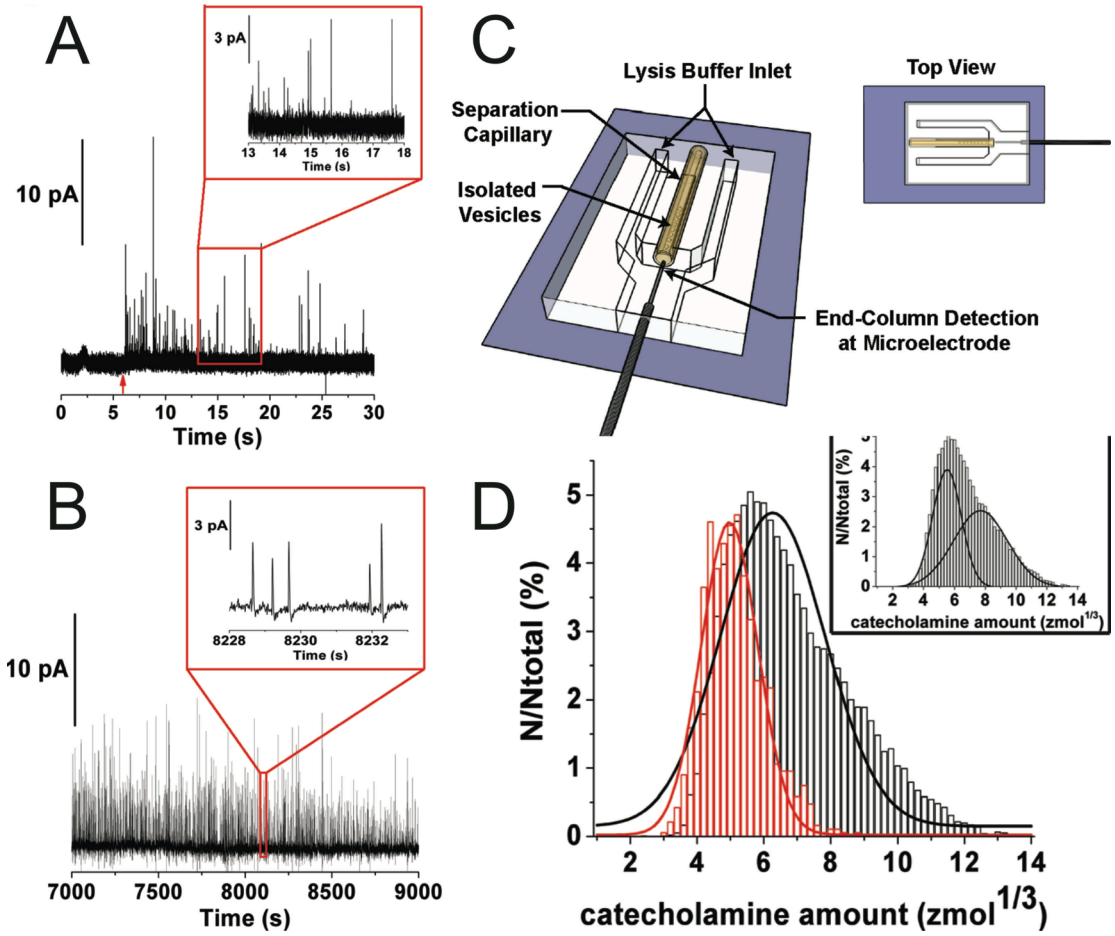


**Figure 1.4 Comparison of single cell exocytosis measurements and characterization of isolated cytoplasmic vesicles in PC12 cells reveals only a fraction of vesicular contents are released during exocytosis**

Using single cell CFMA measurements (A) in combination with the electrochemical analysis of isolated and separated individual secretory vesicles (B) using a microfluidic device (C), Omiatek and colleagues demonstrated that the average amount of catecholamine released from individual secretion events (small histogram centered at ~5 $zmol^{1/3}$) released roughly 40% of the average vesicular contents (large histogram, centered at ~6.5 $zmol^{1/3}$). Adapted with permission from Omiatek et al. (2010) ACS Chem. Neurosci. 1(3), 234-245. Copyright 2010 American Chemical Society.

Importantly, CFMA has been used to demonstrate that formation of a fusion pore does not always lead to full vesicular release during exocytosis; in some cases, the fusion pore recloses in a process known as "kiss-and-run" exocytosis. This "kiss-and-run" process may be a method for cells to send a less than quantal signal and it also represents a more efficient vesicle recycling process. Using CFMA in combination with the microfluidic separation and electrochemical analysis of isolated secretory granules, Ewing and coworkers showed that even during the full exocytosis process vesicles do not extrude all their content, in fact, only 40% of the vesicle is released during PC12 cell exocytosis (Figure 1.4).[41] CFMA experiments show that midbrain neurons release dopamine multiple times from the same vesicle through this mechanism.

CFMA experiments have also contributed to research aiming to determine the contributions of different membrane components, both lipid and protein, that affect the physical and chemical properties of the membrane. Although the lipid and protein composition of the fusion pore is still a topic of debate, CFMA results show that both membrane proteins and lipids influence exocytotic process. The role of membrane proteins, including the SNARE proteins and synaptotagmins discussed later in this chapter, in the biophysical processes of exocytosis have been extensively studied using this technique.[42-44] Similarly, the role of specific phospholipids and their relative abundances in the cellular membrane has also been studied using CFMA demonstrating that phosphotidylserine, phosphatidylethanolamine, sphingomyelin and

phosphatidylcholine influence the exocytotic process by altering the frequency, quantity, and/or kinetics of release.[45,46] Cholesterol, in addition to membrane phospholipids, is another major membrane component found to carry both structural and functional importance in exocytosis.[27,47]

A central theme of the research summarized in this dissertation is to further broaden the scope of CFMA beyond the characterization of fundamental biophysics to include applications exploring the consequences of inflammatory microenvironmental factors on regulated cellular exocytosis in biological signaling networks. Mast cells and the inflammatory response, given their diverse functionality and the inherent complexity of immune cell signaling, is a particularly apt system to explore this this objective.

### 1.3 Mast cells and the immune response

The immune system is comprised of many interconnected elements making up a complex and dynamic barrier to disease and infection. Mast cells (Figure 1.5) are immune cells traditionally known for their role in IgE-mediated type I hypersensitivity reactions; however, they also play several important roles in both the innate and adaptive branches of the immune system.[48,49] To appreciate the larger context of the research in this dissertation, an overview of the immune system is included here, followed by a more specific description of mast cells and their role in various inflammatory processes.

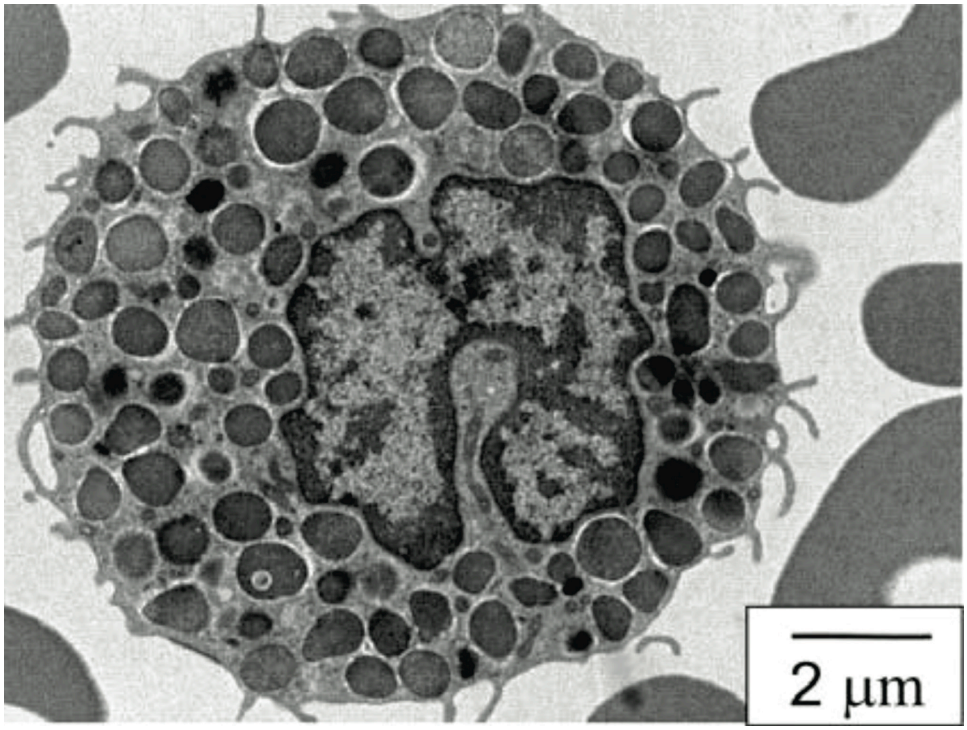


**Figure 1.5 TEM image of a mast cell**
A TEM image of a mouse peritoneal mast cell clearly shows the dense-body granules (secretory vesicles) that contain many biologically active mediators that influence the immune response. Once stimulated, mast cells release these mediators through exocytosis.

### 1.3.1 Overview of the immune system

A discussion of the full breadth of the immune system is beyond the scope of this chapter, however a brief overview of its basic components is warranted to provide the larger context of the research in this dissertation, and to outline the different ways mast cells contribute to the greater functionality of the immune system.

Classically speaking, the immune system is often described in terms of two collaborative and complementary elements; the adaptive and innate immune systems. The adaptive immune system consists largely of B-cells, T-cells, and their respective functions. As its name suggests, the adaptive immune system is capable of memory, and builds upon past pathogen exposure to enhance the body's ability to fend off any future infection. The adaptive immune system, however, requires the mobilization of many different components, especially during a primary response. The innate immune system, on the other hand, is capable of rapid and direct response to a wide variety of pathogen invasions, though it lacks the memory of the adaptive immune system. Often, it is elements of innate immunity that initiate the beginnings of an adaptive immune response. This oversimplified view of the immune system leaves little room for the many elements of the immune system that bridge between innate and adaptive immunity. Nonetheless, it offers a necessary reference point from which any further discussion of the immune system is founded.

#### 1.3.1.1 The adaptive immune system

The key feature of the adaptive immune system is its ability to develop specificity to previously unrecognized foreign pathogens. The precise way this is achieved is beyond the scope of this introduction, however, two categories of leukocytes, B cells and T cells, perform the major functions of the adaptive immune system. In brief, B cells, sometimes referred to as plasma cells, are manufacturers of immunoglobulins (Igs). Immunoglobulins, or antibodies, come in several isotypes, each serving a unique role in

the adaptive immune response, and are responsible for a large part of the specificity of immune reactions. T-cells make up the other prominent component of the adaptive immune system. Two subclasses of T-cells, T-helper ($T_H$) and T-cytotoxic ($T_C$) cells, constitute the majority of T-cell functionality, with a third subclass, T-regulatory ($T_{Reg}$) cells, fulfilling an important, but less understood, role in the immune system. The T-cell equivalent of membrane-bound Ig is the T-cell receptor (TCR). TCRs recognize internalized protein displayed on the surface of many cell types in the context of major histocompatibility complex (MHC). Whereas Igs recognize antigen in its natural conformation, antigen (usually peptides) recognized by TCRs has been processed by an effected cell and displayed on its surface via expressed MHC. In general, $T_C$ cells are directly involved in cell-mediated cytotoxicity, whereas $T_H$ cells recognize MHC class II-associated antigen (expressed only on certain immune cells) and initiate the activation of additional immune system functions.[50] Because of their ability to direct the immune response, $T_H$ cells are particularly interesting for the research of inflammatory disease.[51,52]

Much of the complexity of the immune system is a consequence of the multifunctionality of its many components. Cytokines, which are immunoactive mediators that are both expressed by and act upon the many cells of the immune system, (along with growth factors and other signaling molecules) represent a large portion of this complexity. Because cytokines act on immune cells and alter their function, the local cytokine

microenvironment can have a great influence on the overall immune response.[52,53] This is exemplified by the two distinct subsets, $T_H1$ and $T_H2$, of $T_H$ cells. Both $T_H1$ and $T_H2$ cells recognize antigen in the context of MHC class II, but produce a different cytokine profile, and as a result, favor two very different immune responses.[50,53] For example, allergic disease is typically associated with increased expression of $T_H2$-associated cytokines. Overall, the complexity of the adaptive immune system, in the number of both cell types and functions, manifests as a wide range of possible immune responses. This inherent adaptability affords us the remarkable protection from recurrent infection, but also creates many opportunities for the development of disease in the form of an inappropriate immune response.

#### 1.3.1.2 The innate immune system

The innate immune system is, to a large extent, composed of a different set of immune cells, including macrophages, dendritic cells, neutrophils, and natural killer (NK) cells, as well as the epithelial cells that make up the immediate barrier to infection. These cells use a wide variety of defense mechanisms to directly fend off pathogens, though only a small part of the innate immune system demands attention here. In addition to role of the innate immune system in the direct activity against pathogens, a major function of this system is to secrete mediators that alter the inflammatory microenvironment and recruit additional immune cells to the site of injury.[50]

Innate immune cells perform their role as 'first responders' to pathogens or sites of injury in through several signaling processes, most of which involve a surface receptor-specific cellular response. One example of this is the recognition of infectious agents by toll-like receptors (TLRs).[50,54,55] Unlike the highly selective adaptive immune system receptors, Igs and TCRs that bind very specific antigens, TLRs recognize broad molecular motifs common to families of pathogens. Activation of TLRs can result in a variety of physiological responses depending on the cell type and particular receptor, including increased capacity for phagocytosis.[50] The complement system, activated by three converging pathways, is another powerful defensive mechanism of the innate immune system. All three pathways set off a cascade of proteolytic enzymes that culminates in the formation of large membrane-attack complexes, which in turn perforate the cell wall of invading species.[50] TLR signaling and complement activation are just two examples of the many defense mechanisms of the innate immune response.

In addition to the functions of the innate immune system to directly mitigate pathogens, as described above, much of the activity of the innate immune system culminates in the development of a local inflammatory response through the recruitment of additional leukocytes to the site of infection. In reality, these two functions are often linked. For example, both the activation of immune cells via TLRs and initiation of the complement cascade ultimately trigger the recruitment and infiltration of leukocytes from the peripheral blood. The primary mechanism by which innate immune cells accomplish this

task is through the secretion of chemotactic cytokines (chemokines) and other inflammatory mediators which signal circulating leukocytes to migrate from the blood into the site of injury. To use the previous examples, TLR signaling often results in up-regulation and secretion of chemokines, while several proteolytic byproducts of the complement cascade, C3a and C5a in particular, themselves induce a strong chemotactic response from leukocytes.[50,54,55] Initiation of the inflammatory response plays an important part in the pathogenesis of many diseases, however, the nature of this inflammation varies significantly in both severity and the variety of cell types and mediators involved depending on a wide and complex range of factors. An important aim of this dissertation is to examine mast cell function, taking into account both the complexity and diversity of inflammatory response.

### 1.3.2 Mast cell background

Mast cells are hematopoietic cells found in most connective tissues and mucosal surfaces in the body. As underdeveloped precursors, mast cells circulate in the blood before migrating to various tissues where they undergo final maturation.[55,56] One of their most recognizable features is the presence of many dense-core secretory vesicles that occupy the mast cell cytoplasm (Figure 1.5); the contents of which are released via exocytosis. These granules contain many molecules capable of influencing the immune response, including tumor necrosis factor alpha (TNF-$\alpha$), growth factors such as vascular endothelial growth factor (VEGF), the proteases tryptase and chymase, as well as the bioactive amines histamine and serotonin to name just a few. A list of several mast cell

| Mediators | Main physiological effects |
|---|---|
| **Prestored** | |
| Histamine and serotonin | Vasodilation, angiogenesis, mitogenesis, pain |
| **Chemokines** | |
| IL-8 (CXCL8), MCP-1 (CCL2), MCP-3 (CCL7), MCP-4, RANTES (CCL5), eotaxin (CCL11) | Chemoattraction and tissue infiltration of leukocytes |
| **Enzymes** | |
| Arylsulfatases | Lipid/proteoglycan hydrolysis |
| Carboxypeptidase A | Peptide processing |
| Chymase | Tissue damage, pain, angiotensin II synthesis |
| Kinogenases | Synthesis of vasodilatory kinins, pain |
| Phospholipases | Arachidonic acid generation |
| Tryptase | Tissue damage, activation of protease-activated receptor, inflammation, pain |
| Matrix metalloproteinases | Tissue damage, modification of cytokines/chemokines |
| **Peptides** | |
| Angiogenin | Neovascularization |
| Corticotropin-releasing hormone | Inflammation, vasodilation |
| Endorphins | Analgesia |
| Endothelin | Sepsis |
| Kinins (bradykinin) | Inflammation, pain, vasodilation |
| Leptin | Food intake regulator |
| Renin | Angiotensin synthesis |
| Substance P | Inflammation, pain |
| Urocortin | Inflammation, vasodilation |
| VEGF | Neovascularization, vasodilation |
| Vasoactive intestinal peptide | Vasodilation, mast cell activation |
| **Proteoglycans** | |
| Chondroitin sulfate | Cartilage synthesis, anti-inflammatory |
| Heparin | Angiogenesis, nerve growth factor stabilization |
| Hyaluronic acid | Connective tissue, nerve growth factor stabilization |

**Table 1.1 Examples of bioactive mediators released from mast cell granules**
The table above lists many of the immense variety of mediators that are released from mast cell granules via exocytosis along with some of their known physiological functions. Reprinted with permission from Biochimica et Biophysica Acta, vol. 1822 (1), Theoharides et al. Mast cells and inflammation, pp.21-33, Copyright 2012 with permission from Elsevier.

secreted factors, both granule-associated and de novo synthesized, is included in table 1.1. These bioactive mediators are preformed and stored in mast cell granules along with a sulfated proteoglycan biopolymer matrix, which serves both structural and mechanical functions (the swelling phase of the exocytosis following the formation of a fusion pore).[57] In this work, serotonin is of particular importance because of its electrochemical properties. The ability to measure serotonin release electrochemically offers a unique handle to be able to characterize the kinetic and mechanistic character of mast cell degranulation, providing a label-free way to monitor the release of many mast cell-secreted mediators in a variety of inflammatory contexts.

In addition to the large number and variety of secreted species, mast cells are also capable of responding to a wide range of signaling molecules through a variety of membrane-bound receptors expressed on their surface.[54,58] Table 1.2 lists several of the receptors expressed by mast cells, along with the corresponding ligands for each. Bacterial products, cytokines, proteases, interleukins, neuropeptides, complement proteins, and of course antibodies, are just a few of the types of molecules that have been demonstrated to influence mast cell function in one form or another.[54,58,59]

The breadth of different inflammatory factors that can influence mast cell function also results in the sizeable heterogeneity among mast cell subpopulations that is dependent on the character of a particular inflammatory microenvironment.[60] The goal of the

| Mast cell receptors | Associated agonists |
|---|---|
| Adenosine receptors A2A, A2B, A3 | Adenosine |
| $\beta_2$-Adrenoreceptor | Adrenaline |
| C3a and C5a receptors | C3a and C5a |
| Cannabinoid $CB_2$ receptor | 2-Arachindonoyl-glycerol anandamide |
| CD47 (integrin-associated protein) | Integrins |
| CD200 receptor | CD200 (0X2) |
| Chemokine receptors CXCR1-4, CX3CR1, CCR1,3-5 | Chemokines |
| CRHR-1 and CRHR-2 | Corticotropin-releasing hormone |
| Estrogen receptors (A, B) | Estrogens |
| FcαR | IgA |
| FcεRI | IgE |
| FcγRI, FcγRIIA, FcγRIIB, FcγRIII | IgG |
| GPR34 | Lysophosphatidylserine |
| GPR92, $LPA_1$, $LPA_3$ | Lysophosphatidic acid |
| Histamine receptors H1, H2, H3, H4 | Histamine |
| 5-$HT_{1A}$ | Serotonin |
| Kit receptor tyrosine kinase (CD17) | Stem cell factor |
| Leptin receptor | Leptin |
| Leukotriene receptors 1 and 2 | Leukotrienes |
| MRGX2 | Mastoparan, somatostatin, substance P |
| Neurokinin receptors NK1R, NK2R, NK3R, and VPAC2 | CGRP, Hemokinin-A, substance P, vasoactive intestinal peptide |
| Neurotensin receptor | Neurotensin |
| Neurotrophin receptors TrkA, TrkB, TrkC | NGF, BDGF, neurotrophin 3 |
| Nicotinic acetylcholine receptor | Acetylcholine |
| 0X40 | 0X40 ligand |
| Protease activated receptors 1-4 | Serine proteases (trypsin, tryptase) |
| Progesterone receptor | Progesterone |
| Prostaglandin E receptors $EP_2$, $EP_3$, $EP_4$ | Prostaglandin E |
| Purinoreceptors $P2Y_1$, $P2Y_{12}$, $P2Y_{13}$, $P2Y_2$, $P2Y_{11}$ | ADP, ATP, UTP |
| Sphingosine-1-phosphate receptors $S1P_1$, $S1P_2$, $S1P_3$ | S1P |
| Toll-like receptors 1-9 | Bacterial and viral products |
| Urokiniase receptor | Urokinase |
| Vitamin D receptor | Vitamin D |

**Table 1.2 Summary of mast cell-expressed receptors and their associated ligands**
Mast cells express a large array of difference receptors that allow these cells to participate n and influence the inflammatory environment in response to many different stimuli. Reprinted with permission from Biochimica et Biophysica Acta, vol. 1822 (1), Theoharides et al. Mast cells and inflammation, pp.21-33, 2012 with permission from Elsevier.

research compiled in subsequent chapters is to use a single-cell approach to begin to unravel and isolate specific links in this complex signaling network. To provide the contextual framework for this research, a detailed look at the classical IgE-mediated signaling in mast cells is outlined here, followed by several examples of known mast cell functions within different inflammatory scenarios.

### 1.3.3 IgE signaling and mast cell degranulation

The classic mechanism of mast cell activation is mediated by the interaction between soluble IgE antibody and its membrane-bound receptor (FcεRI) expressed abundantly on the surface of mast cells (Figure 1.6). This is the IgE-mediated type I hypersensitivity (allergic) response for which mast cells are commonly recognized. In allergy, FcεRI binds the constant region of IgE such that the variable regions of the antibody are outwardly displayed, thus allowing the antibody to interact with any corresponding antigen present. Interaction between antigen (or allergen) and a single antibody is not sufficient stimulus to initiate the release of granular contents. Rather, mast cell degranulation (exocytosis of preformed cytosolic vesicles or 'granules') is dependent on the crosslinking of multivalent antigen between two or more FcεRI-bound IgE molecules. Among the many mediators released from stimulated mast cells are histamine in humans, and both serotonin and histamine in mice (structures shown in figure 1.7). Allergic rhinitis is a classic example of IgE-mediated activation, during which the release of excessive amounts of histamine and other immunoactive molecules from mast cells initiates the physiological response associated with an allergic reaction (Table 1.1).

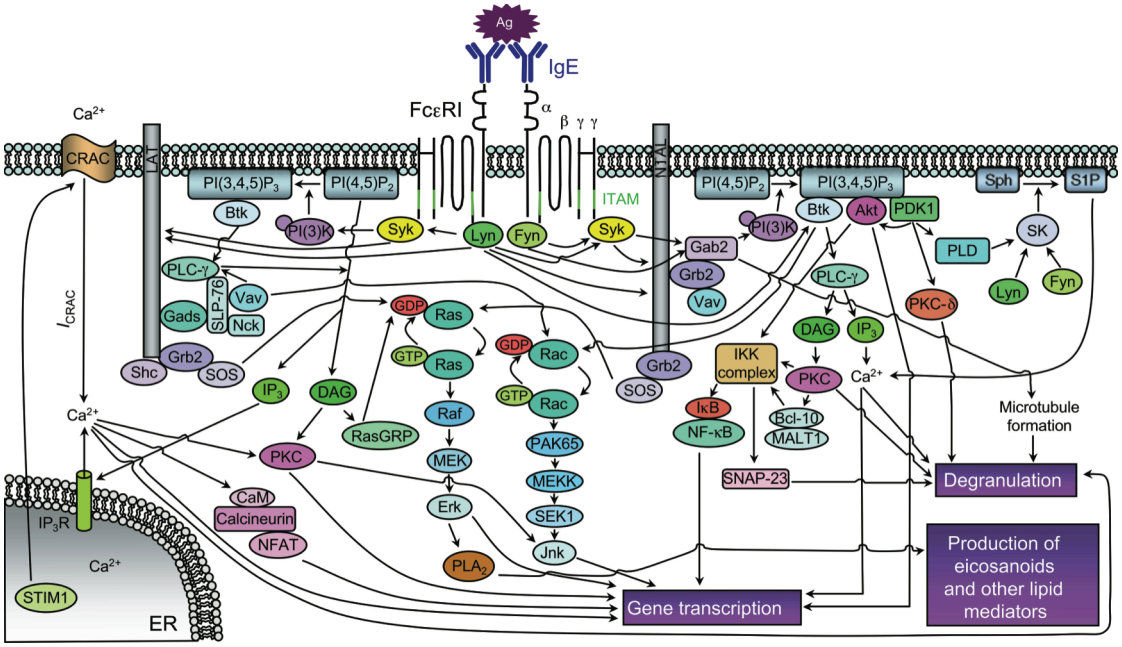


**Figure 1.6 IgE-mediated mast cell signaling**
Mast cell-mediated type I hypersensitivity reactions (allergy) occur in response to the crosslinking of two or more IgE antibodies displayed on the mast cell surface by multivalent antigen. The signaling is regulated by the IgE receptor FcεRI, which is composed of an α subunit, a β subunit, and two γ subunits. Activation of FcεRI initiates a signaling cascade that involves several kinases including Lyn, Syk, and Fyn. Ultimately, activation of both the phosphatidylinositol-3-OH kinase (PI(3)K and Phospholipase Cγ (PLCγ) pathways each culminates in an influx in cytosolic calcium ion, which is critical for the regulation of exocytosis (mast cell degranulation). Reprinted with permission from Macmillan Publishers Ltd.: Nature Immunology, New developments in mast cell biology, Kalesnikoff, J. and Galli, S. J., 2008, 9(11) pp. 1215-1223, copyright 2008.

The IgE-mediated signaling cascade that regulates mast cell degranulation is well characterized. The FcεRI complex is composed of an α subunit responsible for the binding of IgE, a β subunit largely considered to be an amplifier of IgE-mediated signaling, and two γ subunits. The γ subunits are essential for IgE signaling because they

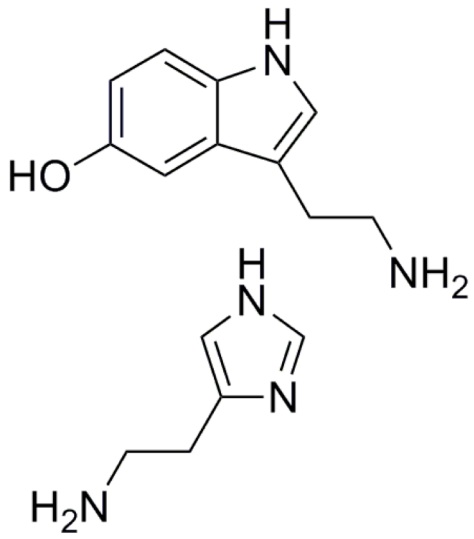


**Figure 1.7 Structures of histamine and serotonin**
Both histamine (bottom) and serotonin (top) are both vasoactive amines released from mast cell granules. Serotonin is oxidized at +700 mV vs. Ag/AgCl and is used to monitor mast cell degranulation during CFMA experiments.

each contain an immunoreceptor tyrosine-based activation motif (ITAM) responsible for initiating the intracellular signaling cascade (Figure 1.6). A complete description of this process is not essential for the purposes of this dissertation. In short, the initial signaling events, upon crosslinking of two IgE receptors, involve several classes of tyrosine kinases,[49,56] and the subsequent phosphorylation events activate numerous other enzymes and adaptor molecules, among them phospholipase Cγ (PLC-γ). PLC-γ ultimately induces the release of calcium from the endoplasmic reticulum, resulting in increased cytosolic calcium concentration. Calcium from the endoplasmic reticulum in turn stimulates the influx of additional extracellular calcium through the activation of calcium release-activated calcium (CRAC) channels; it is this transient cytosolic calcium that is essential for regulation of exocytosis.[49]

The importance of cytosolic calcium pertains to the protein machinery responsible for the docking of mast cell vesicles to the cell membrane (a critical step in exocytosis

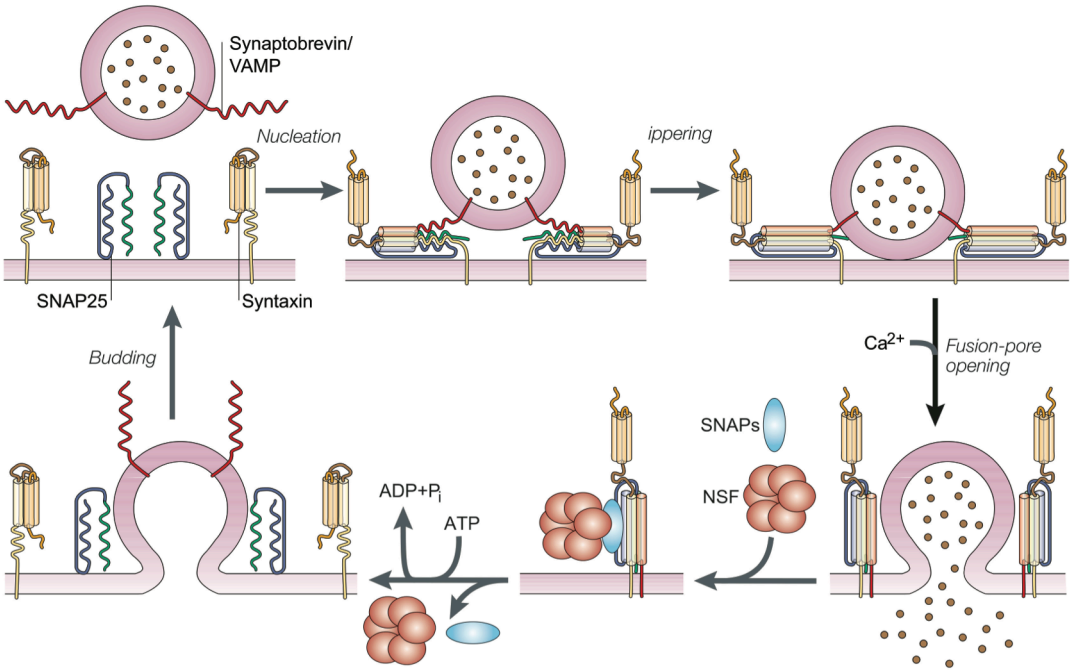


**Figure 1.8 Schematic of docking machinery in exocytosis**
During exocytosis, cytoplasmic vesicles are transported to the cellular membrane where they dock with specialized protein machinery, including SNAREs (SNAP23, SNAP25, and VAMPs are expressed in mast cells). Importantly, increased cytosolic calcium is required for the fusion of the two membranes. Reprinted with permission from Macmillan Publishers Ltd.: Nature Reviews Neuroscience, Snares and Munc18 in synaptic vesicle fusion, Rizo, J and Südhof, T. C., 2002, 3(8) pp. 641-653, copyright 2002.

mentioned earlier in this chapter). These proteins, collectively named soluble N-ethyl-maleimide-sensitive factor- attachment protein receptors (SNAREs), are present on both the vesicle (v-SNAREs) and the interior surface of the target cell membrane (t-SNAREs).[49] Figure 1.8 shows a schematic of SNARE-mediated exocytosis; although

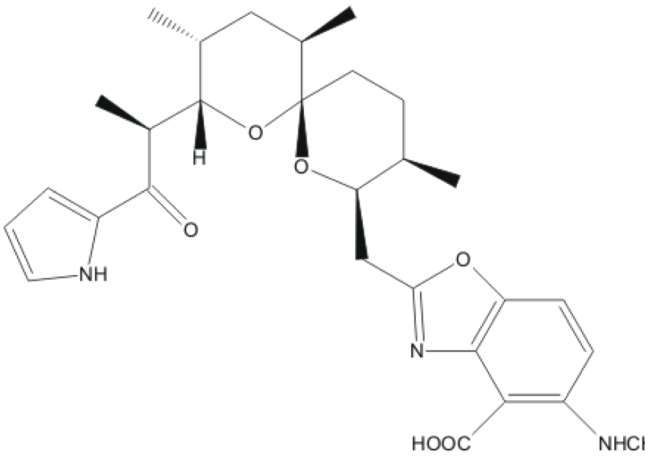


**Figure 1.9 Structure of A23187**
A23187 is a calcium-specific ionophore. Calcium-bound A23187 is lipophilic, and therefore is capable of shuttling calcium ion across the cell membrane.

variations on the specific SNARE proteins exist between different cell types, the basic mechanism of exocytosis is well conserved.[61]

Specifically, mast cells express both synaptosome-associated protein 23 (SNAP-23) and its relative SNAP-25 on their cellular membranes, and vesicle-associated membrane proteins (VAMPs) 2, 3, 7, and 8 as well as SNAP-25 on their granule membranes.[61-63] There are at least two proposed mechanisms by which calcium likely induces exocytosis of mast cell granules. The first is by activating protein kinase C, which in turn acts upon SNARE proteins, making them more readily able to dock vesicles to the cell membrane. The second, and perhaps more important component of calcium-mediated degranulation is through interaction with synaptotagmins.[61] The exact mechanism of synaptotagmin regulation of exocytosis is unclear. Research with synaptotagmin-2 knockout mice has shown the importance of this protein in the regulation of mast cell degranulation.[63] It is important to note the specificity of synaptotagmin-2 regulation for pre-formed mediator release. Neither the synthesis of cytokines such as TNF-α nor the secretion of other de

novo mast cell products were affected by the lack of synaptotagmin-2. The importance of cytosolic calcium for regulation of mast cell degranulation is used to the advantage of researchers studying exocytosis. Calcium ionophores such as A23187, the structure of which is shown in figure 1.9, can be used to bypass several molecular signaling steps and induce degranulation by transporting calcium across the cell membrane.[64,65]

### 1.3.4 Non-allergic functions of mast cells in the immune system

A significant portion of the research conducted on mast cells and their role in the immune system relates to the high-affinity IgE receptor FcεRI and the corresponding activation pathway. Although some of the research in this dissertation explores this element of mast cell physiology, in large part, this work focuses on mast cell function outside of the allergic context, and seeks to characterize the involvement of these cells in a variety of inflammatory environments. The greater thrust of this dissertation is to use a unique, single-cell approach to explore mast cell function in the context of different inflammatory scenarios. To demonstrate the diverse range of interactions between mast cells and the immune system, several examples of established non-allergic mast cell immune functions are outlined below.

Despite the emphasis on their role in allergy, mast cells respond to a diverse set of immune signals (see tables 1.1 and 1.2), through various receptors and their corresponding ligands ranging from interleukins and cytokines to proteases and complement proteins.[54] One of the more basic functions of mast cells is their ability to

initiate the immune response when challenged directly by certain bacterial and viral infections.[55,66,67] This capacity, as discussed earlier, is in part enabled by the expression of several TLRs on the surface of mast cells, and demonstrates how these cells often function in both the innate and adaptive immune systems. The range of TLRs expressed by mast cells can vary based on subpopulation, however, in general, the activation of mast cell TLRs triggers an immune response through the production of cytokines.[55,66,67] Mast cells also respond to a variety of components of the complement cascade, including C3a, C5a and C1q among others.[54,55,67] Like TLRs, the complement receptors induce a range of physiological consequences, and expression can vary by subpopulation. For example, when activated by C3a, some mast cell populations undergo simultaneous degranulation and up-regulation of certain chemokines, whereas activation of the C5a receptor does not.[55,68] TLR activation and complement signaling are just two examples of mast cell involvement in the innate response.

Beyond their role in innate immunity, mast cells are known to act via adaptive mechanisms. Of course, the allergic function of mast cells is mediated by IgE, however, mast cells also express, albeit in smaller numbers, several immunoglobulin G (IgG) receptors (FcγRs).[55,69] Interestingly, FcγRI, FcγRII, and FcγRIII demonstrate different and opposing effects on mast cell degranulation. For example, depending on conditions and the receptor subtype, FcγRs can either stimulate mast cell activation, or inhibit degranulation via FcεRI activation.[69] Both FcγRI and FcγRIII induce mast cell

degranulation via activation similar to the FcεRI pathway.[69,70] However, FcγRII has been shown to inhibit IgE activation.[70] Inhibition of IgE-mediated mast cell activation is particularly interesting because of the potential for the development of new therapies for many atopic disorders.

An additional characteristic of mast cell biology pertinent to this dissertation is the effect of neuropeptide-induced signaling in mast cells and the associated implications for both neurogenic pain and stress-induced inflammatory responses. That stress-related factors are often manifested through inflammatory mechanisms is not a novel concept; however, recent work has provided more tangible experimental evidence of this connection.[71,72] Research done in mice has found an increase in both substance P-producing nerve fibers and the frequency of nerve-mast cell interactions after exposure to stress for periods of 24 and 48 hours.[73] Substance P, as well as other neuropeptides including calcitonin gene-related peptide (CGRP), has long been known to stimulate mast cell degranulation.[71] Pavlovic et al. confirmed a similar increase in substance P producing nerves in both mice exposed to prolonged sonic stress and mice pre-sensitized and challenged with ovalbumin as a model for atopic dermatitis. Furthermore, the same study found that the number of substance P-producing nerves in mice challenged with ovalbumin further increased still when also subjected to the stress treatment.[72] These studies highlight the relationship between stress and mast cell functions, which serves to emphasize the complexity of mast cell physiology and their potential role in the pathogenesis of inflammatory disease.

In short, mast cells are multifunctional effector cells important for many processes of both the adaptive and innate elements of the immune system. Their suspected involvement in such a variety of diseases, both allergic and non-allergic, is a testament to their diverse functionality. The importance of IgE-mediated activation should not be underestimated, however, it is crucial when considering the physiological role of mast cells within a particular physiological system not to overlook the potential influence of a variety of factors, only a few of which were discussed above.

### 1.3.5 Two approaches toward the study of mast cell-immune interactions

In terms of the broad experimental approach, the research projects in this dissertation fit generally into one of two basic paradigms. Although both approaches seek to understand how microenvironmental factors influence mast cell secretory function, they differ from each other in the nature of the altered mast cell function that is examined. The first category consists of research wherein the objective is to monitor the impact of an altered inflammatory environment on mast cell signaling in response to a universal stimulus. This approach is particularly useful for the assessment of mast cell activation potential, especially when the context of the fundamental research question involves a known mast cell stimulation pathway, such as the IgE-activation central to many atopic diseases. In contrast, research in the second category seeks to monitor specific cellular signaling factors that directly induce mast cell degranulation and to characterize the profile of such direct activity of mast cells relative to a standard stimulation condition (such as IgE-

mediated or calcium ionophore-induced degranulation). Both of these approaches were used in this research to provide a more complete picture of mast cell signaling and their participation in a complex inflammatory process, accounting for the individual context of each experimental objective.

### 1.4 Conclusion

The broad application of single-cell carbon-fiber microelectrochemical approaches to explore the fundamentals of exocytosis has established a solid foundation of research that defines our current understanding of this basic and essential cellular function. The central theme of this dissertation is to expand the utility of CFMA to address broader biological questions involving the complex signaling of cellular networks. Mast cell degranulation in the context of inflammatory disease is an ideal, albeit challenging, system in which to demonstrate the applicability of CFMA in this type of setting. To this end, the ensuing four chapters summarize a body of research that includes several examples of how CFMA was used as a unique approach toward the study of mast cell function in response to a particular inflammatory scenario. These chapters encompass a range of different inflammatory contexts, and prove that CFMA, when properly applied, can be an effective tool for the study of cellular communication in complex biological systems.

As the first example of this research effort, Chapter 2 describes a pattern of altered mast cell degranulation in transgenic mice expressing sickle human hemoglobin, a well-characterized model of chronic inflammation, and explores the effects of in vivo

morphine treatment on stimulated mast cell degranulation. Chapter 3 expands on the concept of opioid-induced regulation of mast cell function using knockout mice lacking individual opioid receptors in combination with in vitro morphine exposure. In a change of focus, Chapter 4 transitions away from the 'susceptibility to stimulation' paradigm and applies CFMA to characterize the activity of two specific chemokines and their capacity to directly induce mast cell degranulation, specifically to explore the interaction between airway smooth muscle and mast cells in asthma. Chapter 5, the final chapter of this dissertation, examines the activities of two neuropeptides, Substance P and CGRP, as mast cell-stimulating mediators using CFMA in direct comparison to bulk mast cell degranulation assay data. Collectively, this work represents an attempt to survey the breadth of mast cell functionality within a set of inflammatory scenarios representing just a small sample of the many processes of the inflammatory response.

# Chapter 2

## Carbon-fiber microelectrode amperometry reveals sickle cell-induced inflammation and chronic morphine effects on single mast cells

In part from:

Manning, B. M., Hebbel, R. P., Gupta, K., and Haynes, C. L. *ACS Chem. Bio.* 2012, 7, 3, 543-551

## 2.1 Overview

Sickle cell disease, caused by a mutation of hemoglobin, is characterized by a complex pathophysiology including an important inflammatory component. As discussed in Chapter 1, mast cells are known to influence a range of immune functions in a variety of different ways, largely through the secretion of biologically active mediators from preformed granules. However, it is not understood how mast cells influence the inflammatory environment in sickle cell disease. A notable consequence of sickle cell disease is severe pain. Therefore, morphine is often used to treat this disease. Because mast cells express opioid receptors, it is pertinent to understand how chronic morphine exposure influences mast cell function and inflammation in sickle cell disease. Herein, CFMA was used to monitor the secretion of immunoactive mediators from single mast cells. CFMA enabled the detection and quantification of discrete exocytotic events from single mast cells. Mast cells from two transgenic mouse models expressing human sickle hemoglobin (hBERK1 and BERK) and a control mouse expressing normal human hemoglobin (HbA-BERK) were monitored using CFMA to explore the impact of sickle cell-induced inflammation and chronic morphine exposure on mast cell function. This work, utilizing the unique mechanistic perspective provided by CFMA, describes how mast cell function is significantly altered in hBERK1 and BERK mice, including decreased serotonin released compared to HbA-BERK controls. Furthermore, morphine was shown to significantly increase the serotonin released from HbA-BERK mast cells

and demonstrated the capacity to reverse the observed sickle cell-induced changes in mast cell function.

## 2.2 Introduction

Sickle cell disease (SCD) became the first recognized 'molecular disease' when Linus Pauling discovered the altered electrophoretic mobility of hemoglobin (Hb) in the blood of patients suffering from this painful and often life-threatening disorder.[74] Several years later, the genetic basis for the dysfunctional Hb was determined.[75,76] However, despite its simple origin, the pathophysiology of this disease is complex and highly variable,[76] and relatively few advances in treatment methods have been made. A large part of the diverse manifestation of SCD can be attributed to the significant inflammatory component of the disease.[77-80] Understanding the specific role of inflammation in the development and progression of SCD requires a capacity to monitor the behavior of different cell types that take part in the inflammatory response. In addition to traditional molecular biology methods such as bulk in vitro assays to detect various secreted mediators or immunostaining to observe relative levels of immune cell infiltrate in situ, single cell measurement techniques can provide a complimentary approach to study fundamental cellular functions of the immune system. Understanding how mast cells respond to the chronic inflammation associated with SCD provides an interesting and important perspective on its pathophysiology and progression.

CFMA is a unique analytical tool for the real-time, label-free detection of secreted molecular species from single cells.[81] Single cell electrochemical measurements correlate well with both single vesicle measurements and bulk assays.[36,41] In this case, CFMA was used to measure from single mast cells.[82] As summarized in Chapter 1, CFMA measurements are conducted by holding the microelectrode, placed in contact with a single cell, at a fixed potential sufficient to oxidize the molecular species of interest. Upon stimulation, distinct packets of current are detected as oxidizable species are released from each granule of the cell (Figure 1.3). The ability to quantitatively measure individual exocytosis events from these cells offers a useful handle on the various physiological functions mast cells perform within the immune system.

### 2.2.1 Immune response in SCD

Because they influence a variety of immune responses,[49,60,83] mast cells are subsequently implicated in many inflammatory diseases. SCD is one such example, and because it is painful, patients are often treated with opioids such as morphine.[84-86] One common side effect of morphine treatment is severe itching and reddening, indicating unintentional activation of mast cells, likely exacerbating the symptoms of pain.[87] Morphine-mediated mast cell degranulation is poorly understood and because it occurs at much higher doses than are used for pain management, and it is thought to function independent of opioid receptors.[87-89] Herein, CFMA is used to, first, explore the impact of sickle Hb expression and the subsequent inflammation on mast cell function, and second, gain biophysical insight into the effect of chronic morphine exposure on mast cell degranulation dynamics

at the single cell level. Furthermore, the effect of morphine on mast cell function is also examined in the context of sickle Hb-induced inflammation.

### 2.2.2 Inflammation in SCD

SCD is characterized by a single Glu-Val point mutation of the gene which encodes the β-subunit of Hb,[75] The mutation causes Hb to rapidly polymerize under hypoxic conditions,[95] and the accumulation of polymerized sickle Hb in deoxygenated red blood cells ultimately results in a variety of damaging physiological consequences.[76,78] These include impaired rheological function of red blood cells, anemia, poor oxygenation of tissues, and intermittent vascular occlusion events, which are painful and contribute to organ failure.[76,79] Although vascular occlusion is traditionally implicated as the primary cause of symptoms in SCD patients, underlying inflammation has become recognized as an important contributor to the disease.[79,96-98] Inflammation initiated through oxidative stress and blood cell-endothelium interactions during vascular occlusive events is sustained in sickle cell patients, and proliferates SCD symptoms.[78,97,99] Despite their capacity to influence the immune response, the specific way mast cells function in various inflammatory environments has yet to be extensively explored. Given the chronic state of inflammation in SCD and the integral role of mast cells in many aspects of the immune system, it is critical to explore how mast cells contribute to the development and progression of this disease. Furthermore, because mast cells express opioid receptors and morphine is widely used to treat pain in SCD, it is pertinent to fully understand how

morphine effects mast cell function, both in general and in the context of chronic inflammation.

### 2.2.3 Objective

To better understand the nature of inflammation in SCD and the impact of morphine therapy on mast cells, CFMA was used to monitor the degranulation dynamics of mast cells isolated from two transgenic mouse models, one hemizygous (hBERK) and one homozygous (BERK) for human sickle Hb.[85,100] As a control, mast cells from transgenic mice expressing normal human Hb (HbA-BERK) were used.[100] All three mice were subject to treatment with either morphine or phosphate-buffered saline (PBS). Mast cell degranulation was monitored using CFMA offering insight regarding 1) the change in mast cell function in the presence of SCD-associated inflammation, 2) the effect of morphine on control mast cells alone, and 3) how morphine treatment influences mast cell function in the presence of inflammation. Our results indicate that mast cell function is significantly altered in transgenic mice expressing human sickle Hb through a complex mechanism regulating the exocytosis of stored mediators. Furthermore, in addition to its analgesic effects, this work suggests treatment with morphine may have implications for the state of inflammation in SCD. Ultimately, this research highlights the unique capacity of CFMA to address critical questions relating to mast cell biology and fundamental processes of inflammation.

## 2.3 Experimental approach

### 2.3.1 In vivo morphine treatment

All mice were bred in a germ-free AAALAC accredited animal facility at the University of Minnesota as described previously.[85] Each mouse was genotyped and phenotyped for the expression of human sickle hemoglobin. All animal experiments were performed after Institutional approvals. BERK mice used herein are homozygous for knockout of murine α and β globins, and express human sickle hemoglobin (βS globins). These mice express ~99% human sickle hemoglobin.[100] hBERK1 mice are homozygous for knockout of α globin but hemizygous for β globin. These mice express a single transgene for human α and βS hemoglobin. Both BERK and hBERK1 mice are on a mixed genetic background. Therefore, mice on a similar mixed genetic background, HbA-BERK expressing human α and normal human hemoglobin (βA globin) were used as control.

HbA-BERK, hBERK1 and BERK mice were injected subcutaneously with morphine twice daily at doses of 0.75 mg/kg/day the first week, 1.4 mg/kg/day the second week, and 2.14 mg/kg/day the final week. Each dose of morphine was delivered in 50 μL phosphate buffered saline (PBS) (Invitrogen). Following the third week of exposure, mice were euthanized by $CO_2$ asphyxiation for mast cell isolation by peritoneal lavage.

Due to the low-throughput nature of single cell measurements, three week in vivo exposure protocols were staggered to allow CFMA experiments to be conducted on six

days over the course of three weeks. Measurements from PBS-treated HbA-BERK control mast cells were made in parallel on each day to ensure consistency across all CFMA conditions. One day's experiments were thrown out due to average peak area values exceeding 1.5 standard deviations from the comprehensive mean of PBS-treated HbA-BERK controls, over three times larger than the deviations of the other control data sets.

### 2.3.2 Cell culture

Mouse 3t3 fibroblasts were maintained continuously in lab as described previously. [82] Primary mouse peritoneal mast cells were collected using methods previously described. [39,82] In brief, mice were euthanized by $CO_2$ asphyxiation in accordance with IACUC Protocol #0806A37663 (PI Gupta K; Title: "Opioid activity in endothelium in SCD"). The peritoneal cavity of each mouse was then injected with about 8 mL cold DMEM high glucose media supplemented with 10% (v/v) BCS and 1% penicillin/streptomycin. After 20–30 seconds of massage, the media was extracted and stored on ice. The collected media was centrifuged for 5 minutes at 400xg, and the cell pellet was dispersed in fresh media and plated onto confluent mouse 3t3 fibroblasts previously grown to confluence in 35x10 mm Petri dishes. Mast cells were incubated at 37 ˚C for 24 h prior to measurement by CFMA.

### 2.3.3 CFMA measurements

A general overview of the experimental setup for CFMA was included in Chapter 1. For this work, CFMA experiments were carried out specifically as follows. Cell culture media was removed from the co-cultured mast cells, which were then washed and incubated with warm Tris buffer (12.5 mM Tris(hydroxymethyl)aminomethane hydrochloride, 150 mM NaCl, 4.2 mM KCl, 5.6 mM glucose, 1.5 mM $CaCl_2$, 1.4 mM $MgCl_2$, sterile filtered and pH balanced to 7.2–7.4). The Petri dish was then placed in a plate warmer (Warner Instruments LLC) on an inverted microscope (Nikon). As reported, a polished and backfilled microelectrode was mounted onto a headstage connected to an Axon Instruments Axopatch 200B potentiostat (Molecular Devices Inc.) to permit control of the applied voltage. A pulled glass capillary micropipette, fabricated as described in Chapter 1, was loaded with 10 μM A23187 (Sigma Aldrich) and connected to a Picospritzer III (Parker Hannifin) for controlled delivery of the stimulating solution. Both the micropipette and the headstage-mounted microelectrode were mounted on Burleigh PCS-5000 piezoelectric micromanipulators (Olympus America Inc.). After lowering the microelectrode into solution, its potential was set to +700 mV versus a Ag/AgCl reference electrode. Immediately prior to data collection, the electrode was placed in contact with the cell membrane of a single mast cell, and the stimulating pipette was then placed in close proximity. Upon collection of the amperometric trace, a 3-second dose of 10 μM A23187 was delivered, inducing degranulation. Oxidizing currents corresponding to discrete release events were detected as a function of time.

### 2.3.4 Data analysis and statistics

Amperometric traces were collected using Tar Heel software (Courtesy of Dr. Michael Heien) and processed at 200 Hz with a Bessel low-pass filter before peak parameter analysis using Minianalysis software (Synaptosoft, Inc.). Average peak parameter values were obtained for each amperometric trace representing the exocytosis of granules from a single mast cell.[17]

Within each condition, average peak parameter values from individual cells were statistically analyzed for outliers. The log of the average peak parameters was calculated for all amperometric traces of a given condition. These log averages were then averaged again and a standard deviation was calculated. If a log value for a single amperometric trace fell outside two standard deviations of the average of averages for that peak parameter, the trace was discarded as an outlier for all monitored parameters. For example, if the average Q obtained from a single mast cell was found to be an outlier, the peak frequency, $t_{rise}$, and $t_{1/2}$ values corresponding to that same amperometric trace were also discarded. The log-biased statistical treatment was selected to offset the bias toward larger peaks that results from the data fitting process. After statistical analysis, experimental condition averages were calculated for each peak parameter.[101] The significance of differences between these values was determined using the two-tailed student's t-test with 95% confidence used as the threshold for statistical significance.

## 2.4 Results and discussion

CFMA measurements were conducted on peritoneal mast cells isolated from HbA-BERK, hBERK1 and BERK mice following 3 weeks of morphine treatment (PBS was used for control conditions). Measurement from an individual cell produced a current trace consisting of a collection of current peaks each corresponding to an individual degranulation event. The focus of this work was to explore the role of mast cells in SCD and the influence of morphine on mast cell function, both alone and in the context of chronic inflammation as modeled by the hBERK1 and BERK transgenic mice. Single mast cells were stimulated locally with the calcium ionophore A23187, which was selected as a universal mast cell stimulant that would limit bias toward a specific activation pathway.

### 2.4.1 Individual peak parameters monitored

For the purpose of fulfilling these aims, four characteristics of the CFMA traces, plotted as time versus current, were analyzed among the experimental conditions: peak area (Q), peak frequency, peak half-width ($t_{1/2}$), and peak rise-time ($t_{rise}$) (Figure 1.3e). As outlined in the previous chapter, each peak characteristic reports on a different element of the exocytosis process. Analyzing the perturbations in several peak characteristics between experimental conditions provides a unique description of the mechanisms regulating the observed change in mast cell function.

### 2.4.2 Effects of SCD-associated inflammation on mast cell degranulation in the absence of morphine treatment

To establish the impact of SCD-associated inflammation on mast cell function, mast cells isolated from PBS-treated HbA-BERK controls were compared to those from both hBERK1 and BERK mice (Figure 2.1). The hBERK1 and BERK conditions demonstrated 27% and 58% reductions in Q, respectively (Figure 2.2a). Although this effect was significant in only the BERK mouse, the observed decrease trends with increasing sickle Hb expression. In addition, both hBERK1 and BERK mast cells released their granular content less efficiently, resulting in significantly decreased peak frequencies by 34% and 32%, respectively (Figure 2.2b). When considered in concert versus HbA-BERK controls over the course of a 30 second release, these two effects resulted in a modest, though not statistically significant, decrease in overall serotonin release of 37% ($1.97x10^9$ fewer molecules per cell) for hBERK1 mast cells and a greater, significant decrease of 72% ($3.84x10^9$ fewer molecules per cell) in the BERK condition. These data suggest that the chronic inflammation in SCD induces mast cells to release less serotonin per exocytotic event as a result of either decreased granule loading or decreased percent serotonin released per granule, as regulated by a reduction in secretion driving forces. The relative magnitude of this effect appears to be dependent on disease severity. The reduced frequency of individual release events observed in both hBERK1 and BERK mast cells likely result from a decrease in either granule trafficking or fusion efficiency. Granule trafficking effects often occur due to perturbations of the microtubule

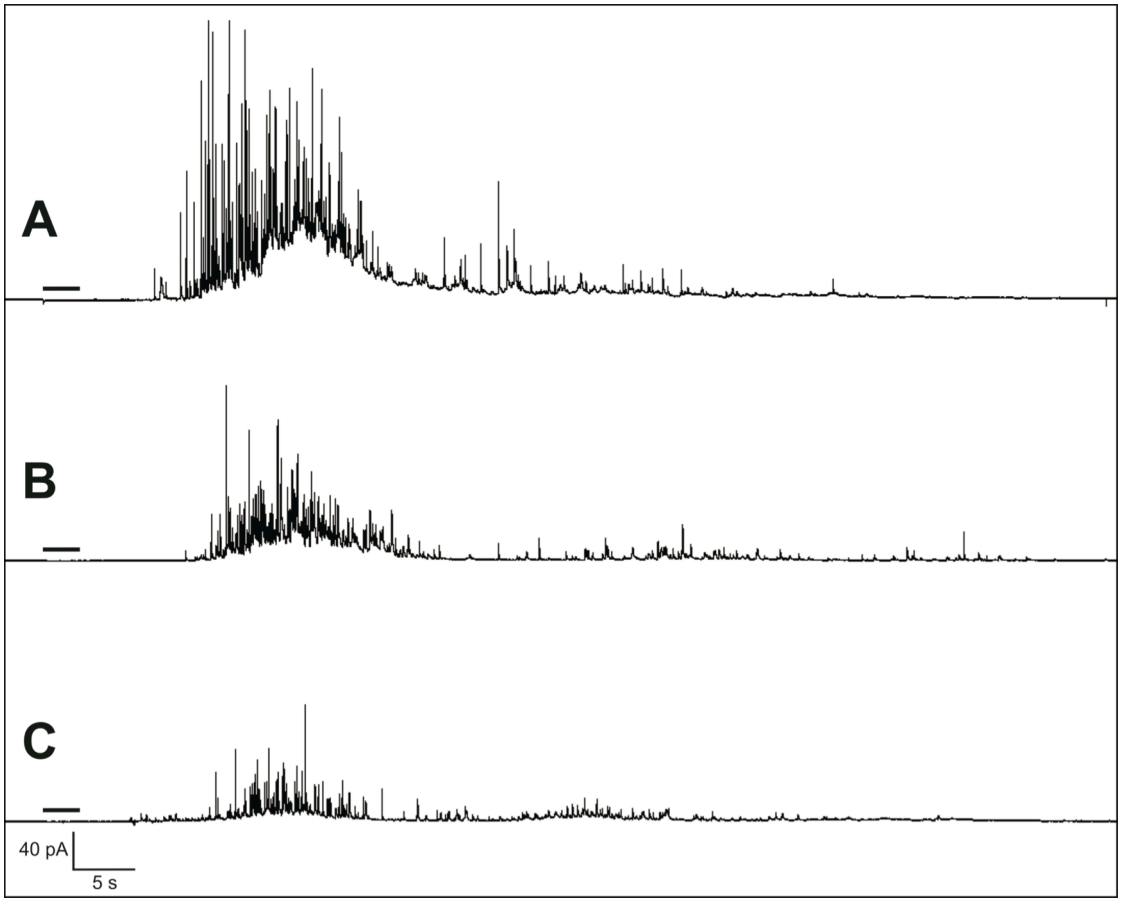


**Figure 2.1 Representative CFMA traces from mast cells isolated from HbA-BERK, hBERK1, and BERK mice**
Representative current traces collected using CFMA to analyze degranulation behavior of mast cells isolated from HbA-BERK (A), hBERK1 (B), and BERK (C) mice in the absence of morphine treatment. Mast cells were stimulated locally with a three second bolus of 10 μM A23187.

transport machinery, whereas fusion efficiency is affected by changes in membrane stability. Unlike the observed changes in Q, changes in peak frequency observed in hBERK1 and BERK mice appear to be independent of disease severity.

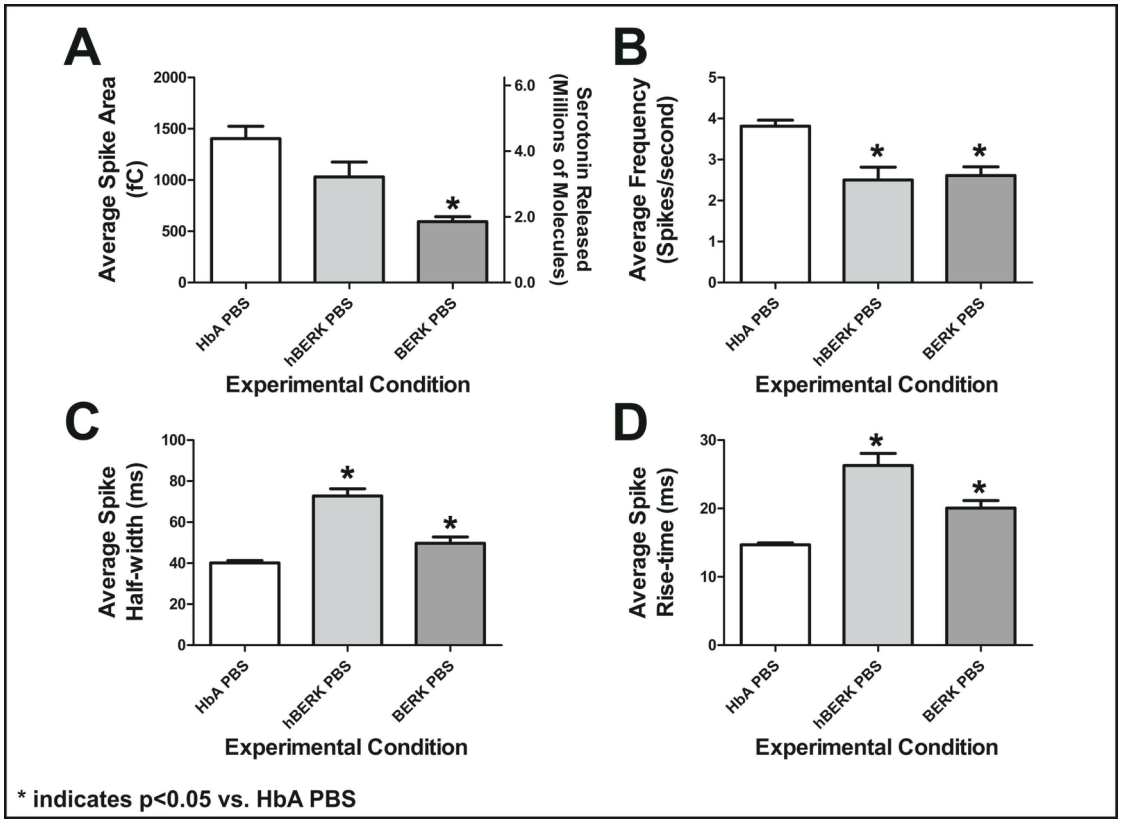


**Figure 2.2 Effects of sickle Hb expression and the corresponding chronic inflammation on mast cell function explored using CFMA**
Mast cells from PBS-treated HbA-BERK (n=77), hBERK1 (n=28), and BERK (n=30) mast cells were analyzed using CFMA. Peak area (A), frequency (B), half-width (C), and rise-time (D) were compared. Statistical significance was determined using the two-tailed Student's t test. Mast cells were stimulated locally with a three second bolus of 10 μM A23187.

Considering the observed sickle Hb-induced decrease in the number of secreted serotonin molecules (as indicated by Q), it is expected that, in the absence of changed release kinetics, $t_{1/2}$ would decrease because it should take less time to release a smaller amount of serotonin. However, mast cells from both hBERK1 and BERK mice demonstrated

significantly larger $t_{1/2}$ values than those from the control mice (Figure 2.2c). Similarly, $t_{rise}$ values increased by 79% and 39%, respectively for hBERK1 and BERK mast cells compared to HbA-BERK controls (Figure 2.2d). This effect is also counter to the expected decrease resulting from the smaller Q values observed for both hBERK1 and BERK mice, with hBERK1 demonstrating the greatest increases in both $t_{1/2}$ and $t_{rise}$, due to the smaller decreases in Q compared to BERK mast cells. It has been shown in other granulated cell types that individual exocytosis events do not release the full mediator content of each granule.[41] Although serotonin loading effects cannot be ruled out entirely, the increase in $t_{1/2}$ and $t_{rise}$ measured herein despite corresponding decreases in Q for both hBERK1 and BERK mast cells suggests a mechanism of decreased serotonin released per granule rather than a decrease in overall granule loading.

Together, the observed decreases in Q and peak frequency, in addition to the somewhat counterintuitive increases in both $t_{1/2}$ and $t_{rise}$ suggest that the chronic inflammation present in both hBERK1 and BERK mice modulates mast cell serotonin secretion through a multifaceted mechanism involving both the serotonin release efficiency as well as membrane driving forces that alter granule fusion. Although the decrease in serotonin released (as indicated by decreased Q values) appears to be controlled in part by both decreased rate of transition from fusion pore to 'full' fusion (as indicated by increased $t_{rise}$ values) and slower biopolymer matrix unfolding (as indicated by decreased $t_{1/2}$ values) rather than decreased serotonin storage, further research will be required to further clarify

the mechanism of this process. Similarly, the frequency effects observed in hBERK1 and BERK mast cells may also result from the same decreased membrane driving forces. The combination of changes in Q, peak frequency, $t_{1/2}$, and $t_{rise}$ observed in mast cells from hBERK1 and BERK mice indicate the serotonin release process in SCD is modulated by multiple compounding mechanisms.

### 2.4.3 Effects of morphine-treatment on mast cell degranulation in the absence of chronic inflammation

To explore the effect of chronic morphine treatment on mast cell function independent of the inflammation associated with SCD, the serotonin release dynamics of mast cells isolated from HbA-BERK mice treated with either morphine or PBS were analyzed. On average, mast cells from morphine-treated mice released 172% more serotonin per granule than those from PBS-treated controls with no significant change in frequency (Figure 2.3A,B). When the effects of Q and peak frequency are combined as a measure of total serotonin released, a 162% increase in overall serotonin released per cell is observed, corresponding to $8.66 \times 10^9$ more serotonin molecules, and is entirely due to increased serotonin released per granule. Interestingly, chronic morphine exposure resulted in a small, significant increase in $t_{1/2}$ (19%), which is expected considering the large observed increase in Q (Figure 2.3C). This expected result reflects the inherent association between $t_{1/2}$ and Q. Other explanations for this $t_{1/2}$ increase require invocation of an unnecessarily complex regulatory mechanism. No morphine-induced increase in $t_{rise}$ was observed for mast cells from HbA-BERK mice (Figure 2.3D).

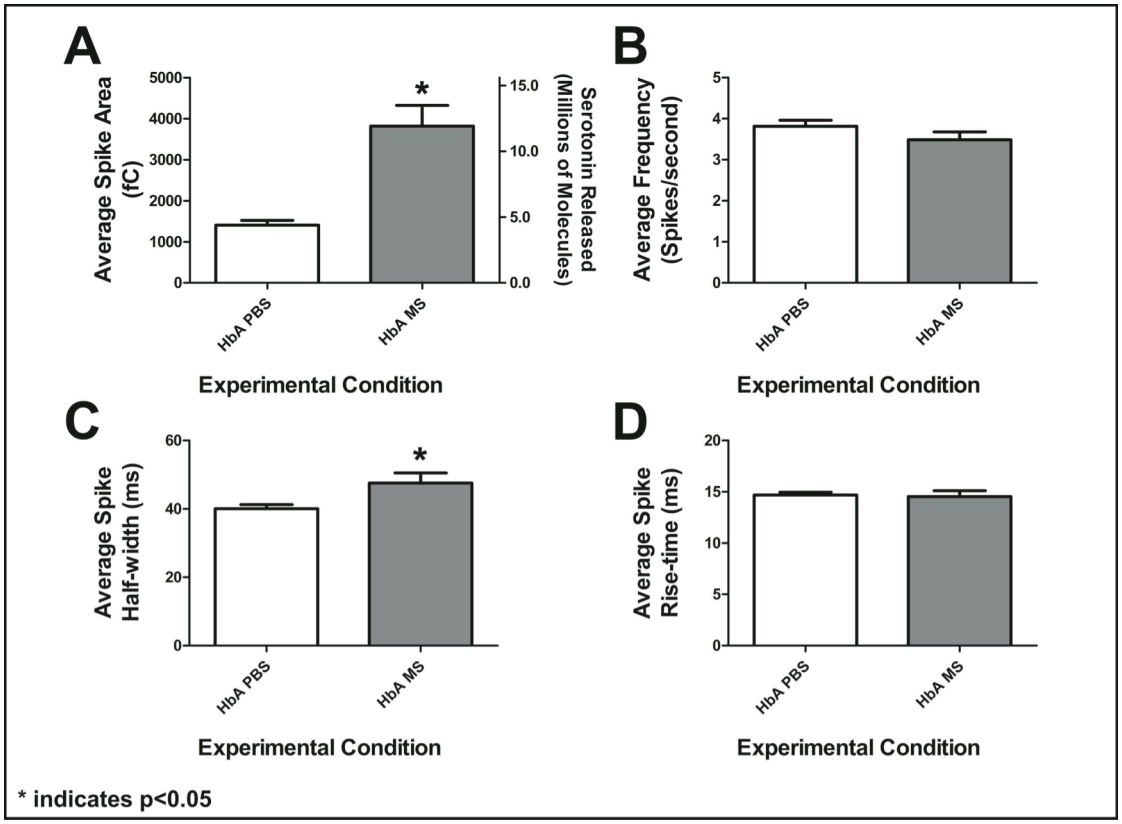


**Figure 2.3 Effect of chronic morphine (MS) treatment on mast cells in the absence of chronic inflammation**
Mast cells from HbA-BERK mice treated with either PBS (n=77) or morphine (n=47) were analyzed by CFMA. Peak area (A), frequency (B), half-width (C), and rise-time (D) were monitored and analyzed for statistical significance using the two-tailed Student's t test. Mast cells were stimulated locally with a three second bolus of 10 µM A23187.

Unlike the complex disease-induced change in mast cell function described above, the observed effect of morphine treatment on mast cells in HbA-BERK mice appears to originate from a simpler mechanism. The large morphine-induced increase in serotonin released per granule is not associated with changes in the monitored peak parameters

other than Q. These data suggest morphine treatment induces mast cells to either store more serotonin per granule or release a greater portion of its granular contents per release event. The lack of unexpected changes in $t_{1/2}$ or $t_{rise}$ suggest that the driving forces of granule fusion are not markedly altered by chronic morphine exposure in mast cells from HbA-BERK mice. Therefore, increased serotonin loading is more likely responsible for the large increase in serotonin released per granule from these mast cells.

### 2.4.4 Effects of morphine treatment on mast cell function in a sickle-induced inflammatory microenvironment

Finally, the effect of chronic morphine treatment on hBERK1- and BERK-derived mast cells was investigated. With respect to the effect on serotonin released per granule, mast cells from BERK mice demonstrated significantly increased Q values sufficient to more than recover the 58% reduction in Q attributed to the expression of sickle Hb (Figure 2.4A). Although statistically insignificant, a smaller recovery trend was also seen in hBERK1-derived mast cells (Figure 2.4A). Interestingly, although in HbA-BERK mice morphine had no effect on release frequency, mast cells from both hBERK1 and BERK mice responded to morphine treatment by reversing the depressed frequencies observed for the PBS conditions in each (Figure 2.4B). In addition, treatment with morphine significantly recovered the sickle Hb-induced increases in $t_{rise}$ in mast cells from both hBERK1 and BERK mice (Figure 2.4D). A similarly significant recovery effect was observed in the $t_{1/2}$ values in the hBERK1 condition (Figure 2.4C), and although a morphine-induced recovery of the $t_{1/2}$ values was not observed for the BERK condition,

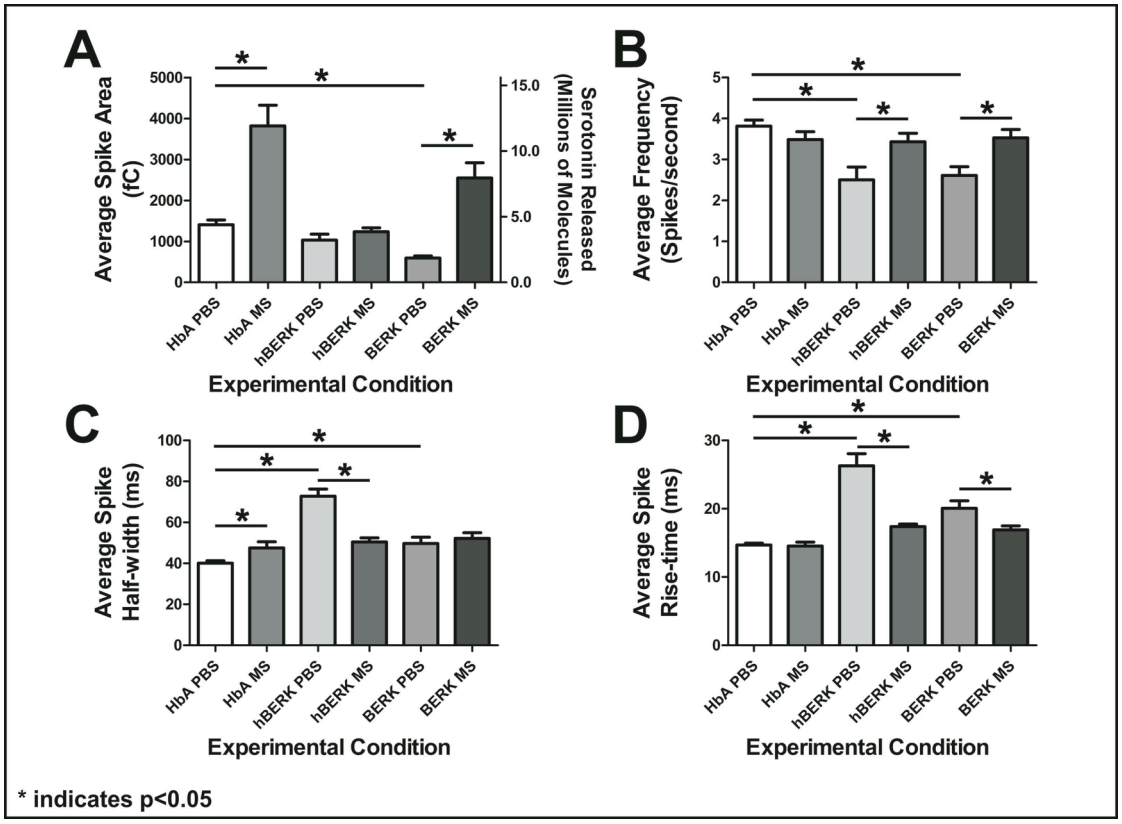


**Figure 2.4 Effect of morphine on mast cell function in SCD mice**
Mast cells from MS-treated HbA-BERK (n=47), hBERK1 (n=52), and HbA-BERK (n=47) mice were compared to PBS-treated controls (n=77 for HbA-BERK, n=28 for hBERK1, n=30 for BERK) and analyzed using CFMA. Peak area (A), frequency (B), half-width (C), and rise-time (D) were monitored and analyzed for statistical significance using the two-tailed Student's t test. Mast cells were stimulated locally with a three second bolus of 10 µM A23187.

this is attributable to the relatively smaller initial sickle Hb-induced effect in these mice (Figure 2.4c).

Given the large morphine-induced increase in Q in mast cells from HbA-BERK control mice, the observed recovery of Q in BERK mice, although important, is perhaps less

surprising compared to the morphine-induced recoveries observed for peak frequency, $t_{rise}$, and $t_{1/2}$ despite the lack of morphine-mediated effects on any of these parameters in the HbA-BERK mice (with the exception of $t_{1/2}$ values in the HbA-BERK mice as mentioned above). For all measured parameters, it is worth noting that the morphine-induced recoveries that were observed did not grossly exceed the corresponding values measured from morphine treated HbA-BERK controls (Figure 2.4). Interestingly, Q was the only measured parameter demonstrating overcompensation behavior in response to treatment with morphine (relative to mast cells from PBS-treated HbA-BERK mice). Nonetheless, Q values in morphine-treated hBERK1 or BERK mice did not exceed those from morphine-treated HbA-BERK mice (Figure 2.4A). It is likely that the increased amount of serotonin released from mast cells from morphine-treated hBERK1 and BERK mice (as demonstrated by an increase in Q) results from a combination of granule loading and increased granule fusion driving forces. Because granule loading was found to be the sole observed mechanism of morphine-mediated regulation of serotonin release in HbA-BERK mast cells, these data indicate that the morphine-induced increase in serotonin loading is independent of inflammation. In contrast, this data suggests the ability of morphine to recover mast cell functionality via regulation of matrix unfolding and membrane driving forces (the mechanisms likely responsible for decreasing the amount of serotonin released from mast cells in hBERK1 and BERK mice) as measured by peak frequency, $t_{rise}$ and $t_{1/2}$, may be limited to levels similar to morphine-treated controls. According to this hypothesis, these findings argue matrix unfolding effects and

membrane driving forces are rate limited under normal conditions, resulting in minimal perturbation of these factors in non-SCD mice upon morphine exposure.

## 2.5 Conclusions

To summarize, this research proposes that chronic inflammation in mice expressing human sickle Hb impairs the secretion of serotonin from mast cells through multiple mechanisms, including fusion pore formation/modulated membrane driving forces and matrix expansion efficiency. Chronic morphine treatment was found to act differently on mast cells from non-sickle cell mice (HbA-BERK) than those expressing human sickle Hb (hBERK1 and BERK). In the absence of SCD-associated inflammation, morphine exposure induced mast cells to increase the amount of serotonin released per granule, a relatively simple mechanism likely resulting from increased serotonin loading. However, morphine treatment induced a more complex change in mast cells isolated from hBERK1 and BERK mice. Whereas only serotonin loading effects were observed in mast cells from HbA-BERK mice, morphine induced marked recovery of all the sickle cell-induced perturbations in mast cell function in both hBERK1 and BERK mice. Morphine was observed to both increase serotonin loading and restore membrane driving forces to levels similar to those of morphine-treated control mice. Given the capacity for mast cells to influence the inflammatory microenvironment and the importance of inflammation in the progression of SCD, these findings offer unique insight into 1) the significantly altered mast cell function in response to sickle-cell induced inflammation, 2) the large morphine-

induced increase in serotonin released per mast cell, and 3) the capacity for morphine to compensate for sickle-cell induced changes in mast cell function.

Any broad-reaching implications of these findings will require significant additional research to characterize both the extent to which mast cells influence the chronic inflammation in SCD as well as the relative importance of morphine in regulating mast cell function when considering available treatment options. Furthermore, in light of tissue-specific mast cell heterogeneity, further work is required to evaluate the universality of these findings. However, it is clear from this study that mast cell function is indeed altered in mice expressing sickle Hb. It is apparent that the use of morphine to treat the pain associated with SCD may also influence the inflammatory state of the disease. Deciphering the root cause of sickle Hb-induced mast cell effects, and determining whether morphine complicates or improves the pathophysiology of SCD, and the extent of either, will be the subject of future collaborative research in this area.

# Chapter 3

## Single cell analysis of mast cells isolated from knockout mice reveals evidence of kappa opioid receptor involvement in the regulation of mast cell degranulation

Gupta, K., Pintar, J. E., and Haynes, C. L. contributed to this work

### 3.1 Overview

The CFMA analysis of mast cell function outlined in Chapter 2 revealed the interesting relationship between in vivo morphine treatment and mast cell functions in chronic inflammation. The research herein delves deeper into the role of opioids and their corresponding receptor system in the regulation of mast cell secretory function. Interactions between immune cells and the peripheral nervous system are critical to many inflammatory diseases. Opioids are widely used for their analgesic properties; however, the extent to which these drugs influence the inflammatory response is less understood. The purpose of this research is to examine the mechanism of the morphine-induced increase in stimulated mast cell degranulation described in Chapter 2 and to characterize the contributions of individual opioid receptors toward the regulation of mast cell function. Specifically, mast cells were isolated from both wild type mice and three knockout variants which each lack one of the three canonical opioid receptors (μ, κ, or δ), as well as a fourth variant lacking all three opioid receptors. Stimulated mast cell degranulation was monitored using CFMA as described in previous chapters. Importantly, the large increase in stimulated mast cell degranulation following in vivo morphine treatment (outlined in Chapter 2) was not reproduced following in vitro treatment, providing strong evidence that this effect was likely a result of downstream microenvironmental effects rather than direct activity of morphine on mast cells. Despite the lack of in vitro morphine-induced alterations in mast cell function, it was discovered that stimulated mast cell degranulation was increased in the kappa knockout variant

relative to wild type controls. CFMA data analysis revealed this effect was a product of both increased granular loading and increased efficiency of granule trafficking and/or fusion. Although an in-depth study of the role of the kappa opioid receptor in the regulation of mast cell degranulation will require further research efforts, these findings provide persuasive evidence that the endogenous opioid receptor system is capable of a constitutive role in regulated mast cell secretory function.

### 3.2 Introduction

Mast cell regulation of allergy is well characterized. [49,102] In addition to the capacity to orchestrate the immune response in an immunoglobulin E (IgE)-mediated manner, mast cells posses a broad capacity to respond to many physiological signals, including several cytokines, bioactive lipids, complement components, and neuropeptides, among others. [59,60,103] One area of particular interest is the role these cells play in neurogenic inflammation and analgesia. The work summarized in Chapter 2 demonstrated and characterized a large morphine-induced increase in murine peritoneal mast cell degranulation. [104] In brief, peritoneal mast cells isolated from mice treated with morphine in vivo demonstrated a much larger degranulation response to a calcium ionophore stimulus relative to untreated controls. Using CFMA enabled a detailed characterization of the altered mast cell function and revealed the increased degranulation was regulated by an increase in the amount of granular contents released per exocytotic event, which was attributed to an increased granule cargo load. To further investigate morphine-induced changes and the potential role of opioid receptors on mast cell degranulation,

CFMA was employed herein to study mast cells isolated from opioid receptor knockout mice at the single cell level.

As described previously in this dissertation, mast cells are bone marrow-derived leukocytes found in most connective tissues, often serving as intermediaries between the innate and adaptive immune systems. [67,105] Our interest in understanding how mast cell function is influenced by the opioid receptor system is rooted in the close association between mast cells and nerve-junctions in tissue as well as the relationship between mast cell-secreted species and neuropathic pain.[106,107] Furthermore, in addition to activation via neuropeptide signaling, mast cells are known to express endogenous opioid peptides.[108,109] Understanding the contributions of the opioid receptor system toward the regulation of mast cell signaling will provide a more complete understanding of the complex relationship between mast cells, inflammation, and the peripheral nervous system.

### 3.2.1 Opioid signaling and the immune system

Opioids such as morphine have long been used therapeutically for their analgesic properties. The canonical mu (μ), delta (δ), and kappa (κ) opioid receptors were first characterized in detail in the late 1980s, and each individual receptor was cloned by several research groups just a few years later. [110,111] Subsequent research efforts have established their primary role in opioid-induced physiological responses, including both analgesic and euphoric effects, largely through inhibition of neuronal activity in both the

peripheral and central nervous systems. [111] Nonetheless, each opioid receptor exhibits distinct, if subtle, differences in their individual signaling. [110,111] Complicating matters further, the μ, δ, and κ opioid receptors are all capable of forming heterodimers, each with a distinct functionality. [111-114] In addition to the discovery of the opioid receptor system, opioid peptides, including the enkephalins, endorphins, and dynorphins, were established as the physiological ligands responsible for endogenous opioid signaling.

Despite the inherent complexity of opioid receptor signaling, the body of research focused on their role in both the central and peripheral nervous systems is well developed. The functions of opioid receptors outside of the nervous system are less understood. In particular, while both endogenous opioid peptides and opioid receptors are expressed on many cells of the immune system, [108,109,115-117] the relationship between the peripheral nervous and immune systems is bidirectional and complex.[118-121] Mast cells, in particular, are associated with both inflammatory and neurogenic pain, as they are found in close proximity to nociceptive nerves and are activated by neuron-secreted species such as substance P and calcitonin gene-related peptide. Upon activation, mast cells also release several mediators including histamine, TNF-α, and nerve growth factor (NGF), as well as endogenous opioids that can act reciprocally on the peripheral nervous system. [106,107] The relationship between mast cells and opioid receptor signaling carries important implications regarding the widespread use of opioids in the treatment of inflammatory pain.

### 3.2.2 CFMA for the study of opioid signaling in mast cells

The entirety of this dissertation focuses on the use of CFMA explicitly because it offers several distinct advantages in the characterization of mast cell degranulation under different physiological scenarios. As described in Chapter 1, beyond the inherent advantage of working at the single-cell level (where cellular heterogeneity is obvious), CFMA leverages the electroactive character of serotonin in combination with the low noise, high sensitivity, and high resolution of the technique to provide direct observation of discrete degranulation events (current spikes) corresponding to the exocytosis of individual cytoplasmic granules. [82,122] Electrochemical detection of serotonin provides a detailed biophysical characterization of mast cell secretion dynamics with minimal interference from the complex biological matrix. Perhaps most importantly, electrochemical detection of serotonin is a label-free technique that allows minimal manipulation of isolated mast cells prior to analysis by CFMA.

### 3.2.3 Objective

The purpose of the research herein is to examine the role of morphine and the endogenous opioid system on mast cell degranulation in detail. Specifically, this work seeks to 1) further explore and characterize the previously reported increase in stimulated mast cell degranulation following in vivo morphine treatment, 2) identify the contributions of specific opioid receptors toward the regulation of mast cell degranulation capacity, and 3) take advantage of the information-rich CFMA data to provide a detailed profile of the fundamental cellular mechanisms that characterize the observed changes in

mast cell secretory function. To achieve these objectives, three different knockout mice, each lacking one of the three opioid receptors, as well as a triple knockout variant, were used in this research. CFMA was used to monitor the degranulation response of individual peritoneal mast cells cultured in vitro from each knockout variant, with or without in vitro morphine treatment.

## 3.3 Experimental approach

### 3.3.1 Opioid receptor knockout mice

Wild type 129S mice and four knockout mice of the same genetic background were used in this research, one for each of three opioid receptors (μ, κ, and δ) as well as a triple knockout variant. All mice were bred at the University of Minnesota in an AAALAC accredited and germ-free facility.

### 3.3.2 Mouse peritoneal mast cell isolation, co-culture, and morphine treatment

In general, mast cells were obtained as outlined in Chapter 2. Briefly, mice were euthanized by $CO_2$ asphyxiation in accordance with an IACUC-approved protocol. Roughly 8 mL of cold cell culture medium (DMEM supplemented with 10% BCS and 1% penicillin/streptomycin) was injected into the peritoneal cavity. Lavage fluid was extracted and stored on ice for transport. The collected cells were then centrifuged for 7 minutes at 400 x g and the resulting cell pellet was dispersed in fresh media. Suspended peritoneal cells were plated onto 35 x 10 mm Petri dishes containing a confluent layer of mouse 3t3 fibroblasts. Morphine-treated conditions were incubated overnight in 1 μM

morphine sulfate while untreated cells received an equal volume of the equivalent vehicle. The co-cultured cells were incubated overnight at 37 ˚C and 5% $CO_2$ prior to CFMA experiments.

### 3.3.3 Carbon-fiber microelectrode amperometry measurements

CFMA measurements were conducted following a similar procedure as described in previous chapters. In short, immediately prior to CFMA measurements, cultured peritoneal mast cells were removed from incubation, the cell culture media was removed, and the cells were washed three times with warm Tris buffer. After the third wash, fresh Tris buffer was added to replace the cell culture media, and the Petri dish was kept at 37 ˚C on a plate warmer mounted on a Nikon inverted microscope. Both a carbon-fiber microelectrode and a glass micropipette (the microelectrode backfilled with an electrolyte solution and mounted on a potentiostat headstage and the micropipette loaded with 10 μM of calcium ionophore A23187 in Tris) were mounted on Burleigh micromanipulators to enable precise placement on each cell. The potential applied to the electrode was controlled by an Axopatch 200B potentiostat (Axon Instruments), and the A23187 stimulating solution was delivered using a Picospritzer III (make). A silver-sliver chloride (Ag/AgCl) electrode (BAS) was used as a reference electrode.

### 3.3.4 Data processing, analysis, and statistical treatment

Data collected from CFMA experiments were exported from the TarHeel CV software package as separate amperometric traces for analysis using MiniAnalysis software. For

each experiment, individual peak analysis for the collected amperometric traces was completed and per-cell averages of the four primary peak parameters (peak area, peak number, peak half-width, and peak rise-time) were obtained as described in previous chapters. Average values of each parameter were pooled according to experimental condition and averaged. Outliers were defined as any trace for which the log of a peak parameter fell outside of two standard deviations of the log mean. If a particular CFMA trace exceeded this outlier criterion for one peak parameter, it was discarded from all data sets.

Due to the technical challenge of single-cell CFMA measurements and the short-lived nature of primary mast cell culture, the number of conditions run per experiment is low. To overcome this limitation, four separate experiments were run in series, one for each of the μ, δ, κ, and triple knockout mice, in which mast cells isolated from both knockout and wild-type mice were collected, and treated with either 1 μM morphine or a vehicle control in vitro. CFMA data from the four WT control conditions, one from each experiment, were then statistically compared using a two-tailed Student's t test with a confidence interval of 95% ($p=0.05$). Once the wild type controls from each experiment were determined to be statistically indistinguishable, the data from all four experiments were combined. Statistical significance between experimental conditions in the combined data set was determined using a one-way ANOVA test, with statistical significance once again determined at the 95% confidence interval.

### 3.4 Results and discussion

The research summarized in Chapter 2 characterized the effects of chronic morphine exposure on mast cell degranulation.[104] In vivo morphine treatment resulted in a large increase in the amount of serotonin released per mast cell as detected by CFMA analysis. It was determined that the observed increase in secreted serotonin was strictly due to increased cargo released per cytoplasmic granule, with no observed changes in the overall frequency or number of granules released. To assess both the influence of morphine-treatment and the possible involvement of opioid receptors in the regulation of mast cell degranulation, CFMA was employed to monitor mast cells isolated from opioid receptor knockout mice with and without in vitro morphine treatment. All mast cells were cultured under identical conditions and stimulated locally with A23187. The resulting current traces were collected and analyzed for individual peak characteristics.[17,123]

#### 3.4.1 Information gained from CFMA analysis

The value of CFMA as an analytical tool is derived from the high degree of detail obtained through an in-depth analysis of each high time resolution amperometric trace. Interpretation of CFMA traces is covered extensively in earlier chapters of this dissertation. In brief, for this research, analysis of CFMA data again focused on the four primary peak parameters (peak area, peak number, peak half-width, and peak rise-time). Peak area relates directly to the number of serotonin molecules released from each granule. Peak number is simply the total number of release events measured from a particular mast cell, and when combined with the average peak area, provides a measure

of the total amount of serotonin released per mast cell. Altered peak area can result from granule loading effects due to changes in the mechanisms of biosynthesis or uptake, as well differences in the fraction of total granular contents released upon granule fusion with the cellular membrane. Peak number generally reflects the efficiency of the granular trafficking and/or docking mechanisms of exocytosis.

While peak area and peak number together offer a fairly concrete description of mast cell degranulation, peak half-width and peak rise-time are each measures of kinetic properties and are therefore less intuitively associated with mechanisms of exocytosis. However, these properties relate to the peak shape and are useful to probe whether the membrane or intragranular matrix driving forces that govern the fusion of the granular and cell membranes are altered. In general, peak half-width is considered a measure of the rate of intragranular matrix expansion, while peak rise-time indicates the degree of 'free-serotonin' not tightly associated with the sulfated proteoglycan matrix that is free to diffuse rapidly to the electrode surface upon fusion pore formation. Of course, these parameters, peak half-width in particular, are not fully independent of peak size, and significant changes in these parameters are always considered in the context of observed changes in measured peak area. In this chapter, a complete analysis of CFMA data was used to characterize effects of opioid receptor system on regulated signaling in mast cells.

As outlined above, the specific aims of this research were to further characterize the previously reported effects of morphine treatment on stimulated mast cell degranulation, to examine the involvement of individual opioid receptors, and to leverage the advantages of single-cell CFMA experimental approach to gain fundamental insight into observed changes in mast cell secretory function. To achieve these aims, mast cells isolated from wild type, μ, δ, κ, and triple knockout mice were monitored using CFMA following in vitro morphine exposure and compared to untreated controls.

### 3.4.2 In vitro morphine exposure does not induce large increases in stimulated mast cell degranulation

With respect to the effect of morphine on mast cell degranulation, in vitro exposure did not produce the large increase in stimulated mast cell degranulation that was previously reported following in vivo treatment (see section 2.4.3). Mast cells isolated from each genetic variant (wild type and all four knockout strains) did not display significant alteration in total serotonin released per cell following morphine treatment. (Figure 3.1) The absence of morphine-induced changes in the total amount of serotonin released per cell was corroborated by a similar absence in morphine effects in each of the other monitored parameters. Interestingly, morphine-treated mast cells isolated from δ opioid receptor knockout mice also demonstrated an increased number of release events per cell (a 44% increase relative

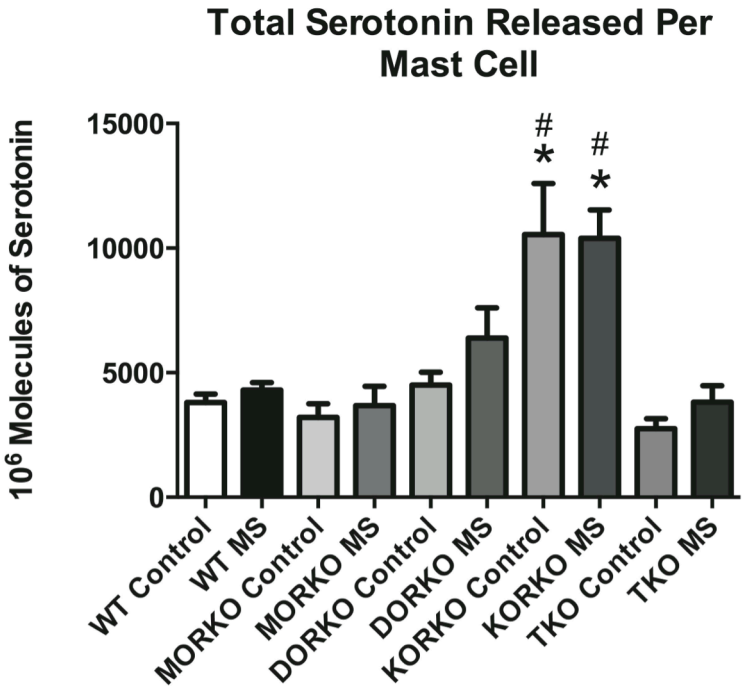


**Figure 3.1 Total serotonin released per mast cell**
CFMA was used to monitor stimulated degranulation from single mast cells isolated from μ (MORKO), δ (DORKO), and κ (KORKO) knockout mice, as well as a triple knockout variant (TKO) relative to wild type (WT) controls. Isolated mast cells were treated overnight with either 1 μM morphine in vitro or an equivalent vehicle control and stimulated locally with a three second bolus of 10 μM A23187. Total serotonin released was calculated using the average peak area (converted to molecules of serotonin) and the number of release events per cell. Statistical significance was determined using a one-way ANOVA at a confidence interval of 95%. * and # indicate $p < 0.05$ versus WT control and WT MS, respectively.

to untreated wild-type controls); however, this effect was not significantly different from either the untreated mast cells from the δ knockout mice nor the morphine-treated mast cells isolated from the wild-type mouse (Figure 3.3). This lack of morphine-induced changes in mast cell degranulation argues strongly that the morphine-induced increase in

stimulated mast cell degranulation following in vivo exposure likely results from an altered inflammatory microenvironment rather than direct activity on mast cells. Our data does not, however, rule out morphine effects on mast cell degranulation in response to other stimuli such as the neuropeptide substance P or direct effects of morphine on mast cell secretory function. Further investigation of these processes will be the focus of additional research efforts.

### 3.4.3 Evidence for κ opioid receptor participation in regulated mast cell degranulation

Having established the morphine-induced alteration of stimulated mast cell degranulation is not due to direct morphine activity, a thorough examination of the endogenous opioid receptor system and the contributions of each opioid receptor to the regulation of mast cell degranulation was explored. Interestingly, a large increase in total serotonin released via stimulated mast cell degranulation was observed in mice lacking the κ opioid receptor (a 177% increase relative to wild-type controls), whereas no significant difference in total secreted serotonin was measured in either of the μ or δ opioid receptor knockout mice relative to the wild-type control (Figure 3.1). Importantly, this effect is not seen in mast cells from the triple knockout mouse, indicating the relationship between κ opioid receptor expression and regulation of mast cell degranulation capacity is complex and suggests a possible role of allosteric interactions between different opioid receptor subtypes.

### 3.4.4 CFMA analysis reveals κ opioid receptor knockout increases both amount of serotonin released per granule and number of release events per cell

A detailed analysis of the CFMA data was then conducted to examine the underlying biophysical mechanism behind the increase in stimulated mast cell degranulation observed in the κ knockout mouse. As described above, average peak area and peak number values offer further insight into the regulation of observed changes in total serotonin released per mast cell. Analysis of average peak area (amount of serotonin released per granule) was significantly elevated in mast cells isolated from κ opioid receptor knockout mice (an increase of 77% relative to wild-type controls), consistent with the observed increase in total serotonin released (Figure 3.2). Similarly consistent with the measured trends in total serotonin data were the absence of significant peak area effects measured in stimulated mast cells from either the μ or δ opioid receptor knockout mice. Consistent with total serotonin data, no significant change in peak area was measured in the triple knockout condition relative to wild type cells.

Further analysis reveals the increased amount of serotonin released per granule was amplified by a corresponding increase in peak number in κ opioid receptor knockout mast cells (increase of 59% relative to WT controls), indicating an increased efficiency of the granule trafficking, docking, and membrane fusion processes (Figure 3.3). Mast cells isolated from μ and triple opioid receptor knockout mice, as well as the untreated mast cells from the δ knockout mice, did not display changes in peak number relative to the

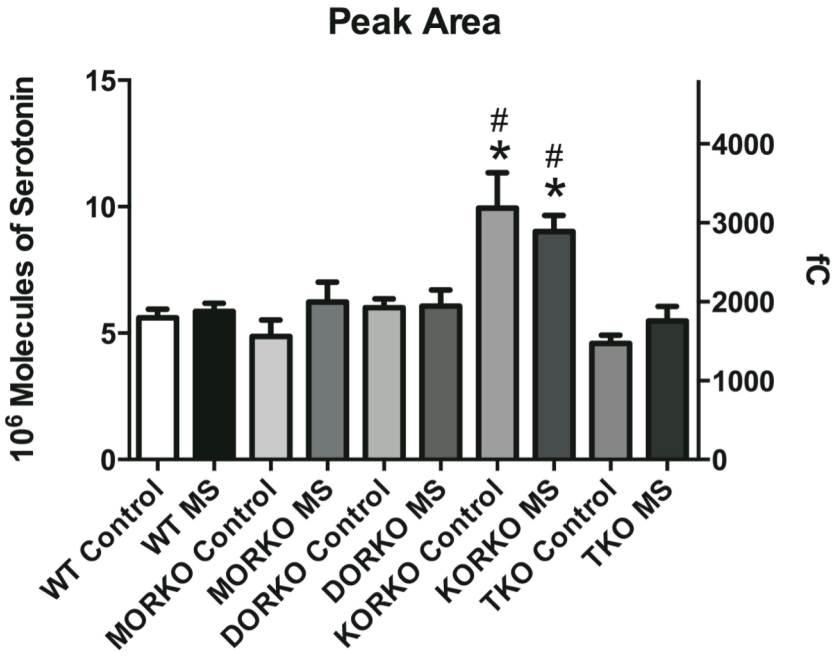


**Figure 3.2 CFMA analysis of serotonin released per granule**
CFMA was used to monitor stimulated degranulation from single mast cells isolated from μ (MORKO), δ (DORKO), and κ (KORKO) knockout mice, as well as a triple knockout variant (TKO) relative to wild type (WT) controls. Isolated mast cells were treated with either 1 μM morphine in vitro or an equivalent vehicle control and stimulated locally with a three second bolus of 10 μM A23187. Average serotonin released per granule was calculated from the average peak area (in fC) using Faraday's law. Mast cells from KORKO mice demonstrated a large increase in serotonin released per granule relative to WT controls, contributing to the observed increase in total serotonin released per cell. Statistical significance was determined using a one-way ANOVA at a confidence interval of 95%. * and # indicate $p < 0.05$ versus WT control and WT MS, respectively.

wild-type controls (morphine-treated mast cells from δ knockout mice were significantly increased relative to untreated wild-type cells, as discussed above, however this effect was not significantly increased relative to either the morphine-treated wild-type or the untreated δ knockout conditions).

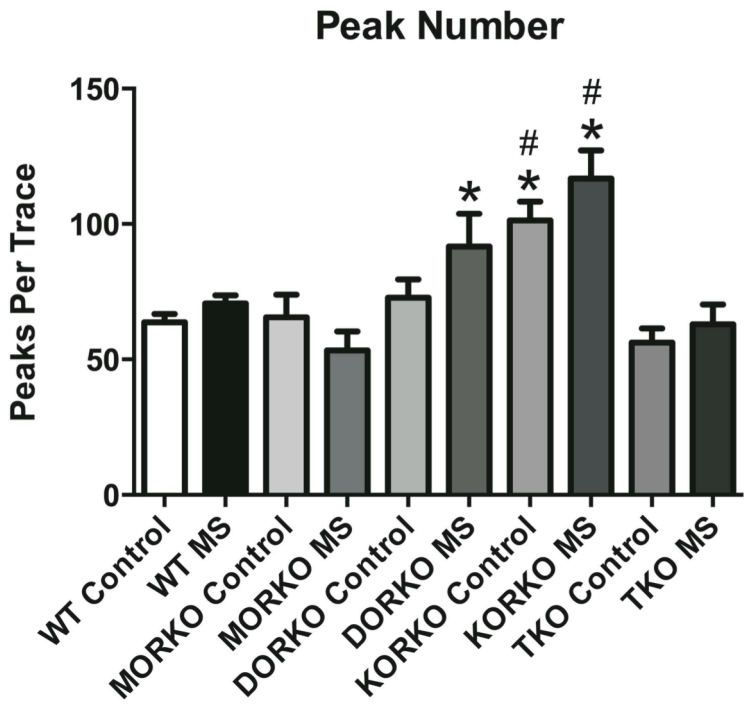


**Figure 3.3 Number of release events per cell**
CFMA was used to monitor stimulated degranulation from single mast cells isolated from μ (MORKO), δ (DORKO), and κ (KORKO) knockout mice, as well as a triple knockout variant (TKO) relative to wild type (WT) controls. Isolated mast cells were treated with either 1 μM morphine in vitro or an equivalent vehicle control and stimulated locally with a three second bolus of 10 μM A23187. Peak number was increased in mast cells isolated from KORKO mice relative to WT controls, contributing to the overall increase in serotonin released per cell. Statistical significance was determined using a one-way ANOVA at a confidence interval of 95%. * and # indicate $p < 0.05$ versus WT control and WT MS, respectively.

With the observed increase in stimulated serotonin release from mast cells isolated from κ opioid receptor knockout mice attributed to corresponding increases in both peak area and peak number, secretion kinetics data were then compared. Analysis of peak half-width and peak rise-time, particularly in the context of concurrent trends in peak area, can

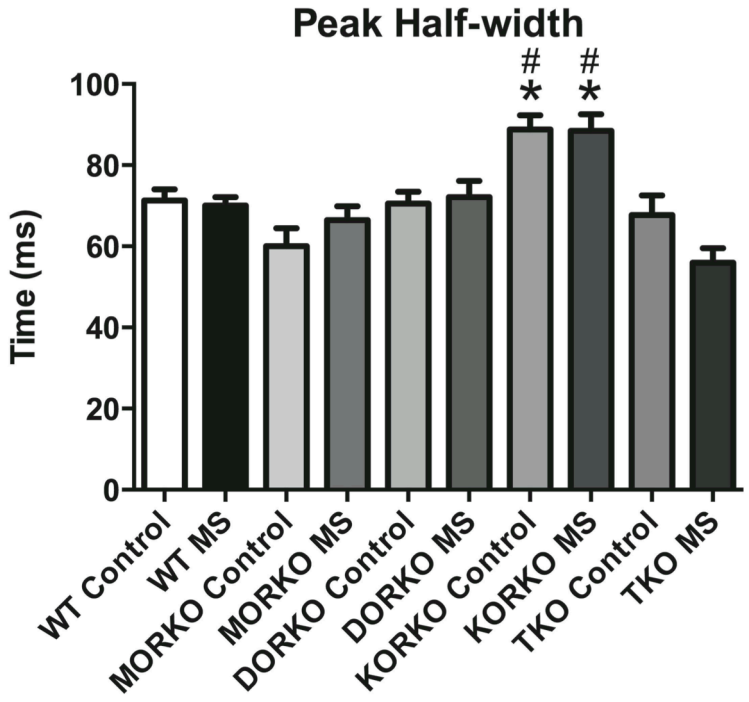


**Figure 3.4 Average peak half-width**
CFMA was used to monitor stimulated degranulation from single mast cells isolated from μ (MORKO), δ (DORKO), and κ (KORKO) knockout mice, as well as a triple knockout variant (TKO) relative to wild type (WT) controls. Isolated mast cells were treated with either 1 μM morphine in vitro or an equivalent vehicle control and stimulated locally with a three second bolus of 10 μM A23187. Calculated peak half-width was increased in mast cells isolated from KORKO mice, consistent with the corresponding increase in peak area. Statistical significance was determined using a one-way ANOVA at a confidence interval of 95%. * and # indicate $p < 0.05$ versus WT control and WT MS, respectively.

provide additional insight into how mast cells from these knockout mice regulate the stimulated release of granular contents. For example, in previously reported work, mast cells from transgenic mice expressing human sickle hemoglobin (and therefore inducing a state of chronic systemic inflammation) demonstrated a decrease in total serotonin

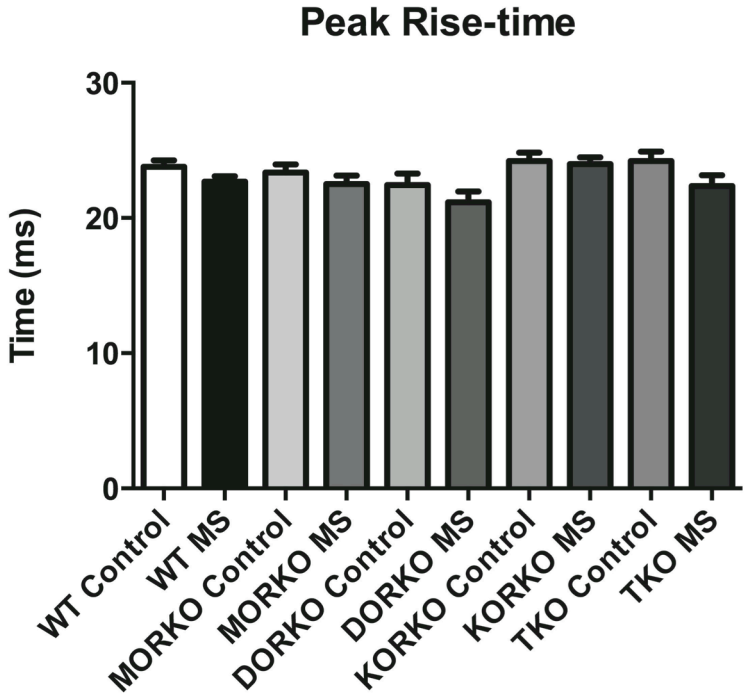


**Figure 3.5 Average peak rise-time**
CFMA was used to monitor stimulated degranulation from single mast cells isolated from μ (MORKO), δ (DORKO), and κ (KORKO) knockout mice, as well as a triple knockout variant (TKO) relative to wild type (WT) controls. Isolated mast cells were treated with either 1 μM morphine in vitro or an equivalent vehicle control and stimulated locally with a three second bolus of 10 μM A23187. Calculated peak rise-time was unchanged across all monitored conditions, suggesting membrane and intragranular matrix driving forces are not involved in the increased serotonin released per granule in the KORKO mice. Statistical significance was determined using a one-way ANOVA at a confidence interval of 95%. * and # indicate $p < 0.05$ versus WT control and WT MS, respectively.

released per cell (see section 2.4.2). CFMA analysis of this revealed a decrease in peak area that was accompanied by increases in both peak half-width and rise-time.[104] This negative correlation between the size of the average release event and the peak half-width

and rise-time indicated membrane driving forces and the intragranular matrix were altered independently from the peak size, and likely participated in the regulation mechanisms resulting in decreased serotonin released per granule.[104] In the present study, in contrast, the observed increase in peak area in the κ opioid receptor knockout was associated with a 25% increase in measured peak half-width (Figure 3.4). No significant peak half-width effects were observed in mast cells isolated from the μ, δ, or triple knockout mice relative to wild type controls. The increased peak half-width in the κ knockout condition, in context of the larger amount of serotonin released per granule, argues against the presence of altered membrane and intragranular matrix driving forces. Peak rise-time data also support this conclusion, as no significant variations in peak rise-time were observed across any of the experimental conditions (Figure 3.5). Together, the small increase in half-width and absence of rise-time effects suggest increased granule loading is likely the driver of increased serotonin released per granule.

### 3.5 Conclusion

In summary, single cell analysis using CFMA has revealed that stimulated mast cells isolated from κ opioid receptor knockout mice release significantly more serotonin per cell relative to wild-type controls, while mast cells from μ, δ, and triple knockout mice did not demonstrate this change in degranulation. Individual peak analysis of the CFMA data shows very clearly that the increased degranulation intensity in the κ knockout mice is a function of both increased serotonin released per granule and increased number of release events per mast cell, indicating that both granule loading as well as granule

trafficking and docking processes are altered in mast cells from these mice. In vitro morphine treatment did not result in any significantly altered mast cell degranulation in any of the mouse strains studied, providing strong evidence that previously reported in vivo morphine exposure-induced changes in mast cell degranulation is likely due to downstream effects of an altered inflammatory microenvironment, rather than direct activity through opioid receptors expressed on mast cells. This work highlights a previously unexplored relationship between the endogenous opioid system and mast cell degranulation, and emphasizes the need for a greater understanding of the impact of opioid signaling in the immune system. A detailed investigation of κ opioid receptor participation in mast cell function, as well as that of both heterodimeric receptor complexes and allosteric interactions, will be the focus of further research efforts.

# Chapter 4

## Single-cell analysis of mast cell degranulation induced by airway smooth muscle-secreted chemokines

Meyer, A. F., Gruba, S. M., and Haynes, C. L. contributed to this work

## 4.1 Overview

In a transition away from opioid signaling, the work in this chapter focuses on the use of CFMA to explore mast cell degranulation as it relates to the specific interaction between mast cells and structural smooth muscle cells of the airways in asthmatic inflammation. Asthma is a chronic inflammatory disease characterized by narrowed airways, bronchial hyper-responsiveness, mucus hyper-secretion, and irreversible airway remodeling.[124-126] Due to the complexity of the inflammatory response, our fundamental understanding of the underlying pathology of asthma is incomplete. It has been shown that mast cell infiltration into the airway smooth muscle is a defining feature of asthma, and the interplay between these two cell types has become the focus of much research.[127-132] Although commonly recognized as orchestrators of allergic response, mast cells participate in many non-allergic processes within the immune system. Notably, mast cells release a variety of pro-inflammatory molecules capable of promoting the $T_H2$-type immune response typical of asthma. Furthermore, it is now understood that ASM also regulates the inflammatory response.[129,133] Specifically, airway smooth muscle cells secrete several chemokines, including CXCL10 and RANTES, which recruit immune cells and alter the inflammatory microenvironment.[133-135] The research presented in this chapter demonstrates the utility of CFMA to study the effects of airway smooth muscle-secreted chemokines on mast cell degranulation in real-time and at the single-cell level. We've shown the capacity of both CXCL10 and RANTES to directly induce mast cell degranulation and leveraged the information-rich CFMA data to characterize the

biophysical mechanisms that underlie pathway-dependent regulation of mast cell degranulation.

## 4.2 Introduction

Affecting 22 million people in the United States alone, asthma is a common chronic respiratory disease.[124] However, relatively little is known about the mechanisms by which it develops and progresses. Additionally, although the use of inhaled glucocorticoid steroids is effective for many patients, a significant percentage don't respond to these drugs.[124-126] Understanding the pathophysiology of asthma is essential for the development of novel therapies and treatments.

### 4.2.1 Asthma and inflammation

Traditionally, eosinophils have been considered the central orchestrators of asthmatic inflammation. However, recent advances have called this paradigm into question.[125-128] Most notably, a cohort of asthmatic patients exhibits airway inflammation that lacks eosinophil infiltration. A thorough comparison between asthma and eosinophillic bronchitis, a common and reversible inflammatory disease of the airway, suggests that mast cells rather than eosinophils are critical to asthma development. Specifically, mast cell localization to the airway smooth muscle (ASM) is of particular importance. [128,129] As a result, interactions between ASM and mast cells in asthma have become a major focus of research, seeking to better characterize the cellular mechanisms of asthma and to develop improved treatment options for patients with steroid-resistant disease.

### 4.2.2 Mast cells and inflammation

Mast cells and their capacity to influence the immune response has been covered extensively in previous chapters of this dissertation. In short, mature mast cells are identified by the expression of c-kit and the high affinity IgE receptor FcεRI, as well as the large number of dense-body granules that occupy the mast cell cytoplasm. The dense body granules contain many immunoactive mediators, including TNF-α, histamine, serotonin, tryptase, and a sulfated proteoglycan matrix, which are released upon stimulation via exocytosis. In addition to the release of preformed immunoactive molecules, mast cells also secrete many cytokines, chemokines and growth factors, as well as prostaglandins and leukotrienes that are synthesized de novo upon activation.[58,60,105]

Although their role in allergy has been well studied, mast cell participation in non-allergic inflammatory diseases is less clearly defined[58,59,102]. In addition to IgE-mediated activation, mast cells selectively secrete several mediators in response to many other stimuli, including bacterial lipopolysaccharaide, the neuropeptides substance P and calcitonin gene-related protein, C3a and C5a of the complement cascade, as well as many other signaling molecules.[58,60,105,128] In asthma, mast cells are thought to play an important role in displayed symptoms due to their elevated density and activated phenotype in the asthmatic lung.[130] Additionally, they release proinflammatory factors that can induce the Th2-type of inflammation observed in asthma.[127,131,132] Furthermore,

many cases of asthma are atopic and present with elevated levels of serum IgE, arguing for the importance of mast cell degranulation in these patients.[128] While there are many proposed roles for mast cell regulation of asthmatic inflammation, the mechanisms of action are not clear, and early attempts to use mast cell-specific therapeutic interventions have been largely ineffective.

### 4.2.3 Airway smooth muscle and mast cells in asthma

It has long been recognized that ASM hyperresponsiveness and increased ASM mass are critical characteristics of asthma pathology.[130,133,134] However, only recently have these structural cells been understood to play an active role in the inflammatory response that drives the disease. In particular, studies comparing the inflammation associated with asthma to that of eosinophillic bronchitis, as mentioned above, have highlighted the importance of ASM-mast cell interactions in the development of this disease.

Microlocalization of mast cells into the ASM bundles is likely regulated through chemokines secreted by ASM cells in the asthmatic lung. Specifically, CXCL10 and RANTES have been implicated in the recruitment of mast cells via the chemokine receptors CXCR3 and both CCR1 and CCR3, respectively.[133-135] The activity of CXCL10 and RANTES on mast cell function has largely been considered chemotactic in nature. Limited evidence has suggested these chemokines may additionally promote partial degranulation behavior in mast cells.[136,137] Our findings provide strong confirmation that both CXCL10 and RANTES directly induce mast cell degranulation. This, in turn, likely

contributes to the structural remodeling and hypersensitive ASM phenotype observed in asthma.[138-140] Furthermore, we describe a unified biophysical mechanism by which regulation of mast cell degranulation is differentially modulated in a pathway-dependent manner.

### 4.2.4 Objective

To study the effects of CXCL10 and RANTES on mast cell degranulation, CFMA was used, offering real time, direct analysis of CXCL10- and RANTES-induced mast cell degranulation at the single cell level. As previously covered in earlier chapters, carbon-fiber microelectrodes have high sensitivity and a low, stable background that facilitates single-cell analysis of mast cell degranulation.[39,82,122,141,142] These characteristics of CFMA allow the direct, real-time detection and detailed monitoring of individual vesicle fusion events from single mast cells following direct, local stimulation via a micropipette (Figure 1.3).

A detailed description of the information gained from the individual peak analysis of CFMA data is provided in previous chapters. To summarize, the data from each CFMA measurement is manifested as a series of individual current peaks, each corresponding to the contents of a single mast cell granule released to the extracellular space. Characterization of individual current peaks allows quantification of mast cell secretory function.[82,104,143] In this study, five key parameters were monitored: total serotonin per mast cell, peak area (Q), peak frequency, peak half-width ($t_{1/2}$), and peak rise time ($t_{rise}$),

as well as the calculated total serotonin released per cell. Again, total serotonin reflects the general intensity of mast cell degranulation. Peak area relates to the number of serotonin molecules released per granule. Peak frequency is measured as the number of release events detected over the course of degranulation and reflects the overall efficiency of the granule trafficking, docking, and fusion processes of exocytosis. Peak half-width and peak rise-time are measurements related to the kinetics of exocytosis, reflecting the rate of intragranular matrix expansion and the amount of 'free-serotonin' initially released upon fusion of the granular and cell membranes, respectively. Together, these parameters allow changes in mast cell secretory function to be described in concrete terms and are useful for the characterization of processes that regulate mast cell degranulation within the context of asthma.

## 4.3 Experimental approach

### 4.3.1 Mast cell isolation and co-culture

Murine peritoneal mast cells were obtained from age-matched, sex-matched C57BL/6 mice (Jackson Laboratories) following IACUC approved guidelines (Protocol #0806A37663). Mast cells were isolated by peritoneal lavage and cultured as described in earlier chapters. [104,141] Briefly, the peritoneal cavity was injected with 8-10 mL of DMEM high glucose media supplemented with 10% bovine calf serum and 1% penicillin/streptomycin (all from ThermoFisher Scientific, Pittsburgh, PA). Extracted lavage fluid is stored on ice for transport and the collected cells are washed via centrifugation at 400 x g for 7 minutes followed by re-suspension in warm, fresh cell

culture media containing either 0.5 μg/mL anti-TNP IgE (BD Biosciences, San Jose, CA), or vehicle for control conditions. The resuspended cells are then plated onto 35 x 10 mm Petri dishes containing a confluent layer of murine 3t3 fibroblasts purchased from American Type Cell Culture (Manassas, VA) to create a co-culture environment and incubated over night. Immediately before use in CFMA experiments, the cell culture media was removed and the cells were washed three times with warm Tris buffer (12.5 mM tris(hydroxymethyl)aminomethane hydrochloride, 150 mM NaCl, 4.2 mM KCl, 5.6 mM glucose, 1.5 mM $CaCl_2$, 1.4 mM $MgCl_2$, sterile filtered and pH balanced to 7.2−7.4).

### 4.3.3 CFMA experiments

CFMA experiments were conducted as described in earlier chapters [82,104]. Briefly, cultured peritoneal mast cells, with or without anti-trinitrophenol (anti-TNP) IgE pre-incubation, were mounted on a temperature controlled Petri dish holder (Warner Instruments, Hamden, CT) and positioned on the stage of an inverted microscope (Nikon, Tokyo, Japan). Prior to measurement, a carbon-fiber microelectrode connected to a headstage and a pulled glass micropipette loaded with a stimulating substance were mounted on Burleigh PCS-5000 piezoelectric micromanipulators (Olympus America, Center Valley, PA) to permit fine positional control in three dimensions. The electrical potential of the microelectrode was controlled by an Axopatch 200B potentiostat (Molecular Devices, Sunnyvale, CA) and Tar Heel CV software (National Instruments, Austin, TX), written by Michael L.A.V. Heien, was used to control computer interface settings and record data for each amperometric trace.

For each measurement, the carbon-fiber microelectrode was lowered onto the surface of a single mast cell and set to +700 mV versus a Ag/AgCl reference electrode. Upon collection of data, a bolus of stimulating substance, 10 μM A23187 (Sigma Aldrich, St. Louis, MO) or 200 ng/mL of either TNP-modified ovalbumin (TNP-OVA) (ThermoFisher Scientific, Pittsburgh, PA), CXCL10 (Shenandoah Biotechnology, Warwick, PA), or RANTES (Shenandoah Biotechnology) in Tris buffer, was delivered locally to the cell. Serotonin released to the electrode surface was detected as current over the course of a 90 s collection period.

### 4.3.4 Data analysis and statistics

Each amperometric trace obtained from a single CFMA experiment (and thus, representing the degranulation behavior of a single mast cell) was filtered at 200 Hz through a low-pass Bessel filter and exported as a text file prior to conversion, using the ABF Utility provided in the MiniAnalysis software package (Synaptosoft, Fort Lee, NJ), to the .ABF file format required for peak parameter analysis. Using the MiniAnalysis software, each trace was analyzed for the several peak parameters discussed above, and an average value for each cell was obtained. Average parameter values for each trace were pooled across similar experimental conditions. Outliers were defined as any trace for which the experimental values were found to be more than two log standard deviations from the log mean for that condition. For example, if a given trace produced all but one parameter within the criteria, the trace would be discarded as an outlier for all

measured parameters. Following the removal of outliers, the mean peak parameter values for each trace were averaged and compared to other experimental conditions using the two-tailed Student's t test with statistical significance determined at the 95 percent confidence interval ($p \leq 0.05$). Comparison of stimulation conditions was carried out in three separate experiments, each with TNP-OVA-stimulated mast cells as a control condition. The error bars for the TNP-OVA condition on all graphs are represented as a standard error measurement calculated using a weighted average of the variances the three separate TNP-OVA data sets.

### 4.4 Results and discussion

Investigation of mast cell secretory function in response to various ASM-associated inflammatory mediators was initiated using high performance liquid chromatography (HPLC) equipped with electrochemical detection.[36] Levels of serotonin released from primary mouse peritoneal mast cells, cultured in concert with macrophages and other cells collected by peritoneal lavage, were characterized using this bulk measurement technique to study the effect of pre-incubation with ASM-associated chemokines on IgE-mediated mast cell degranulation. These early experiments, however, suggested surprisingly that CXCL10 and RANTES directly induced mast cell degranulation independent of the IgE-mediated stimulation. The observed effect, although small relative to IgE-mediated stimulation, warranted further investigation.

### 4.4.1 Approach

To specifically explore the direct induction of mast cell degranulation by ASM products, CFMA was used to monitor real time mast cell secretory function at the single cell level. The degranulation behavior of individual mouse peritoneal mast cells cultured in vitro and incubated with anti-TNP IgE was monitored using CFMA following direct local exposure to either CXCL10 or RANTES, as well as both TNP-OVA, as a model for IgE-mediated degranulation, and the calcium ionophore A23187 as separate positive controls. An additional experimental condition consisted of A23187-stimulated mast cells without IgE pre-incubation.

### 4.4.2 CXCL10 and RANTES directly activate mast cell degranulation

The results of these experiments clearly demonstrate the ability of both CXCL10 and RANTES to directly induce mast cell degranulation and highlight the distinct differences in degranulation behavior between alternative modes of stimulation. Figure 4.1 shows representative CFMA traces recorded from each experimental condition. Calculation of total serotonin released per cell reveals that CXCL10 directly stimulated secretion; however, CXCL10-stimulated mast cells released 52% less serotonin than IgE-mediated degranulation (Figure 4.2). RANTES-stimulated mast cells, released an even lower amount, equal to 89% less serotonin than the IgE-mediated degranulation (Figure 4.2). In contrast to the CXCL10 and RANTES stimulation, calcium ionophore-induced degranulation (A23187) was observed to be more intense than the IgE-mediated condition. A23187, both with and without IgE incubation, inducing stronger mast cell

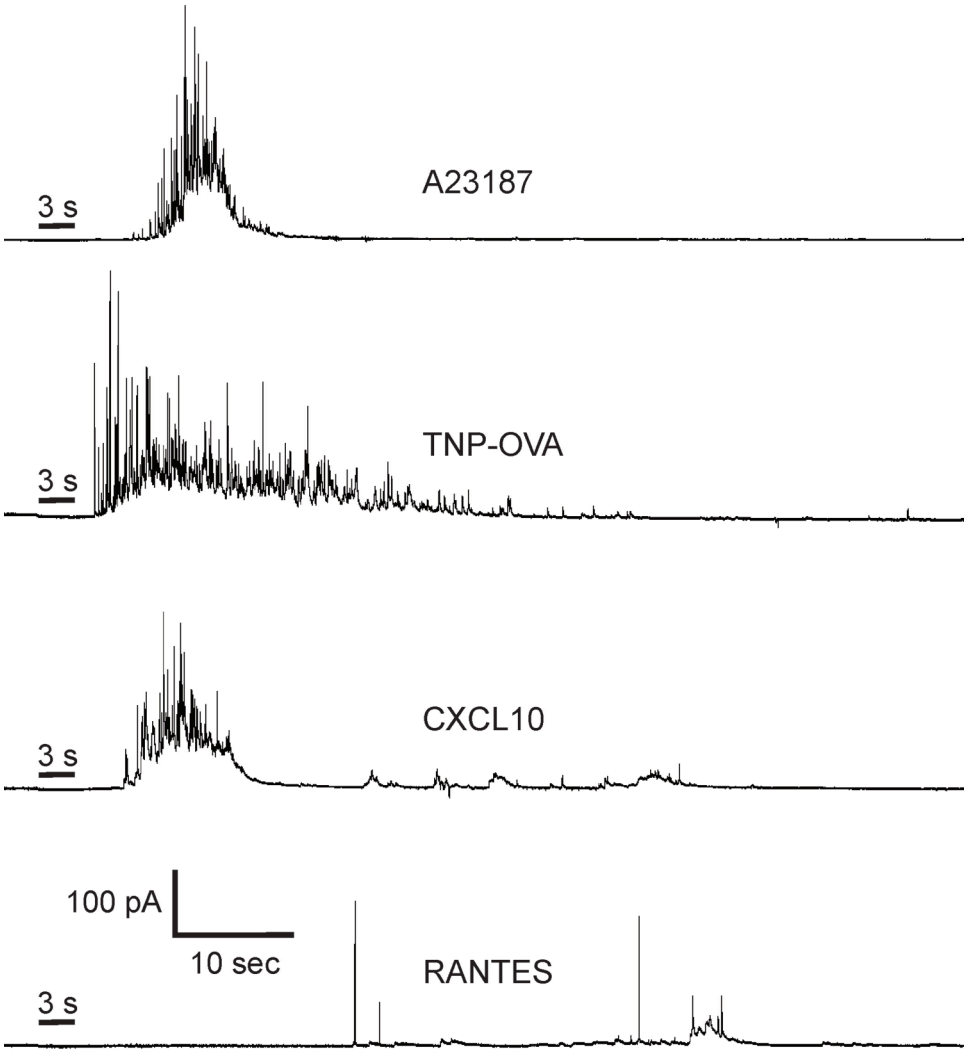


**Figure 4.1 Representative CFMA traces**
Representative CFMA traces from mast cells pre-incubated with 0.5 μg/mL anti-TNP IgE and stimulated with 10 μM A23187, 200 ng/mL TNP-OVA, 200 ng/mL CXCL10 or 200 ng/mL RANTES. Both CXCL10 and RANTES were able to directly induce mast cell degranulation.

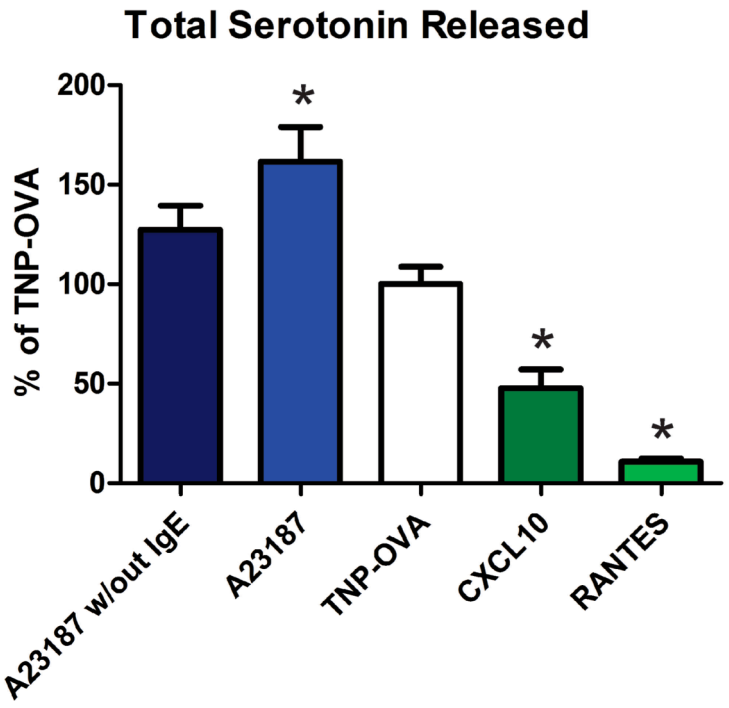


**Figure 4.2 Total serotonin released per mast cell**
Total serotonin released from mast cells stimulated with A23187 without IgE pre-incubation (n=18), A23187 with IgE pre-incubation (n=17), TNP-OVA (n=19), CXCL10 (n=26), or RANTES (n=16). Total serotonin is calculated using the amount of serotonin released per granule and the number of release events per cell. * indicates $p<0.05$ vs. TNP-OVA.

degranulation responses, releasing 62% and 27% more serotonin per cell, respectively, than the TNP-OVA stimulation (Figure 4.2). However, only the A23187-stimulated mast cells with anti-TNP IgE were found to be significantly different from TNP-OVA-stimulated counterparts. These data confirm the direct mast cell degranulation activities of both CXCL10 and RANTES and highlight the ability of CFMA to directly compare

stimulatory conditions and reveal distinct stimulation-dependent mast cell degranulation patterns. In addition to demonstrating the promising potential for the application of CFMA for the comparative analysis of alternate modes of mast cell activation, these findings suggest a dual role of ASM-secreted products in asthma pathogenesis. RANTES and CXCL10 may be central to not only the microlocalization of mast cells to the ASM, but also the mast cell activation and degranulation thought to influence the proinflammatory ASM phenotype in asthma. This work supports the emphasis on IgE-independent modes of mast cell activation, particularly via ASM-secreted products, as promising pathways to target for the development of novel asthma therapies.

### 4.4.3 Analysis of CXCL10- and RANTES-induced mast cell degranulation

In addition to demonstrating the ability of CXCL10 and RANTES to directly induce mast cell degranulation at the single cell level, CFMA facilitates characterization of the secretory function of individual cells in real time and with precise control of stimulatory conditions. In particular, CFMA allowed the characterization of the partial degranulation observed in mast cells stimulated via CXCL10 or RANTES. The results presented here clearly suggest that mast cells regulate the degree of degranulation in a stimulation-dependent manner across a wide dynamic range. Individual peak analysis was conducted to investigate the biophysical mechanism by which mast cell degranulation is differentially regulated.

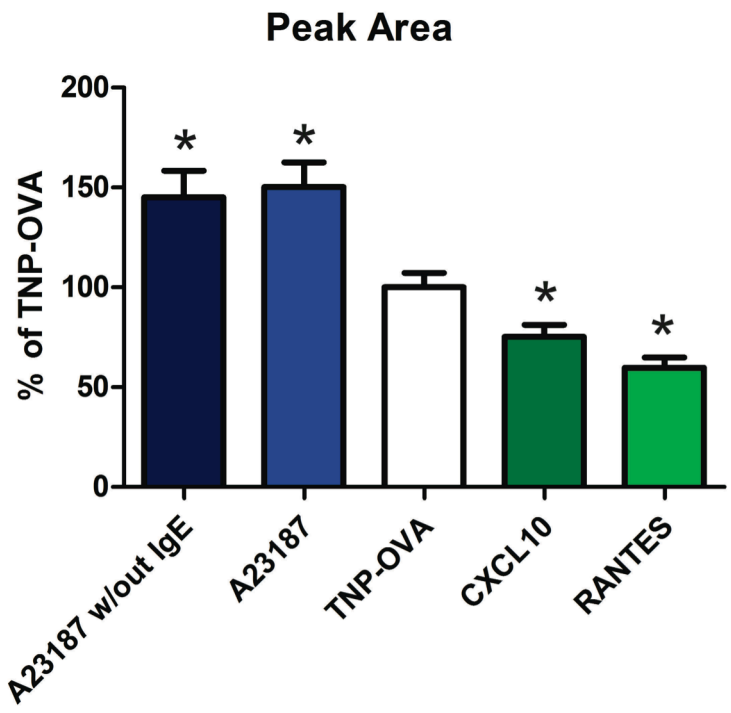


**Figure 4.3 Average amount of serotonin released per granule**
Average peak area values for mast cells stimulated with A23187 without IgE pre-incubation (n=18), A23187 with IgE pre-incubation (n=17), TNP-OVA (n=19), CXCL10 (n=26), or RANTES (n=16). The number of molecules of serotonin released per granule is calculated using the integrated area of each peak and Faraday's law. * indicates $p<0.05$ vs. TNP-OVA.

Across all conditions, the serotonin released per granule, as measured by peak area values, corresponded directly to the amount of total serotonin released per cell. A23187 stimulated mast cells pre-treated with anti-TNP IgE released 150% of the serotonin released per granule observed in the TNP-OVA condition; slightly more than (though statistically similar to) the 145% of TNP-OVA observed from mast cells stimulated with

A23187 without IgE incubation (Figure 4.3). Conversely, CXCL10- and RANTES-stimulated mast cells released only 75% and 60%, respectively, of TNP-OVA-stimulated mast cells (Figure 4.3). All observed changes were statistically significant ($p<0.05$). Because all incubation conditions were identical (with the exception of A23187-stimulated mast cells without IgE pre-treatment), it is unlikely the observed stimulation-dependent changes in serotonin released per granule are due to altered granule loading. Rather, our results suggest CXCL10- and RANTES-induced partial degranulation in mast cells is a regulated process and involves modulated release of granular contents.

The contributions of altered peak area to the total amount of serotonin released per cell were amplified by changes in measured peak frequency. A23187-stimulated mast cells, both with and without IgE incubation, were found to undergo degranulation at measured frequency values 34% and 16% greater than TNP-OVA-stimulated cells, respectively, though the latter was not statistically significant ($p=0.09$) (Figure 4.4). In contrast, stimulation with CXCL10 and RANTES produced degranulation frequency values 48% and 75% lower, respectively, than the TNP-OVA condition (Figure 4.4). These findings are clear evidence that granule trafficking and docking efficiency are also regulated in a stimulation-dependent manner that influences the degree of mast cell degranulation.

Therefore, our findings argue that, compared to IgE-mediated degranulation, the relatively lower total serotonin released from mast cells directly stimulated by CXCL10

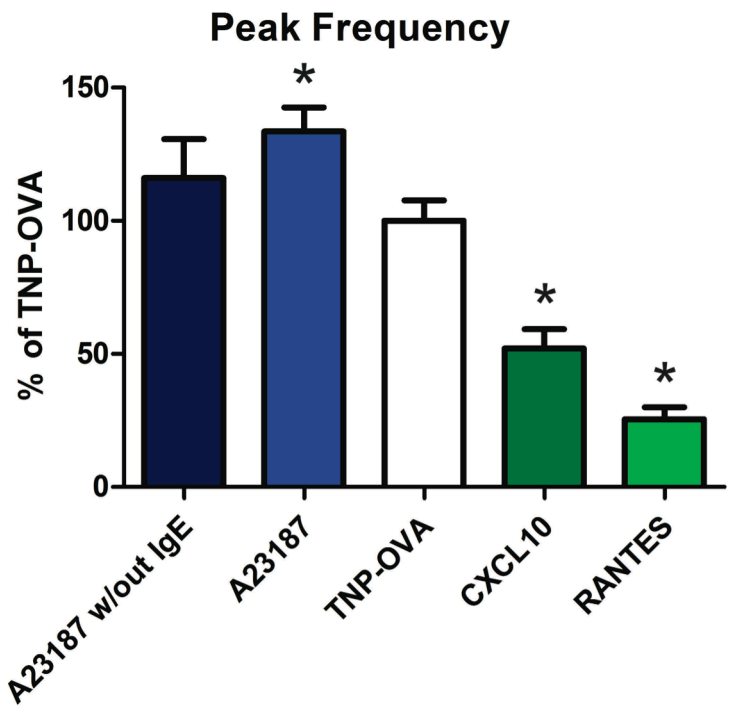


**Figure 4.4 Average frequency of release events**
Average peak frequency values for mast cells stimulated with A23187 without IgE pre-incubation (n=18), A23187 with IgE pre-incubation (n=17), TNP-OVA (n=19), CXCL10 (n=26), or RANTES (n=16). Average peak frequency is calculated as the number of release events over time. * indicates $p<0.05$ vs. TNP-OVA.

and RANTES results from both decreased serotonin released per granule and decreased frequency of release events. Similarly, the relatively larger amount of serotonin released from A23187-stimulated mast cells is due to both greater amounts of serotonin released per granule and increased granule trafficking, docking, and fusion. Interestingly, the A23187-stimulated mast cells lacking IgE pre-incubation demonstrated increased

serotonin released per granule, however, the increase in degranulation frequency was insufficient to influence the total serotonin released from these cells in a statistically significant fashion relative to the TNP-OVA condition. This implies surface-bound IgE may influence mast cell degranulation by removing barriers to granule trafficking and docking efficiency. Overall, these data suggest a unified biophysical mechanism by which mast cells exhibit pathway-dependent modulation of degranulation intensity. Most importantly, mast cell degranulation induced by RANTES and CXCL10 are distinct from IgE-mediated activation. These findings highlight the variations in mast cell degranulation that demand consideration when evaluating the role of mast cells in asthma.

Given the role of both peak area (serotonin released per granule) and peak frequency (granule transport, docking, and/or fusion efficiency) in the regulation of mast cell degranulation, further peak analysis was conducted to gain more insight into this process. Both peak half-width and peak rise-time were monitored as indicators of the intragranular matrix and membrane driving forces that are important to the exocytosis process. Consistent trends were observed for these parameters across all monitored conditions. As peak area decreased, both peak half-width and peak rise-time increased significantly (Figure 4.5 and 4.6).

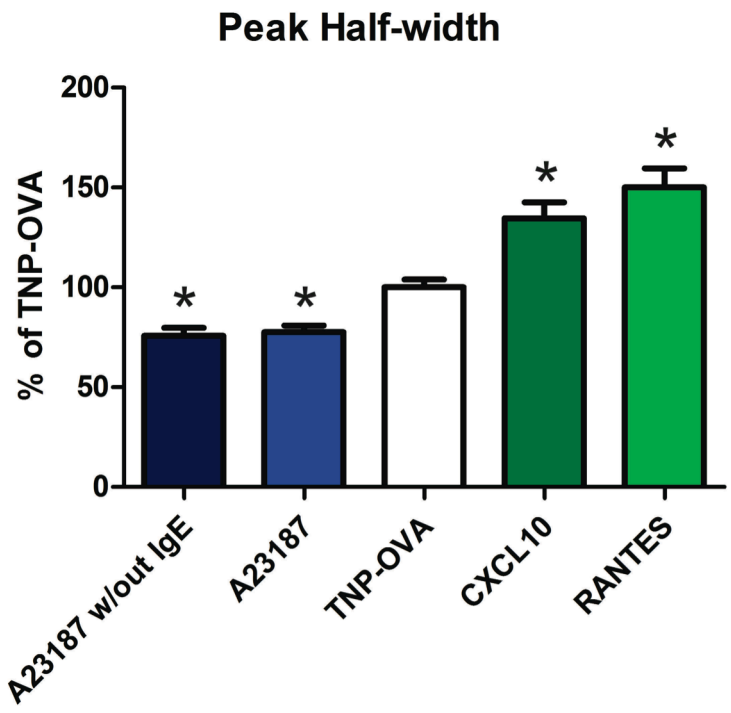


**Figure 4.5 Average peak half-width**
Average peak half-width values for mast cells stimulated with A23187 without IgE pre-incubation (n=18), A23187 with IgE pre-incubation (n=17), TNP-OVA (n=19), CXCL10 (n=26), or RANTES (n=16). Peak half-width is calculated as full width at half max of each peak in a CFMA trace. * indicates $p<0.05$ vs. TNP-OVA.

For example, considering the observed 50% increase in peak area measured for A23187-stimulated mast cells with anti-TNP IgE incubation versus TNP-OVA, the same condition demonstrated a 22% decrease in peak half-width (Figure 4.5). Similarly, A23187-stimulated mast cells without IgE incubation showed a 45% increase in peak area and a 24% decrease in peak half-width compared to the TNP-OVA-stimulated

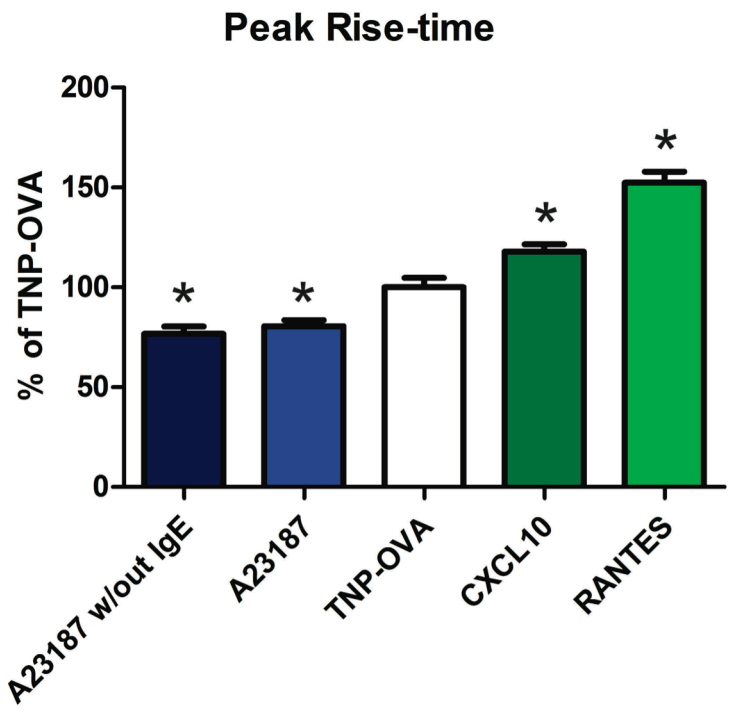


**Figure 4.6 Average peak rise-time**
Average peak rise-time values for mast cells stimulated with A23187 without IgE pre-incubation (n=18), A23187 with IgE pre-incubation (n=17), TNP-OVA (n=19), CXCL10 (n=26), or RANTES (n=16). Peak rise is calculated as the time from 10% to 9% of peak height. * indicates $p<0.05$ vs. TNP-OVA.

condition (Figure 4.5). Following the same trend, the CXCL10- and RANTES-stimulated mast cells, which released 25% and 40% less serotonin per granule versus TNP-OVA, responded with peak half-widths increased by 35% and 50% compared to IgE-mediated degranulation, respectively (Figure 4.5). These findings strongly support a critical role for membrane driving forces in regulating the degree of granular content release. In the

absence of altered membrane dynamics, larger peak area values normally correspond to increases in peak half-width due to increased time to release more granular cargo. The opposite trends observed in this work suggest that these driving forces participate in the regulation of mast cell degranulation.

Additionally, A23187-stimulated mast cells with and without IgE demonstrated peak rise-time values 19% and 23% less, respectively, compared to TNP-OVA values despite the observed increases in serotonin released per granule (Fig. 4.6). In contrast, CXCL10- and RANTES-stimulated mast cells demonstrated increased peak rise-time values 18% and 52% greater, respectively, than TNP-OVA-stimulated mast cells suggesting intragranular matrix effects and/or altered fusion pore stability may also participate in the regulatory mechanism of mast cell degranulation (Figure 4.6). As with peak half-width, in the absence of intragranular matrix effects or changes to fusion pore formation, an increase in peak area normally coincides with an increase in peak rise-time due to increased cargo released. The opposite effect observed in this data suggests either or both of these processes are likely involved in the stimulation-dependent regulation of mast cell degranulation.

### 4.5 Conclusion

This research demonstrates the utility of CFMA for the direct observation of mast cell degranulation behavior at the single cell level, and specifically for the study of asthma-relevant ASM products on mast cell function. These findings confirm the capacity of the

ASM-secreted chemoattractants CXCL10 and RANTES for the direct induction of mast cell degranulation despite total secretion levels significantly lower than conventional mast cell degranulation pathways. The dual activity of CXCL10 and RANTES on mast cell function, suggests a simple model of mast cell microlocalization to the ASM and subsequent activation in asthma, presumably upon exposure to a threshold concentration of either cytokine. Importantly, this work reveals consistent trends in the biophysical mechanism of regulated mast cell degranulation in response to different stimuli. Across all experimental conditions, increased mast cell degranulation intensity was accomplished by a combination of increased serotonin released per granule and an increased frequency of release events. Conversely, decreased mast cell degranulation was accounted for by both decreased serotonin released per granule and a decreased frequency of release events. Furthermore, observed trends in kinetic parameters ($t_{1/2}$ and $t_{rise}$) also suggest a consistent role of intragranular matrix and membrane driving forces in the stimulation-dependent release of granular contents. These findings argue for a unified biophysical mechanism of regulated degranulation that incorporates control over granule trafficking, transport, and/or docking machinery as well as intragranular matrix and membrane driving forces. The extent to which this model of regulated degranulation is conserved across all modes of mast cell stimulation will be the subject of further study. A complete understanding of the relationship between ASM and mast cells in the pathogenesis of asthma will require extensive further research, including various other chemokines, co-culture of cell types, or in vivo studies. Nonetheless, the findings outlined here emphasize

the need for a more nuanced understanding of the multidimensional and complex nature of immune cell signaling in asthma.

# Chapter 5

## Using CFMA to characterize the effects of substance P and calcitonin gene-related peptide on mast cell degranulation at the single cell level

Meyer, A. F., Gruba, S. M., and Haynes, C. L. contributed to this work

## 5.1 Overview

Following an approach similar to the work in Chapter 4, the research herein details an effort to characterize at the single cell level the biophysical processes of degranulation in mast cells upon direct stimulation with different stimuli. However, rather than using CFMA to study airway smooth muscle-associated chemokines, this work focuses on two neuropeptides central to the development of neurogenic inflammation, substance P and CGRP, and their direct effects on mast cell degranulation. Both substance P and CGRP were found to induce mast cell degranulation following a very similar biophysical mechanism at the single cell level. In addition to the characterization of substance P- and CGRP-induced mast cell degranulation using CFMA, bulk assay analysis of mast cell degranulation using an HPLC with electrochemical detection capability was conducted in parallel with CFMA experiments. This approach revealed distinct differences between substance P and CGRP at the bulk level that were indiscernible using CFMA alone. Specifically, substance P was able to induce concentration-dependent degranulation from peritoneal mast cells while CGRP did not induce significant degranulation at the bulk level, despite a similar mechanism of degranulation from single cells. This discrepancy was likely due to effective stimulation of a smaller percentage of the mast cell population by CGRP relative to substance P. Bulk analysis was also used to characterize the effects of monomeric IgE pre-incubation on the sensitivity of mast cell populations to neuropeptide-induced degranulation. This work revealed a previously unreported effect of surface-bound IgE and the desensitization of mast cells toward substance P-induced

degranulation. Together these findings demonstrate the advantages and utility of both single-cell CFMA and bulk assay HPLC experiments used in combination to study mast cell signaling in the context of neurogenic inflammation.

### 5.2 Introduction to neurogenic inflammation

Neurogenic inflammation plays an important role in the pathophysiology of many diseases, including atopic dermatitis, interstitial cystitis, asthma, arthritis, and irritable bowel syndrome, among others.[144-147] In response to injury or stress, afferent nerve fibers release several inflammatory mediators that initiate a local immune response.[106,107,146,148,149] In particular, damaged or activated nerves release the neuropeptides substance P and CGRP, discussed in detail below, which in turn act on both vasculature and tissue-resident immune cells resulting in vasodilation, swelling, leukocyte infiltration and activation, and hyperalgesia.[106,107,149,150] Mast cell degranulation, particularly in response to secreted neuropeptides, is critical to the development of neurogenic inflammation. Activation of mast cells via neuropeptides results in the secretion of a variety of mediators such as histamine and tumor necrosis factor, which act on afferent peripheral neurons, further propagating the inflammatory response.[146] However, immune cell interactions with the peripheral nervous system are not limited to proinflammatory pathways. For example, immune cell production of analgesic opioid peptides is well documented.[116] Nonetheless, the complex relationship between neuropeptides and mast cell degranulation is critical to neurogenic inflammation, and beyond the limited use of whole-cell patch clamp techniques and

fluorescence spectroscopy,[151] neuropeptide-induced mast cell degranulation has not been studied extensively at the single cell level. In this work, CFMA was applied to characterize the activities of two common neuropeptides, substance P and CGRP, on mouse peritoneal mast cells to explore neurogenic inflammation. Additionally, preliminary experiments suggested a possible role for surface-bound monomeric IgE (in the absence of antigen) in the regulation of neuropeptide-induced mast cell degranulation; therefore, IgE effects were also explored at the bulk level using an HPLC outfitted with electrochemical detection capability.

### 5.2.1 Mast cell contributions to neurogenic inflammation

Although many immune cells participate in neurogenic inflammation, including macrophages, neutrophils and eosinophils, mast cells are thought to play a central role, largely due to the importance of histamine and its activity on peripheral nerves. As discussed thoroughly in previous chapters, mast cells, in response to immune signals (including the crosslinking of surface-bound IgE by multivalent antigen), degranulate to release histamine and many other signaling molecules from their cytoplasmic vesicles (granules) (Table 1.1). During neurogenic inflammation, mast cells degranulate in response to neuropeptides released from the peripheral nervous system. Several products of mast cell degranulation, and histamine in particular, subsequently act directly on peripheral nerve fibers, initiating an axonal reflex in the sensory nerve, stimulating neighboring axons to also secrete neuropeptides, and thus, propagating the inflammatory response.[149] In addition to the effects of mast cell-secreted histamine on the propagation

of neurogenic inflammation, research also suggests direct cell-to-cell contact between mast cells and peripheral nerve terminals, mediated in part by N-cadherins, is involved in the regulated mast cell degranulation.[107] TNF-α, which is also a product of mast cell degranulation, has been shown to act directly on sensory nerve fibers, increasing mechanical sensitization.[152] These examples highlight the demand for tools such as CFMA that enable the direct detection of mast cell degranulation behavior to explore the many different neuro-immune interactions.

### 5.2.2 Substance P and CGRP

Although a number of neuropeptides, such as neurokinin A and corticotropin-releasing factor, are known to participate in neuro-immune functions, substance P and CGRP are particularly important for the initiation of neurogenic inflammation.[153,154] Substance P is a member of the tachykinin class of peptides which act through the neurokinin family of receptors (NKRs).[150,155] CGRP, as its name suggests, is derived through an alternative splicing product of the calcitonin gene and acts through the calcitonin receptor-like receptor (CRL).[150,156] Both substance P and CGRP are released from the same subset of capsaicin-sensitive primary afferent neurons and are co-localized in, and co-released from, dense-core secretory granules at peripheral axon terminals.[150,155] Similarly, both substance P and CGRP have been shown to induce mast cell degranulation as part of the pro-inflammatory functionality of these neuropeptides.[155] However, although substance P-induced mast cell degranulation is well established, the data supporting the effects of CGRP on mast cell degranulation are mixed.[146,148,157,158] Furthermore, despite mast cell

expression of both CRL and NKRs, it also suggested that substance P- and CGRP-induced mast cell degranulation is likely due to direct activation of GTP-binding (G) proteins rather than receptor signaling.[155,158,159] Because mouse peritoneal mast cells are numerous and an easily accessible model system for research purposes, it is useful to characterize the capacity of both substance P and CGRP to directly induce mast cell degranulation in this model system.

### 5.2.3 Objective

The research summarized in this chapter seeks to measure and characterize mast cell degranulation upon stimulation by substance P and CGRP using both single-cell and bulk assay techniques. The use of electrochemical detection in both bulk and single-cell experiments affords a highly compatible comparison between the two approaches. While single-cell approaches such as CFMA offer biophysical and mechanistic information not achieved through traditional assays, the application of complementary bulk assays are particularly useful when they provide information that reflects the collective activity of a cell population within the larger context of a complex cellular environment, particularly under conditions that induce only partial stimulation of a given mast cell population. The research described in this chapter seeks to 1) use CFMA to characterize the biophysical properties of substance P and CGRP-induced mast cell degranulation, 2) apply a bulk HPLC assay to explore the effect of monomeric IgE incubation on the susceptibility of a collection of mast cells to neuropeptide-induced degranulation, and 3) correlate single-cell CFMA results with bulk level HPLC data to better understand the differences

between substance P and CGRP as mast cell stimulants, as well as cellular microenvironment effects on mast cell secretory function.

## 5.3 Experimental approach

### 5.3.1 Mast cell isolation and culture

Mouse peritoneal mast cells were isolated and cultured as described in previous chapters. All mice were handled in accordance with an approved IACUC protocol (Protocol # 0806A37663) For CFMA experiments, three male age-matched C57BL/6 mice were euthanized and mast cells were collected by peritoneal lavage. Washed and resuspended peritoneal cells were then plated in 2 mL aliquots onto 35 x 10 mm Petri dishes over a confluent layer of mouse 3t3 fibroblasts. Co-cultured mast cells were then incubated overnight at 37 ˚C and 5% $CO_2$ until use in CFMA experiments.

A similar mast cell isolation and culture procedure was followed for bulk assay experiments, with the following variations to account for the detection limit of the HPLC method as well as the number of both biological and instrumental replicates for statistical analysis. For an experiment with 12 conditions, 12 age-matched male C57BL/6 mice were euthanized and mast cells were collected as described above. Rather than 35 x 10 mm Petri dishes, 500 µL aliquots of peritoneal cells were co-cultured with a confluent layer of murine 3t3 fibroblasts in two 24 well plates. Conditions that required IgE-mediated pretreatment were incubated with 500 ng/mL anti-TNP IgE. Co-cultured cells

were then incubated overnight prior to stimulation and extraction of supernatants for HPLC analysis of secreted serotonin as outlined below.

### 5.3.2 Carbon-fiber microelectrode amperometry

CFMA experiments were conducted as previously described in this dissertation. Briefly, cell culture parameters were kept the same for all experimental conditions. Peritoneal mast cells were stimulated locally via micropipette with 1 μM substance P, 1 μM CGRP, or 10 μM A23187 (a calcium ionophore), and the subsequent degranulation was monitored using CFMA (Figure 1.3).

### 5.3.3 Monitoring mast cell degranulation using HPLC with electrochemical detection

Like CFMA, electrochemical detection of secreted serotonin is beneficial because it is a highly selective and label-free method with low limits of detection sufficient to detect serotonin levels secreted from a relatively small number of mast cells. In parallel with single-cell CFMA conditions, co-cultured peritoneal cells were washed three times with warm Tris buffer. After the third wash, 250 μL of the appropriate mast cell stimulation solution was added to each well and incubated at 37 ˚C and 5% $CO_2$ for 30 minutes. Following the incubation period, supernatants were removed and filtered using a 96 well filtration plate (Millipore) which was centrifuged at 3000 x g for 10 minutes. 180 μL of the filtered supernatants were then diluted to 200 μL with 0.5 M $HClO_4$ containing a 5 μM dopamine internal standard (for a final internal standard concentration of 0.5 μM). A

five point calibration curve was also made in 0.5 μM $HClO_4$, ranging from 0.0625 to 1.000 μM serotonin, with each containing an 0.5 μM dopamine internal standard. Ahead of mast cell secretion analysis, calibration curves were created using the ratio of serotonin to dopamine peak area values. Both calibrants and experimental samples were run on an Agilent 1200 HPLC instrument, as described in the literature,[36] using a 5 μm, 4.6 x 150 mm Eclipse XDB C18 column attached to a Waters 2465 electrochemical detector with a glassy carbon electrode. As in CFMA experiments, the working potential of the electrode was set to 700 mV vs. an in situ Ag/AgCl reference electrode.

### 5.3.4 Data analysis and statistical treatment

CFMA data collection and individual peak analysis was conducted as described in previous chapters. In short, peak area (Q), peak number, peak half-width ($t_{1/2}$) and peak rise time ($t_{rise}$), as well as the calculated total serotonin per cell, were monitored for each individual mast cell. Following the exclusion of outliers, average values for each parameter were calculated, and statistical significance between experimental conditions was determined using the unpaired student's T test and a confidence interval of 95%.

For HPLC experiments, serotonin concentration values were calculated as integrated peak area values correlated to a calibration curve created as described above. HPLC peaks were integrated using Agilent Chemstation software. Statistical significance between experimental conditions was determined using a one-way ANOVA test and a confidence interval of 95%.

## 5.4 Results and Discussion

To achieve the objectives outlined above, direct activation of degranulation from peritoneal mast cells by substance P and CGRP was characterized using both single cell CFMA measurements and parallel bulk experiments. In the bulk experiments, secretion from stimulated mast cells was monitored using an HPLC outfitted with electrochemical detection to permit the measurement of secreted serotonin. In addition to the fundamental characterization of neuropeptide-induced degranulation, these studies revealed that substance P- and CGRP-induced mast cell degranulation was altered if cells were pre-incubated with monomeric IgE (during experiments in which the neuropeptide stimulation conditions were directly compared to an IgE-mediated stimulation control). A thorough comparison of CFMA and HPLC data reveals similarities between substance P and CGRP at the single cell level that are not observed through bulk analysis, likely due to differences in the relative percentages of the mast cell subpopulations effectively stimulated by each neuropeptide.

### 5.4.1 Single cell analysis of neuropeptide-stimulated mast cell degranulation

During CFMA experiments, mast cells stimulated directly with either substance P or CGRP were compared to a population of mast cells stimulated with the calcium ionophore A23187. Importantly, both substance P and CGRP were capable of initiating degranulation in vitro from primary peritoneal mast cells in the absence of other exogenous stimulant. (Figure 5.1) Analysis of the CFMA data for each condition revealed that mast cells stimulated with either substance P or CGRP released similar levels of total

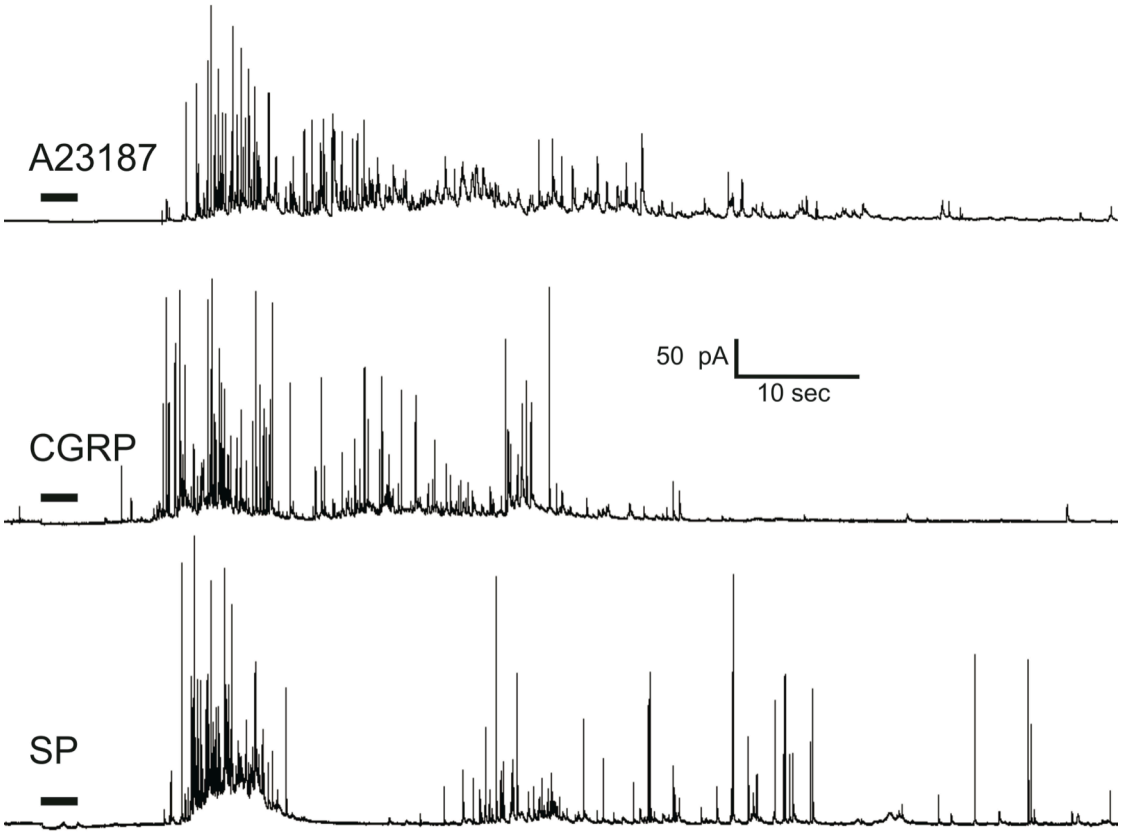


**Figure 5.1 Representative CFMA traces from neuropeptide-stimulated mast cells**
Representative CFMA traces from mast cells stimulated locally with a three second bolus of 10 μM A23187, 1 μM substance P, or 1 μM CGRP.

serotonin per cell. Both neuropeptides stimulated mast cells to release less total serotonin than A23187-stimulated controls (substance P- and CGRP stimulated mast cells released 39% less serotonin per cell than the A23187-stimulated cells). (Figure 5.2) Further analysis of the CFMA data reveals this marked difference in the degree of mast cell

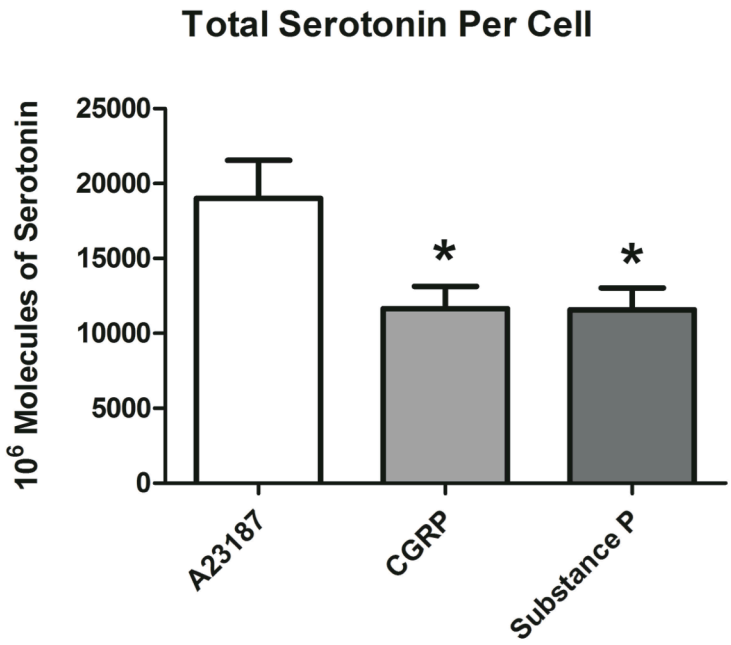


**Figure 5.2 Total serotonin per cell released from neuropeptide-stimulated mast cells**
Total serotonin released per mast cell following local stimulation with 10 μM A23187 (n=17), 1 μM CGRP (n=18), or 1 μM substance P (n=14). * indicates $p<0.05$ vs. A23187.

degranulation is largely accounted for by a lower amount of serotonin released per granule, with no measureable difference in the number of release events per cell. (Figure 5.3 and 5.4) Substance P- and CGRP-stimulated mast cells released 29% and 34% less serotonin per granule, respectively, relative to A23187-stimulated controls, with negligible changes in the number of peaks detected per trace. The stimulation-dependent alterations in peak area observed in the absence of different cell culture conditions suggests regulated control of the amount of chemical messenger released per granule

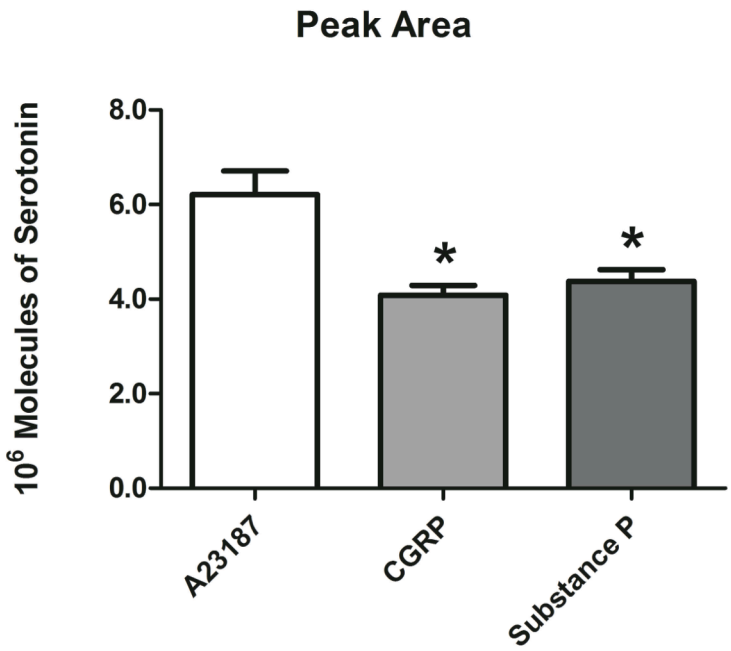


**Figure 5.3 Average serotonin released per granule following neuropeptide-stimulated mast cell degranulation**
Average amount of serotonin per granule following local stimulation with 10 µM A23187 (n=17), 1 µM CGRP (n=18), or 1 µM substance P (n=14). CGRP and substance P-stimulated mast cells released 34% and 29% less serotonin per granule relative to A23187-stimulated controls, respectively. * indicates $p<0.05$ vs. A23187.

rather than altered granule loading effects, which in theory, could occur in the event of differences in microenvironmental factors (cell incubation conditions). The absence of peak number effects also suggests that the granule trafficking and/or docking machinery can be regulated independently of the processes that regulate the percentage of granular contents released during degranulation.

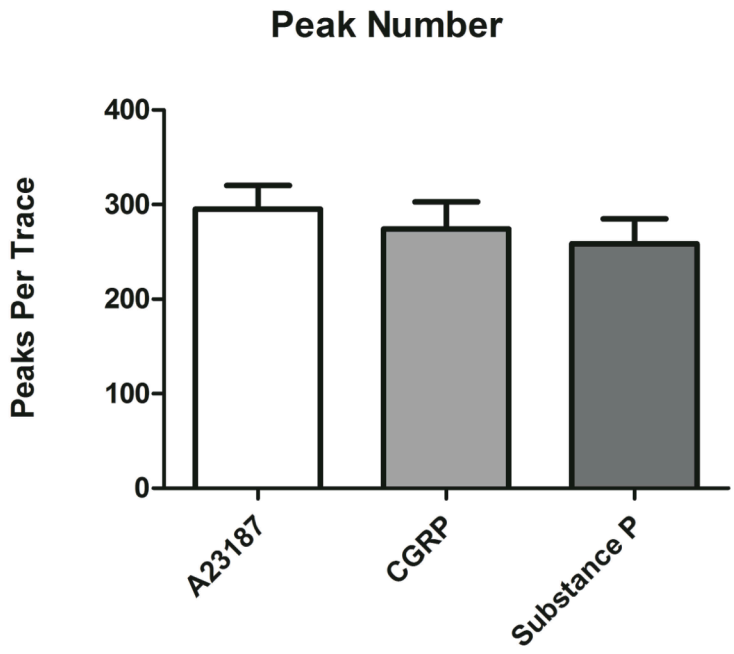


**Figure 5.4 Average number of release events per mast cell following neuropeptide stimulation**
Average number of release events following local stimulation with 10 µM A23187 (n=17), 1 µM CGRP (n=18), or 1 µM substance P (n=14). CGRP and substance P-stimulated mast cells did not demonstrate significantly altered number of release events relative to A23187-stimulated controls. * indicates $p<0.05$ vs. A23187.

Analysis of the kinetic parameters of mast cell degranulation revealed that the substantially smaller peak area values observed in the substance P- and CGRP-stimulated mast cells were not associated with measureable differences in either peak half-width or peak rise-time. (Figure 5.5) Although it is common to observe a correlation between a decrease in the percent of released granular contents and altered kinetic parameters such as $t_{1/2}$ and $t_{rise}$ (see chapter 3), these data present additional mechanistic insight that

suggests the fraction of serotonin released per granule may be regulated in a manner that does not result in altered membrane or intragranular matrix driving forces.

### 5.4.2 Substance P-induced mast cell degranulation is inhibited by pre-incubation with monomeric IgE

Substance P- and CGRP-stimulated mast cells presented remarkably similar degranulation profiles at the single-cell level; in contrast, at the bulk level, substance P produced a more robust stimulation than CGRP, where low μM CGRP concentrations did not produce a significant increase in secreted serotonin (Figure 5.6). Interestingly, several attempts were made, with limited success, to monitor substance P- and CGRP-induced mast cell degranulation using CFMA in direct comparison to IgE-mediated degranulation. During these experiments wherein all conditions were pre-incubated with monomeric anti-TNP IgE, control mast cells were stimulated with TNP-OVA as previously described (Chapter 3), little or no stimulation was measured. Given these findings, HPLC was subsequently used to explore the effect of IgE pre-incubation on neuropeptide-stimulated mast cell degranulation in a larger population of cells.

Serotonin levels in the supernatants of cultured peritoneal mast cells were monitored following a 30-minute incubation with the stimulation conditions outlined above. Substance P-stimulated mast cell degranulation in a concentration-dependent manner. In the absence of IgE pre-incubation, mast cells stimulated with 10 μM and 100 μM

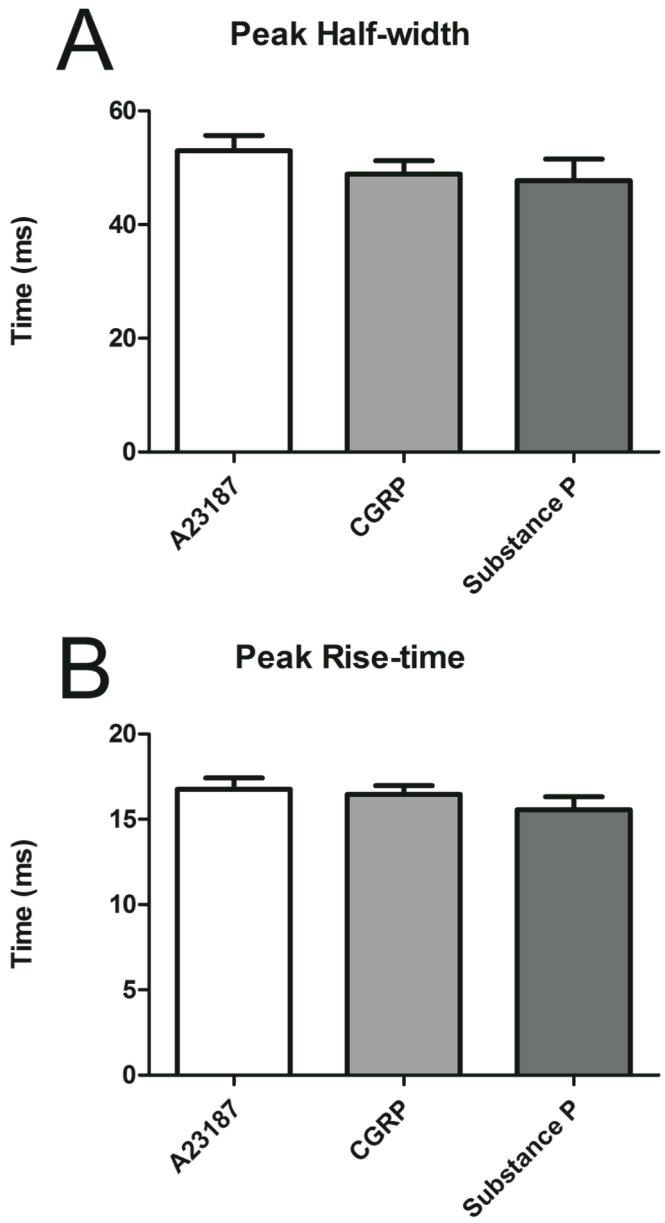


**Figure 5.5 Average peak half-width and rise-time from neuropeptide-stimulated mast cells**

Average peak half-width (A) and rise-time (B) values following local stimulation with 10 µM A23187 (n=17), 1 µM CGRP (n=18), or 1 µM substance P (n=14). CGRP and substance P-stimulated mast cells did not demonstrate significantly altered kinetics relative to A23187-stimulated controls.

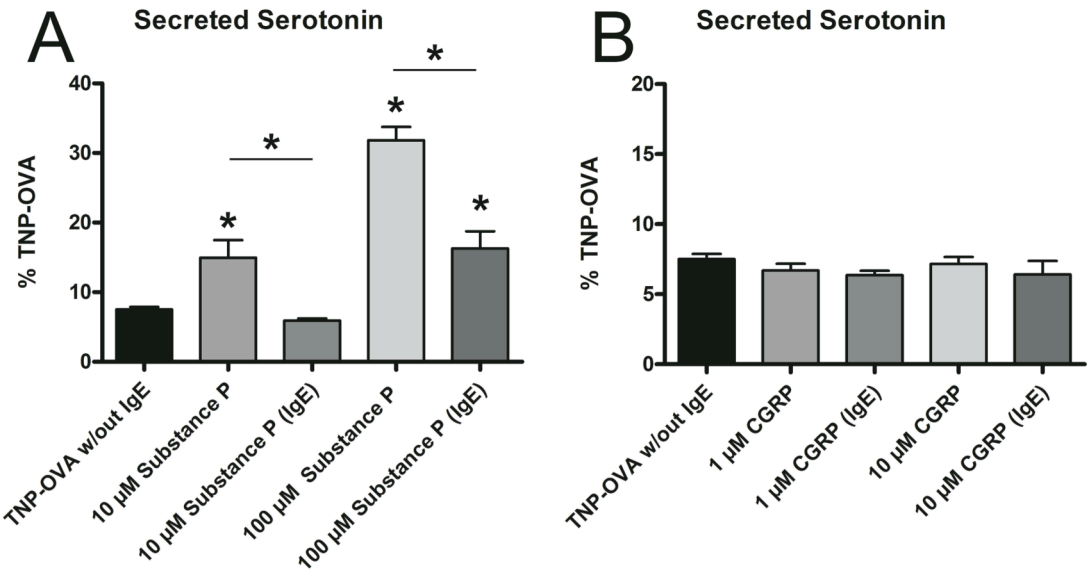


**Figure 5.6 Bulk analysis of mast cell degranulation using HPLC with electrochemical detection**

Serotonin concentration in supernatants from peritoneal mast cells co-cultured with 3t3 fibroblasts were measured using HPLC with electrochemical detection capability. Mast cells were stimulated with 10 µM or 100 µM substance P, 1 µM or 10 µM CGRP, or 200 ng/mL TNP-OVA with or without pre-incubation with 0.5 µg/mL anti-TNP IgE. Serotonin levels are represented as a percentage of the TNP-OVA with IgE pre-incubation condition. Statistical significance was determined using a one-way ANOVA test and a confidence interval of 95%. * indicates $p<0.05$ vs. TNP-OVA without IgE (unless indicated otherwise).

substance P released 15% and 32% of the serotonin, respectively, relative to TNP-OVA-stimulated control cells (Figure 5.6a). However, mast cells pre-incubated with monomeric IgE (as in the TNP-OVA stimulated condition) demonstrated significantly less mast cell degranulation. Supernatants from IgE-incubated mast cells stimulated with 10 µM substance P did not release significantly more serotonin than negative controls,

while IgE-incubated mast cells stimulated with 100 μM substance P released only 16% of the TNP-OVA control condition (Figure 5.6a). These results provide strong evidence that surface-bound monomeric IgE (via FcεRI) desensitizes mast cells to substance P-induced degranulation. Furthermore, this observation, which to the best of our knowledge has not been reported in the literature, is consistent with the difficulty obtaining single cell data in CFMA experiments in which neuropeptide-stimulated mast cells were pre-incubated with IgE. IgE-regulated desensitization towards neuropeptide stimulation may have important implications for the pathogenesis of diseases, especially those associated with either atopic or neurogenic processes.[71,103]

### 5.4.3 Comparison between bulk and single-cell patterns of substance P- and CGRP-induced mast cell degranulation

Interestingly, despite the capacity to induce mast cell degranulation at the single cell level upon direct, localized stimulation (Figures 5.1 and 5.2), HPLC analysis of bulk CGRP-stimulated mast cells did not reveal significantly increased levels of serotonin (Figure 5.6b). When considered in parallel with the similar degranulation profile observed between both substance P and CGRP at the single cell level, these data suggest the strong possibility that differences in the percentage of stimulated mast cells is the primary factor contributing to the differences observed between the two neuropeptides at the bulk level. Although the possible contributions of reuptake channels and/or serotonin biosynthetic pathways cannot be ruled out given the inherent complexity of the peritoneal cell/3t3 fibroblast co-culture system, we hypothesize that a smaller percent of the CGRP-treated

mast cells were stimulated to undergo degranulation than those treated with substance P. This hypothesis is also supported by the qualitative observation that the CGRP was a less consistent mast cell stimulant than substance P during single-cell CFMA experiments. However, further investigation will be required to verify the greater efficiency of substance P-induced mast cell degranulation.

The notable similarity between the degranulation profiles of substance P- and CGRP-stimulated mast cells at the single cell level suggests that the subpopulation of mast cells that are effectively stimulated by either neuropeptide initiate degranulation through a similar signaling pathway. Therefore, the similar degranulation profiles at the single-cell level, in combination with the relatively high (μM) concentrations required to induce mast cell degranulation, is consistent with the proposal that both neuropeptides activate mast cell degranulation through a receptor-independent pathway involving direct activation of G proteins.[155] Further characterization of the inhibitory effects of IgE on substance P- and CGRP-induced mast cell degranulation, as well as an in-depth examination of neuropeptide-induced G protein activation in mast cells will be the focus of additional research efforts.

### 5.5 Conclusion

In summary, the research contained in this chapter demonstrates and characterizes the capacities of both substance P and CGRP to directly induce degranulation in mouse peritoneal mast cells. Both single-cell CFMA measurements and bulk analysis of

degranulation using HPLC were used to reveal subtle differences between each of these neuropeptides in terms of their relative activities as mast cell stimulants. CFMA data revealed individual mast cells stimulated by both substance P and CGRP present remarkably similar degranulation profiles; information that was not discernable from bulk assay experiments. Parallel analysis of mast cell degranulation at the bulk level provided complementary insight into the differences between the two neuropeptides. Substance P-induced degranulation proved both concentration- and IgE-dependent, whereas CGRP was unable to sufficiently stimulate mast cells at the bulk level to produce a significant increase in measured serotonin from cultured peritoneal cell supernatants. Although concentration effects cannot be ruled out, a comparison between the bulk and single-cell data suggests substance P is likely more efficient than CGRP in terms of the relative efficiency with which each is capable of stimulating mast cell degranulation, while both likely stimulate mast cell degranulation by activating G proteins, as is widely reported in the literature. Finally, the IgE-dependence of substance P-induced mast cell degranulation has not been reported and may be an important element of neurogenic inflammation in atopic disease.

# Chapter 6

## Summary and future directions

## 6.1 Summary

The collection of work in this dissertation presents CFMA as a valuable technique for the study of cellular signaling networks in the immune system. Taken together, the findings summarized in the previous chapters provide a representative portrait of mast cell degranulation in response to inflammatory microenvironmental factors and the variety of regulatory mechanisms that influence mast cell secretory function. There are several considerations that are critical for the effective use of CFMA for any research focusing on the biological implications of cellular exocytosis.

Importantly, using CFMA to study cellular communication networks (as opposed to the investigation of strictly intracellular biophysical processes) introduces additional constraints on the design of an appropriate experimental model. An optimal model system from the perspective of a particular biological question may be incompatible (or suboptimal) for CFMA analysis and vice versa. Traditional model systems used in CFMA experiments (both in terms of the cell types studied and the stimulation conditions used to activate exocytosis) were preferred, in part, because they offered high levels of a secreted analyte to enhance signal-to-noise ratios and improved analysis of the biophysical parameters of exocytosis, or simply because these cell types were easier to culture in vitro (immortal cell lines, for example). However, selection of a model system based on cell secretion properties alone is a luxury not afforded to research applications involving biologically relevant cellular networks. As a result, it's often necessary to

compromise – opting to work within a system (cell type, stimulation condition, etc.) that is suboptimal from an analytical perspective but provides access to the relevant biological question at hand. Improving the accessibility of model systems that are simultaneously biologically relevant and CFMA-compatible is a significant hurdle facing the continued development of CFMA for applications in new biological contexts. Fortunately for this dissertation, there's no shortage of interesting biological questions involving mast cells and their role in various inflammatory processes. Nonetheless, variables including heterogeneity between mast cell subtypes, tissue of origin, and differences between animal species (or between different strains of the same species) demand scrutiny during the experimental design process.

The interpretation of CFMA data is similarly constrained by the biological context and aims of each particular research project. In general, for the study of cell-cell communication, this translates as an emphasis on the total amount of mediator released per cell, as this parameter is directly related to the biological consequences of exocytosis. Kinetic parameters of exocytosis ($t_{1/2}$ and $t_{rise}$) are important and provide valuable insight into the regulatory biophysical mechanisms that underlie changes in total secretion. However, these factors are secondary to the more concrete parameters such as peak area and peak number/frequency, which exhibit a more intuitive and direct connection to the amount of biological mediators released from the cell. Nonetheless, the interconnectedness of the measured parameters in CFMA analysis cannot be overstated.

For example, altered membrane dynamics that induce measurable changes in $t_{1/2}$ and $t_{rise}$ can impact the efficiency of the fusion process, and thereby influence the number of granules released per cell.

Despite the additional constraints that must be considered in order to use CFMA effectively for the study mast cells and inflammation, when appropriately applied, CFMA offers a valuable perspective that is inaccessible using traditional bulk assay methods alone. Perhaps the most important takeaway from this dissertation is the highly regulated and variable nature of mast cell degranulation, particularly in terms of the wide range of biophysical mechanisms that exert control over the relative amount of bioactive mediators released.

This work contains several examples wherein mast cells isolated from different in vivo microenvironments demonstrated altered degranulation in response to a universal stimulus (mast cells isolated from sickle Hb-expressing mice with and without morphine treatment in Chapter 2, and mast cells isolated from kappa opioid receptor knockout mice relative to wild type controls in Chapter 3). In each case, the biophysical processes regulating the measured change in function were distinctly different. For example, in the absence of chronic inflammation, in vivo morphine treatment dramatically increased the amount of serotonin released from mast cells, driven entirely by an increased cargo released per granule. On the other hand, mast cells from sickle Hb-expressing mice

| **Mast cells isolated from different in vivo microenvironments following similar stimulation conditions** | | | | | |
|---|---|---|---|---|---|
| | Total 5HT per cell | Concrete parameters | | Kinetic parameters | |
| | | 5HT Released per granule | Peak number or frequency | Peak Half-width | Peak Rise-time |
| **Chapter 2** | | | | | |
| Chronic inflammation effect (sickle-Hb without morphine treatment) | Decreased | Decreased | Decreased | Increased | Increased |
| In vivo morphine (normal Hb) | Increased | Increased | No change | Increased | No change |
| Morphine effect (sickle Hb-expressing mice) | Increased | Increased | Increased | Decreased | Decreased |
| **Chapter 3** | | | | | |
| MCs from KORKO mice vs. WT | Increased | Increased | Increased | Increased | No change |
| **Mast cells isolated from similar in vivo microenvironments respond to different stimuli** | | | | | |
| **Chapter 4** | | | | | |
| A23187-stimulated MCs vs. TNP-OVA | Increased | Increased | Increased | Decreased | Decreased |
| ASM-secreted chemokine stimulation vs. TNP-OVA | Decreased | Decreased | Decreased | Increased | Increased |
| **Chapter 5** | | | | | |
| Neuropeptide-stimulated MCs vs. A23187-stimulated controls | Decreased | Decreased | No change | No change | No change |

**Table 6.1 Summary of different modes of regulated mast cell degranulation**
Various modes of regulated mast cell (MC) degranulation in response to both altered in vivo microenvironmental factors and different stimulation conditions are summarized above.

demonstrated reduced degranulation intensity associated with a biophysical mechanism involving all four monitored peak parameters. The degranulation response recorded from mast cells isolated from kappa opioid receptor knockout mice was different still. CFMA measurements of mast cells from these mice, relative to wild type controls, revealed an increase in total degranulation regulated by both increased granular contents and an increased number of release events per cell, with a small increase in peak half-width

(associated with larger peak size) and no measurable change in peak rise-time (Table 6.1).

Furthermore, experiments in which mast cells isolated from the same mice were activated via different stimuli also revealed a high degree of variability in the regulation of mast cell degranulation (mast cells stimulated with ASM-secreted chemokines CXCL10 and RANTES in Chapter 4 and neuropeptide-stimulated mast cells in Chapter 5). Relative to IgE-mediated degranulation, A23187-stimulated mast cells released more serotonin per cell, while CXCL10- and RANTES-stimulated mast cells released less; both trends adhered to a similar profile of regulated degranulation (increased serotonin per granule was associated with increased peak area and frequency, and decreased kinetic parameters). Finally, in yet another unique pattern of degranulation, substance P- and CGRP- stimulated mast cells released less serotonin per cell, relative to A23187 stimulated controls, through a process strictly involving a decrease in serotonin released per granule with no measureable change in either of the three remaining parameters (Table 6.1).

### 6.2 Future directions

The remarkable variation between different modes of regulated degranulation (Table 6.1), as revealed by CFMA analysis, is imperceptible at the bulk level and typifies the advantage of a single-cell approach to the study of cell-cell communication. Future work in this field will undoubtedly improve the faculty of CFMA for the study of cellular

signaling in inflammation and disease. Two avenues of future work are particularly promising.

First, the continued improvement of CFMA as an analytical method for the study of intercellular signaling will depend on the development of additional CFMA-compatible model systems and/or the optimization of existing cell models not currently used in the microelectrochemistry field. For example, the ability to use CFMA to monitor degranulation behavior in mast cells isolated from skin and other connective tissues is of immediate interest because of known associations between mast cells and several inflammatory diseases specific to these sites. Not only will the introduction of different cell types widen the scope of CFMA-accessible biological questions, it will also address questions surrounding the biological relevance of currently used model systems while simultaneously characterizing the tissue-specific heterogeneity between cell subtypes (e.g. skin mast cells vs. peritoneal mast cells).

The second promising area of future work is the development of novel co-culture systems that will facilitate the study of direct cell-cell contact effects in the regulation of mast cell degranulation. There are many examples of the importance of cell-cell contact in various immune system processes (including the mast cell-ASM interactions and mast cell-nervous system interactions explored in Chapters 4 and 5, respectively). However, the mechanisms of cell-cell contact-mediated regulation of mast cell function has not been

explored extensively at the single cell level and poses an interesting technical challenge for the further development of CFMA as an analytical tool.

### 6.3 Closing remarks

A convincing case has been made, hopefully, that CFMA is a unique and valuable tool for the study of mast cell signaling in inflammation and holds great potential for future applications in this field. However, this dissertation also represents an effort to build upon a large and hard-earned foundation of work formed by numerous previous research efforts. It is time well spent to pause and appreciate the greater context of this thesis. Countless past contributions have produced both the technical capabilities and the fundamental knowledge that laid the groundwork for the research presented herein. The time, energy, and resources spent to, for example, enable the use of microelectrochemistry in biological systems or facilitate the characterization of basic cellular functions, is worth acknowledging. To contribute in a small way to this collective effort has been both a humbling and rewarding experience.

## Bibliography


(1) Adams, R. Carbon paste electrodes. *Anal. Chem.* **1958**, *30*, 1576–1576.

(2) Bard, A. J.; Faulkner, L. R. *Electrochemical Methods: Fundamentals and Applications*; Swain, E., Ed. 2nd ed. John Wiley & Sons, Inc., 2001.

(3) Wightman, R. M.; Jankowski, J. A.; Kennedy, R. T.; Kawagoe, K. T.; Schroeder, T. J.; Leszczyszyn, D. J.; Near, J. A.; Diliberto, E. J.; Viveros, O. H. Temporally resolved catecholamine spikes correspond to single vesicle release from individual chromaffin cells. *Proc. Natl. Acad. Sci. U.S.A.* **1991**, *88*, 10754–10758.

(4) Leszczyszyn, D. J.; Jankowski, J. A.; Viveros, O. H.; Diliberto, E. J.; Near, J. A.; Wightman, R. M. Nicotinic receptor-mediated catecholamine secretion from individual chromaffin cells - chemical evidence for exocytosis. *J. Biol. Chem.***1990**, *265*, 14736–14737.

(5) Troyer, K. P. Temporal separation of vesicle release from vesicle fusion during exocytosis. *J. Biol. Chem.* **2002**, *277*, 29101–29107.

(6) Borges, R.; Diaz-Vera, J.; Dominguez, N.; Rosa Arnau, M.; Machado, J. D. Chromogranins as regulators of exocytosis. *J. Neurochem.* **2010**, *114*, 335–343.

(7) *Single-Channel Recording*; Sakmann, B.; Neher, E., Eds. 2nd ed. Springer, 2009.

(8) Robinson, D. L.; Venton, B. J.; Heien, M.; Wightman, R. M. Detecting subsecond dopamine release with fast-scan cyclic voltammetry in vivo. *Clin. Chem.* **2003**, *49*, 1763–1773.

(9) Omiatek, D. M.; Santillo, M. F.; Heien, M. L.; Ewing, A. G. Hybrid capillary-microfluidic device for the separation, lysis, and electrochemical detection of vesicles. *Anal. Chem.* **2009**, *81*, 2294–2302.

(10) Venton, B. J.; Wightman, R. M. Psychoanalytical electrochemistry: dopamine and behavior. *Anal. Chem.* **2003**, *75*, 414 A–421 A.

(11) Michael, D.; Travis, E. R.; Wightman, R. M. Color images for fast-scan CV. *Anal. Chem.* **1998**, *70*, 586A–592A.

(12) Jackson, B. P.; Dietz, S. M.; Wightman, R. M. Fast-scan cyclic voltammetry of 5-hydroxytryptamine. *Anal. Chem.* **1995**, *67*, 1115–1120.

(13) Heien, M. L.; Ewing, A. G. Quantitative chemical analysis of single cells. In *Micro and Nano Technologies in Bioanalysis*, Lee, J. W. and Foote, R. S., Eds. Methods in Molecular Biology vol. 544; Humana Press: New York, **2009**; pp 153-162.

(14) Pihel, K.; Schroeder, T. J.; Wightman, R. M. Rapid and selective cyclic voltammetric measurements of epinephrine and norepinephrine as a method to measure secretion from single bovine adrenal medullary cells. *Anal. Chem.* **1994**, *66*, 4532–4537.

(15) Heien, M. L. A. V.; Johnson, M. A.; Wightman, R. M. Resolving neurotransmitters detected by fast-san cyclic voltammetry. *Anal. Chem.* **2004**,

*76*, 5697–5704.

(16) Zhang, B.; Alysandratos, K.-D.; Angelidou, A.; Asadi, S.; Sismanopoulos, N.; Delivanis, D.-A.; Weng, Z.; Miniati, A.; Vasiadi, M.; Katsarou-Katsari, A.; Miao, B.; Leeman, S. E.; Kalogeromitros, D.; Theoharides, T. C. Human mast cell degranulation and preformed TNF secretion require mitochondrial translocation to exocytosis sites: relevance to atopic dermatitis. *J. Allergy Clin. Immunol.* **2011**, *127*, 1522–31.e8.

(17) Mosharov, E. V.; Sulzer, D. Analysis of exocytotic events recorded by amperometry. *Nat. Meth.* **2005**, *2*, 651–658.

(18) Chen, T. K.; Luo, G. O.; Ewing, A. G. Amperometric monitoring of stimulated catecholamine release from rat pheochromocytoma (PC12) cells at the zeptomole level. *Anal. Chem.* **1994**, *66*, 3031–3035.

(19) Jankowski, J. A.; Schroeder, T. J.; Ciolkowski, E. L.; Wightman, R. M. Temporal characteristics of quantal secretion of catecholamines from adrenal medullary cells. *J. Biol. Chem.* **1993**, *268*, 14694–14700.

(20) Schroeder, T. J.; Jankowski, J. A.; Kawagoe, K. T.; Wightman, R. M.; Lefrou, C.; Amatore, C. Analysis of diffusional broadening of vesicular packets of catecholamines released from biological cells during exocytosis. *Anal. Chem.* **1992**, *64*, 3077–3083.

(21) Travis, E. R.; Wang, Y. M.; Michael, D. J.; Caron, M. G.; Wightman, R. M. Differential quantal release of histamine and 5-hydroxytryptamine from mast cells of vesicular monoamine transporter 2 knockout mice. *Proc. Natl. Acad. Sci. U.S.A.* **2000**, *97*, 162–167.

(22) Amatore, C.; Arbault, S.; Bouret, Y.; Guille, M.; Lemaître, F.; Verchier, Y. Invariance of exocytotic events detected by amperometry as a function of the carbon fiber microelectrode diameter. *Anal. Chem.* **2009**, *81*, 3087–3093.

(23) Travis, E. R.; Wightman, R. M. Spatio-temporal resolution of exocytosis from individual cells. *Annu. Rev. Biophys. Biomol. Struct.* **1998**, *27*, 77–103.

(24) Sombers, L. A.; Hanchar, H. J.; Colliver, T. L.; Wittenberg, N.; Cans, A.; Arbault, S.; Amatore, C.; Ewing, A. G. The effects of vesicular volume on secretion through the fusion pore in exocytotic release from PC12 cells. *J. Neurosci.* **2004**, *24*, 303–309.

(25) Segura, F.; Brioso, M. A.; Gomez, J. F.; Machado, J. D.; Borges, R. Automatic analysis for amperometrical recordings of exocytosis. *J. Neurosci. Methods* **2000**, *103*, 151–156.

(26) Chow, R. H.; Vonruden, L.; Neher, E. Delay in vesicle fusion revealed by electrochemical monitoring of single secretory events in adrenal chromaffin cells. *Nature* **1992**, *356*, 60–63.

(27) Ge, S.; White, J. G.; Haynes, C. L. Critical role of membrane cholesterol in exocytosis revealed by single platelet study. *ACS Chem. Biol.* **2010**, *5*, 819–828.

(28) Borges, R.; Jaen, R.; Freire, F.; Gomez, J. F.; Villafruela, C.; Yanes, E.

Morphological and functional characterization of beige mouse adrenomedullary secretory vesicles. *Cell Tissue Res.* **2001**, *304*, 159–164.
(29) Zhou, Z.; Misler, S. Amperometric detection of stimulus-induced quantal release of catecholamines from cultured superior cervical-ganglion neurons. *Proc. Natl. Acad. Sci. U.S.A.* **1995**, *92*, 6938–6942.
(30) Pothos, E. N.; Davila, V.; Sulzer, D. Presynaptic recording of quanta from midbrain dopamine neurons and modulation of the quantal size. *J. Neurosci.* **1998**, *18*, 4106–4118.
(31) Rayport, S.; Sulzer, D.; SHI, W. X.; Sawasdikosol, S.; Monaco, J.; Batson, D.; Rajendran, G. Identified postnatal mesolimbic dopamine neurons in culture - morphology and electrophysiology. *J. Neurosci.* **1992**, *12*, 4264–4280.
(32) Hochstetler, S. E.; Puopolo, M.; Gustincich, S.; Raviola, E.; Wightman, R. M. Real-time amperometric measurements of zeptomole quantities of dopamine released from neurons. *Anal. Chem.* **2000**, *72*, 489–496.
(33) Bruns, D. Detection of transmitter release with carbon fiber electrodes. *Methods* **2004**, *33*, 312–321.
(34) Bruns, D.; Jahn, R. Real-time measurement of transmitter release from single synaptic vesicles. *Nature* **1995**, *377*, 62–65.
(35) Ge, S.; Wittenberg, N. J.; Haynes, C. L. Quantitative and real-time detection of secretion of chemical messengers from individual platelets. *Biochemistry* **2008**, *47*, 7020–7024.
(36) Ge, S.; Woo, E.; White, J. G.; Haynes, C. L. Electrochemical measurement of endogenous serotonin release from human blood platelets. *Anal. Chem.* **2011**, *83*, 2598–2604.
(37) Tatham, P. E. R.; Duchen, M. R.; Millar, J. Monitoring exocytosis from single mast-cells by fast voltammetry. *Pflugers Archiv.-Eur. J. Physiol.* **1991**, *419*, 409–414.
(38) de Toledo, G. A.; Fernández-Chacón, R.; Fernández, J. M. Release of secretory products during transient vesicle fusion. *Nature* **1993**, *363*, 554–558.
(39) Pihel, K.; Hsieh, S.; Jorgenson, J. W.; Wightman, R. M. Electrochemical detection of histamine and 5-hydroxytryptamine at isolated mast cells. *Anal. Chem.* **1995**, *67*, 4514–4521.
(40) Amatore, C.; Arbault, S.; Bonifas, I.; Bouret, Y.; Erard, M.; Ewing, A. G.; Sombers, L. A. Correlation between vesicle quantal size and fusion pore release in chromaffin cell exocytosis. *Biophys. J.* **2005**, *88*, 4411–4420.
(41) Omiatek, D. M.; Dong, Y.; Heien, M. L. A. V.; Ewing, A. G. Only a fraction of quantal content is released during exocytosis as revealed by electrochemical cytometry of secretory vesicles. *ACS Chem. Neurosci.* **2010**, *1*, 234–245.
(42) Jackson, M. B.; Chapman, E. R. The fusion pores of Ca2+-triggered exocytosis. *Nat. Struct. Mol. Biol.* **2008**, *15*, 684–689.
(43) Ngatchou, A. N.; Kisler, K.; Fang, Q.; Walter, A. M.; Zhao, Y.; Bruns, D.; Sorensen, J. B.; Lindau, M. Role of the synaptobrevin C terminus in fusion

pore formation. *Proc. Natl. Acad. Sci. U.S.A.* **2010**, *107*, 18463–18468.
(44) Fang, Q.; Berberian, K.; Gong, L.-W.; Hafez, I.; Sorensen, J. B.; Lindau, M. The role of the C terminus of the SNARE protein SNAP-25 in fusion pore opening and a model for fusion pore mechanics. *Proc. Natl. Acad. Sci. U.S.A.* **2008**, *105*, 15388–15392.
(45) Amatore, C.; Arbault, S.; Bouret, Y.; Guille, M.; Lemaître, F.; Verchier, Y. Regulation of exocytosis in chromaffin cells by trans-insertion of lysophosphatidylcholine and arachidonic acid into the outer leaflet of the cell membrane. *Chem. Bio. Chem.* **2006**, *7*, 1998–2003.
(46) Uchiyama, Y.; Maxson, M. M.; Sawada, T.; Nakano, A.; Ewing, A. G. Phospholipid mediated plasticity in exocytosis observed in PC12 cells. *Brain Res.* **2007**, *1151*, 46–54.
(47) Zhang, J.; Xue, R.; Ong, W.-Y.; Chen, P. Roles of Cholesterol in vesicle fusion and motion. *Biophys. J.* **2009**, *97*, 1371–1380.
(48) Bischoff, S. C. Role of mast cells in allergic and non-allergic immune responses: comparison of human and murine data. *Nat. Rev. Immunol.* **2007**, *7*, 93–104.
(49) Kalesnikoff, J.; Galli, S. J. New developments in mast cell biology. *Nat. Immunol.* **2008**, *9*, 1215–1223.
(50) Kindt, T. J.; Osborne, B. A.; Goldsby, R. A. *Kuby Immunology*; 6 ed. W. H. Freeman & Co., **2007**.
(51) Leung, D. Y.; Bieber, T. Atopic dermatitis. *Lancet* **2003**, *361*, 151–160.
(52) Spergel, J.; Mizoguchi, E.; Oettgen, H. Roles of TH1 and TH2 cytokines in a murine model of allergic dermatitis. *J. Clin. Invest.* **1999**, *103*, 1103-1111.
(53) Horsmanheimo, L.; Harvima, I. T.; Järvikallio, A.; Harvima, R. J.; Naukkarinen, A.; Horsmanheimo, M. Mast cells are one major source of interleukin-4 in atopic dermatitis. *Br. J. Dermatol.* **1994**, *131*, 348–353.
(54) Marshall, J. S. Mast-cell responses to pathogens. *Nat. Rev. Immunol.* **2004**, *4*, 787–799.
(55) Beaven, M. A. Our perception of the mast cell from Paul Ehrlich to now. *Eur. J. Immunol.* **2009**, *39*, 11–25.
(56) Galli, S. J.; Kalesnikoff, J.; Grimbaldeston, M. A.; Piliponsky, A. M.; Williams, C. M. M.; Tsai, M. Mast cells as "tunable" effector and immunoregulatory cells: recent advances. *Annu. Rev. Immunol.* **2005**, *23*, 749–786.
(57) Amatore, C.; Bouret, Y.; Travis, E. R.; Wightman, R. Interplay between membrane dynamics, diffusion and swelling pressure governs individual vesicular exocytotic events during release of adrenaline by chromaffin cells. *Biochimie* **2000**, *82*, 481–496.
(58) Theoharides, T. C.; Alysandratos, K.-D.; Angelidou, A.; Delivanis, D.-A.; Sismanopoulos, N.; Zhang, B.; Asadi, S.; Vasiadi, M.; Weng, Z.; Miniati, A.; Kalogeromitros, D. Mast cells and inflammation. *Biochim. Biophys. Acta* **2012**,

*1822*, 21–33.
(59) Galli, S. J.; Tsai, M. Mast cells: versatile regulators of inflammation, tissue remodeling, host defense and homeostasis. *J. Dermatol. Sci.* **2008**, *49*, 7–19.
(60) Moon, T. C.; St Laurent, C. D.; Morris, K. E.; Marcet, C.; Yoshimura, T.; Sekar, Y.; Befus, A. D. Advances in mast cell biology: new understanding of heterogeneity and function. *Mucosal. Immunol.* **2010**, *3*, 111–128.
(61) Logan, M. R.; Odemuyiwa, S. O.; Moqbel, R. Understanding exocytosis in immune and inflammatory cells: the molecular basis of mediator secretion. *J. Allergy Clin. Immunol.* **2003**, *111*, 923–932.
(62) Guo, Z.; Turner, C.; Castle, D. Relocation of the t-SNARE SNAP-23 from lamellipodia-like cell surface projections regulates compound exocytosis in mast cells. *Cell* **1998**, *94*, 537–548.
(63) Melicoff, E.; Sansores-Garcia, L.; Gomez, A.; Moreira, D. C.; Datta, P.; Thakur, P.; Petrova, Y.; Siddiqi, T.; Murthy, J. N.; Dickey, B. F.; Heidelberger, R.; Adachi, R. Synaptotagmin-2 controls regulated exocytosis but not other secretory responses of mast cells. *J. Biol. Chem.* **2009**, *284*, 19445–19451.
(64) Bennett, J. P.; Cockcroft, S.; Gomperts, B. D. Ionomycin stimulates mast cell histamine secretion by forming a lipid-soluble calcium complex. *Nature* **1979**, *282*, 851–853.
(65) Nash, G.; Niedt, G.; MacDermott, R. P. Ionophore-A23187-induced cellular cytotoxicity: a cell fragment mediated process. *Immunology* **1980**, *40*, 265-272.
(66) Varadaradjalou, S.; Féger, F.; Thieblemont, N.; Hamouda, N. B.; Pleau, J.-M.; Dy, M.; Arock, M. Toll-like receptor 2 (TLR2) and TLR4 differentially activate human mast cells. *Eur. J. Immunol.* **2003**, *33*, 899–906.
(67) Dawicki, W.; Marshall, J. S. New and emerging roles for mast cells in host defence. *Cur. Opin. Immunol.* **2007**, *19*, 31–38.
(68) Venkatesha, R.; Thangam, E.; Zaidi, A.; Ali, H. Distinct regulation of C3a-induced MCP-1/CCL2 and RANTES/CCL5 production in human mast cells by extracellular signal regulated kinase and PI3 kinase. *Mol. Immunol.* **2005**, *42*, 581–587.
(69) Tkaczyk, C.; Okayama, Y.; Metcalfe, D. D.; Gilfillan, A. M. Fcγ Receptors on mast cells: activatory and inhibitory regulation of mediator release. *Int. Arch. Allergy Immunol.* **2004**, *133*, 305–315.
(70) Daeron, M.; Malbec, O.; Latour, S.; Arock, M.; Fridman, W. H. Regulation of high-affinity IgE receptor-mediated mast cell activation by murine low-affinity IgG receptors. *J. Clin. Invest.* **1995**, *95*, 577–585.
(71) Arndt, J.; Smith, N.; Tausk, F. Stress and atopic dermatitis. *Curr. Allergy Asthma Rep.* **2008**, *8*, 312–317.
(72) Pavlovic, S.; Daniltchenko, M.; Tobin, D. J.; Hagen, E.; Hunt, S. P.; Klapp, B. F.; Arck, P. C.; Peters, E. M. J. Further exploring the brain–skin connection: stress worsens eermatitis via substance P-dependent neurogenic inflammation in mice. *J. Investig. Dermatol.* **2007**, *128*, 434–446.

(73) Peters, E. M. J.; Kuhlmei, A.; Tobin, D. J.; Müller-Röver, S.; Klapp, B. F.; Arck, P. C. Stress exposure modulates peptidergic innervation and degranulates mast cells in murine skin. *Brain Behav. Immun.* **2005**, *19*, 252–262.
(74) Pauling, L.; Itano, H. A.; Singer, S. J.; Wells, I. C. Sickle cell anemia, a molecular disease. *Science* **1949**, *110*, 543–548.
(75) Ingram, V. M. Gene mutations in human haemoglobin: the chemical difference between normal and sickle cell haemoglobin. *Nature* **1957**, *180*, 326–328.
(76) Frenette, P. S.; Atweh, G. F. Sickle cell disease: old discoveries, new concepts, and future promise. *J. Clin. Invest.* **2007**, *117*, 850–858.
(77) Kaul, D. Sickle cell disease. In *Comprehensive Physiology* **2008**; pp 769-793.
(78) Kaul, D. Insights into vascular pathobiology of sickle cell disease. *Hématologie* **2009**, *15*, 446–457.
(79) Conran, N.; Franco-Penteado, C. F.; Costa, F. F. Newer aspects of the pathophysiology of sickle cell disease vaso-occlusion. *Hemoglobin* **2009**, *33*, 1–16.
(80) Rees, D. C.; Williams, T. N.; Gladwin, M. T. Sickle-cell disease. *Lancet* **2010**, *376*, 2018–2031.
(81) Kita, J. M.; Wightman, R. M. Microelectrodes for studying neurobiology. *Curr. Opin. Chem. Biol.* **2008**, *12*, 491–496.
(82) Marquis, B. J.; McFarland, A. D.; Braun, K. L.; Haynes, C. L. Dynamic measurement of altered chemical messenger secretion after cellular uptake of nanoparticles using carbon-fiber microelectrode amperometry. *Anal. Chem.* **2008**, *80*, 3431–3437.
(83) Kalesnikoff, J.; Galli, S. J. Antiinflammatory and immunosuppressive functions of mast cells. *Methods Mol. Biol.* **2011**, *677*, 207–220.
(84) Darbari, D. S.; Minniti, C. P.; Rana, S.; van den Anker, J. Pharmacogenetics of morphine: Potential implications in sickle cell disease. *Am. J. Hematol.* **2008**, *83*, 233–236.
(85) Kohli, D. R.; Li, Y.; Khasabov, S. G.; Gupta, P.; Kehl, L. J.; Ericson, M. E.; Nguyen, J.; Gupta, V.; Hebbel, R. P.; Simone, D. A.; Gupta, K. Pain-related behaviors and neurochemical alterations in mice expressing sickle hemoglobin: modulation by cannabinoids. *Blood* **2010**, *116*, 456–465.
(86) Darbari, D. S.; Neely, M.; van den Anker, J.; Rana, S. Increased clearance of morphine in sickle cell disease: implications for pain management. *J. Pain* **2011**, *12*, 531–538.
(87) Blunk, J.; Schmelz, M.; Zeck, S.; Skov, P.; Likar, R. Opioid-induced mast cell activation and vascular responses is not mediated by μ-opioid receptors: An in vivo microdialysis study in human skin. *Anesth. Analg.* **2004**, *98*, 364–370.
(88) Klinker, J. F.; Seifert, R. Morphine and muscle relaxants are receptor-independent G-protein activators and cromolyn is an inhibitor of stimulated G-protein activity. *Inflamm. Res.* **1997**, *46*, 46–50.
(89) Barke, K. E.; Hough, L. B. Opiates, mast cells and histamine release. *Life Sci.*

**1993**, *53*, 1391–1399.
(90) Okayama, Y.; Kawakami, T. Development, migration, and survival of mast cells. *Immunol. Res.* **2006**, *34*, 97–115.
(91) Zdravkovic, V.; Pantovic, S.; Rosic, G.; Tomic-Lucic, A.; Zdravkovic, N.; Colic, M.; Obradovic, Z.; Rosic, M. Histamine blood concentration in ischemic heart disease patients. *J. Biomed. Biotechnol.* **2011**, *2011*, 1–8.
(92) Wojtecka-Lukasik, E.; Ksiezopolska-Orlowska, K.; Gaszewska, E.; Krasowicz-Towalska, O.; Rzodkiewicz, P.; Maslinska, D.; Szukiewicz, D.; Maslinski, S. Cryotherapy decreases histamine levels in the blood of patients with rheumatoid arthritis. *Inflamm. Res.* **2010**, *59 Suppl. 2*, S253–5.
(93) Schwartz, L. B.; Irani, A. M.; Roller, K.; Castells, M. C.; Schechter, N. M. Quantitation of histamine, tryptase, and chymase in dispersed human T and TC mast cells. *J. Immunol.* **1987**, *138*, 2611–2615.
(94) Shore, P. A.; Burkhalter, A.; Cohn, V. H. A method for the fluorometric assay of histamine in tissues. *J. Pharmacol. Exp. Ther.* **1959**, *127*, 182–186.
(95) Kaul, D. K.; Fabry, M. E.; Windisch, P.; Baez, S.; Nagel, R. L. Erythrocytes in sickle cell anemia are heterogeneous in their rheological and hemodynamic characteristics. *J. Clin. Invest.* **1983**, *72*, 22–31.
(96) Hagar, W.; Vichinsky, E. Advances in clinical research in sickle cell disease. *Brit. J. Haematol.* **2008**, *141*, 346–356.
(97) Conran, N.; Costa, F. F. Hemoglobin disorders and endothelial cell interactions. *Clin. Biochem.* **2009**, *42*, 1824–1838.
(98) Ballas, S. K. Current issues in sickle cell pain and its management. *Hematology Am. Soc. Hematol. Educ. Program* **2007**, 97–105.
(99) Hebbel, R. P.; Osarogiagbon, R.; Kaul, D. The endothelial biology of sickle cell disease: inflammation and a chronic vasculopathy. *Microcirculation* **2004**, *11*, 129–151.
(100) Paszty, C.; Brion, C. M.; Elizabeth, M.; Witkowska, H. E.; Stevens, M. E.; Mohandas, N.; Rubin, E. M. Transgenic knockout mice with exclusively human sickle hemoglobin and sickle cell disease. *Science* **1997**, *278*, 876–878.
(101) Colliver, T. L.; Hess, E. J.; Pothos, E. N.; Sulzer, D.; Ewing, A. G. Quantitative and statistical analysis of the shape of amperometric spikes recorded from two populations of cells. *J. Neurochem.* **2000**, *74*, 1086–1097.
(102) Amin, K. The role of mast cells in allergic inflammation. *Respir. Med.* **2012**, *106*, 9–14.
(103) Theoharides, T. C.; Enakuaa, S.; Sismanopoulos, N.; Asadi, S.; Papadimas, E. C.; Angelidou, A.; Alysandratos, K.-D. Contribution of stress to asthma worsening through mast cell activation. *Ann. Allergy Asthma Immunol.* **2012**, *109*, 14–19.
(104) Manning, B. M.; Hebbel, R. P.; Gupta, K.; Haynes, C. L. Carbon-fiber microelectrode amperometry reveals sickle-cell-induced inflammation and chronic morphine effects on single mast cells. *ACS Chem. Biol.* **2012**, *7*, 543–

551.
(105) Metz, M.; Grimbaldeston, M. A.; Nakae, S.; Piliponsky, A. M.; Tsai, M.; Galli, S. J. Mast cells in the promotion and limitation of chronic inflammation. *Immunol. Rev.* **2007**, *217*, 304–328.
(106) Machelska, H. Dual peripheral actions of immune cells in neuropathic pain. *Arch. Immunol. Ther. Exp. (Warsz.)* **2011**, *59*, 11–24.
(107) Ren, K.; Dubner, R. Interactions between the immune and nervous systems in pain. *Nat. Med.* **2010**, *16*, 1267–1276.
(108) Martin, J.; Prystowsky, M. B.; Angeletti, R. H. Preproenkephalin mRNA in T-cells, macrophages, and mast cells. *J. Neurosci. Res.* **1987**, *18*, 82–87.
(109) Busch-Dienstfertig, M.; Stein, C. Opioid receptors and opioid peptide-producing leukocytes in inflammatory pain - Basic and therapeutic aspects. *Brain Behav. Immun.* **2010**, *24*, 683–694.
(110) Goldstein, A.; Naidu, A. Multiple Opioid Receptors - Ligand selectivity profiles and binding-site signatures. *Mol. Pharmacol.* **1989**, *36*, 265–272.
(111) Corbett, A. D.; Henderson, G.; McKnight, A. T.; Paterson, S. J. 75 years of opioid research: the exciting but vain quest for the Holy Grail. *Brit. J. Pharmacol.* **2006**, *147*, S153–S162.
(112) Devi, L. A. Heterodimerization of G-protein-coupled receptors: pharmacology, signaling and trafficking. *Trends Pharmacol. Sci.* **2001**, *22*, 532–537.
(113) Berg, K. A.; Rowan, M. P.; Gupta, A.; Sanchez, T. A.; Silva, M.; Gomes, I.; McGuire, B. A.; Portoghese, P. S.; Hargreaves, K. M.; Devi, L. A.; Clarke, W. P. Allosteric Interactions between delta and kappa Opioid Receptors in Peripheral Sensory Neurons. *Mol. Pharmacol.* **2012**, *81*, 264–272.
(114) Filizola, M.; Devi, L. A. Structural biology: How opioid drugs bind to receptors. *Nature* **2012**, *485*, 314–317.
(115) Bidlack, J. M.; Khimich, M.; Parkhill, A. L.; Sumagin, S.; Sun, B.; Tipton, C. M. Opioid Receptors and Signaling on Cells from the Immune System. *J. Neuroimmune Pharm.* **2006**, *1*, 260–269.
(116) Stein, C.; Machelska, H. Modulation of Peripheral Sensory Neurons by the Immune System: Implications for Pain Therapy. *Pharmacol. Rev.* **2011**, *63*, 860–881.
(117) Sharp, B. M. Multiple opioid receptors on immune cells modulate intracellular signaling. *Brain Behav. Immun.* **2006**, *20*, 9–14.
(118) Williams, J. P.; Lambert, D. G. Editorial II: Opioids and the neuroimmune axis. *Br. J. Anaesth.* **2005**, *94*, 3–6.
(119) Pol, O.; Puig, M. M. Expression of opioid receptors during peripheral inflammation. *Curr. Top. Med. Chem.* **2004**, *4*, 51–61.
(120) McCarthy, L.; Wetzel, M.; Sliker, J. K.; Eisenstein, T. K.; Rogers, T. J. Opioids, opioid receptors, and the immune response. *Drug Alcohol Depen.* **2001**, *62*, 111–123.
(121) Verburg-van Kemenade, B. M. L.; Van der Aa, L. M.; Chadzinska, M.

Neuroendocrine-immune interaction: regulation of inflammation via G-protein coupled receptors. *Gen. Comp. Endocrinol.* **2013**, *188*, 94-101.
(122) Kim, D.; Koseoglu, S.; Manning, B. M.; Meyer, A. F.; Haynes, C. L. Electroanalytical eavesdropping on single cell communication. *Anal. Chem.* **2011**, *83*, 7242–7249.
(123) Wightman, R. M.; Schroeder, T. J.; Finnegan, J. M.; Ciolkowski, E. L.; Pihel, K. Time course of release of catecholamines from individual vesicles during exocytosis at adrenal medullary cells. *Biophys. J.* **1995**, *68*, 383–390.
(124) Asthma, E. P. O. T. M. O. *Expert Panel Report 3: Guidelines for the diagnosis and management of asthma*; US Patent Office, 2007; pp. 1–440.
(125) Bradding, P. Asthma: eosinophil disease, mast cell disease, or both? *Allergy Asthma Clin. Immunol.* **2008**, *4*, 84–8490.
(126) Poon, A. H.; Eidelman, D. H.; Martin, J. G.; Laprise, C.; Hamid, Q. Pathogenesis of severe asthma. *Clin. Exper. Allergy* **2012**, *42*, 625–637.
(127) Holgate, S. T.; Davies, D. E. Rethinking the pathogenesis of asthma. *Immunity* **2009**, *31*, 362–367.
(128) Bradding, P.; Walls, A. F.; Holgate, S. T. The role of the mast cell in the pathophysiology of asthma. *J. Allergy Clin. Immunol.* **2006**, *117*, 1277–1284.
(129) Brightling, C. E.; Bradding, P.; Symon, F. A.; Holgate, S. T.; Wardlaw, A. J.; Pavord, I. D. Mast-cell infiltration of airway smooth muscle in asthma. *N. Engl. J. Med.* **2002**, *346*, 1699–1705.
(130) Carter, R. J. F.; Bradding, P. The role of mast cells in the structural alterations of the airways as a potential mechanism in the pathogenesis of severe asthma. *Curr. Pharm. Des.* **2011**, *17*, 685–698.
(131) Finkelman, F. D.; Boyce, J. A.; Vercelli, D.; Rothenberg, M. E. Key advances in mechanisms of asthma, allergy, and immunology in 2009. *J. Allergy Clin. Immunol.* **2010**, *125*, 312–318.
(132) Kaur, D.; Saunders, R.; Berger, P.; Siddiqui, S.; Woodman, L.; Wardlaw, A.; Bradding, P.; Brightling, C. E. Airway smooth muscle and mast cell-derived CC chemokine ligand 19 mediate airway smooth muscle migration in asthma. *Am. J. Respir. Crit. Care Med.* **2006**, *174*, 1179–1188.
(133) Hershenson, M. B.; Brown, M.; Camoretti-Mercado, B.; Solway, J. Airway smooth muscle in asthma. *Annu. Rev. Pathol. Mech. Dis.* **2008**, *3*, 523–555.
(134) Marthan, R.; Berger, P.; Girodet, P.; Tunon-de-Lara, J. Airway smooth muscle interaction with mast cells. In *Airway smooth muscle in asthma and COPD*; Chung, K. F., Ed.; John Wiley & Sons: Chicester, U.K., **2008**, pp 127–139.
(135) Yeganeh, B.; Xia, C.; Movassagh, H.; Koziol-White, C.; Chang, Y.; Al-Alwan, L.; Bourke, J. E.; Oliver, B. G. G. Emerging mediators of airway smooth muscle dysfunction in asthma. *Pulm. Pharmacol. Ther.* **2013**, *26,* 105-111.
(136) Willox, I.; Mirkina, I.; Westwick, J.; Ward, S. G. Evidence for PI3K-dependent CXCR3 agonist-induced degranulation of human cord blood-derived mast cells. *Mol. Immunol.* **2010**, *47*, 2367–2377.

(137) Zhao, Z. Z.; Sugerman, P. B.; Zhou, X. J.; Walsh, L. J.; Savage, N. W. Mast cell degranulation and the role of T cell RANTES in oral lichen planus. *Oral Dis.* **2001**, *7*, 246–251.
(138) Murphy, D. M.; O'Byrne, P. M. Recent advances in the pathophysiology of asthma. *Chest* **2010**, *137*, 1417–1426.
(139) Alkhouri, H.; Hollins, F.; Moir, L. M.; Brightling, C. E.; Armour, C. L.; Hughes, J. M. Human lung mast cells modulate the functions of airway smooth muscle cells in asthma. *Allergy* **2011**, *66*, 1231–1241.
(140) Bradding, P. Mast cell regulation of airway smooth muscle function in asthma. *Eur. Respir. J.* **2007**, *29*, 827–830.
(141) Mundroff, M. L.; Wightman, R. M. Amperometry and cyclic voltammetry with carbon fiber microelectrodes at single cells. In *Current. Protocols in Neuroscience*; John Wiley & Sons: Chicester, U.K. **2002**, Supplement 18, Unit 6.14.
(142) Adams, K. L.; Puchades, M.; Ewing, A. G. In vitro electrochemistry of biological systems. *Annu. Rev. Anal. Chem.* **2008**, *1*, 329–355.
(143) Mosharov, E. V. Analysis of single-vesicle exocytotic events recorded by amperometry. *Methods Mol. Biol.* **2008**, *440*, 315–327.
(144) Veres, T. Z.; Rochlitzer, S.; Braun, A. The role of neuro-immune cross-talk in the regulation of inflammation and remodelling in asthma. *Pharmacol. Ther.* **2009**, *122,* 203-214.
(145) Elsenbruch, S. Abdominal pain in Irritable Bowel Syndrome: a review of putative psychological, neural and neuro-immune mechanisms. *Brain Behav. Immun.* **2011**, *25*, 386–394.
(146) Rosa, A. C.; Fantozzi, R. Histamine in the neurogenic inflammation. *Brit. J. Pharmacol.* **2013**, DOI 10.1111/bph.12266.
(147) O'Connor, T. M.; O'Connell, J.; O'Brien, D. I.; Goode, T.; Bredin, C. P.; Shanahan, F. The role of substance P in inflammatory disease. *J. Cell. Physiol.* **2004**, *201*, 167–180.
(148) Kawana, S.; Liang, Z.; Nagano, M.; Suzuki, H. Role of substance P in stress-derived degranulation of dermal mast cells in mice. *J. Dermatol. Sci.* **2006**, *42*, 47–54.
(149) Black, P. H. Stress and the inflammatory response: A review of neurogenic inflammation. *Brain Behav. Immun.* **2002**, *16*, 622–653.
(150) Maggi, C. A. Tachykinins and calcitonin gene-related peptide (CGRP) as co-transmitters released from peripheral endings of sensory nerves. *Prog. Neurobiol.* **1995**, *45*, 1-98.
(151) Lorenz, D.; Wiesner, B.; Zipper, J.; Winkler, A.; Krause, E.; Beyermann, M.; Lindau, M.; Bienert, M. Mechanism of peptide-induced mast cell degranulation: translocation and patch-clamp studies. *J. Gen. Physiol.* **1998**, *112*, 577–591.
(152) Levy, D. Endogenous mechanisms underlying the activation and sensitization

of meningeal nociceptors: the role of immuno-vascular interactions and cortical spreading depression. *Curr. Pain Headache Rep.* **2012**, *16*, 270–277.
(153) Holzer, P. Neurogenic vasodilatation and plasma leakage in the skin. *Gen. Pharmacol.* **1998**, *30*, 5–11.
(154) Birklein, F.; Schmelz, M. Neuropeptides, neurogenic inflammation and complex regional pain syndrome (CRPS). *Neurosci. Lett.* **2008**, *437*, 199–202.
(155) Roosterman, D.; Goerge, T.; Schneider, S. W.; Bunnett, N. W.; Steinhoff, M. Neuronal control of skin function: the skin as a neuroimmunoendocrine organ. *Physiol. Rev.* **2006**, *86*, 1309–1379.
(156) Watkins, H. A.; Rathbone, D. L.; Barwell, J.; Hay, D. L.; Poyner, D. R. Structure-activity relationships for alpha calcitonin gene-related peptide. *Brit. J. Pharmacol.* **2012**, DOI: 10.1111/bph.12072.
(157) De Jonge, F.; De Laet, A.; Van Nassauw, L.; Brown, J. K.; Miller, H. R. P.; van Bogaert, P. P.; Timmermans, J. P.; Kroese, A. B. A. In vitro activation of murine DRG neurons by CGRP-mediated mucosal mast cell degranulation. *Am. J. Physiol. - Gastrointest. Liver Physiol.* **2004**, *287*, 178–191.
(158) Kulka, M.; Sheen, C. H.; Tancowny, B. P.; Grammer, L. C.; Schleimer, R. P. Neuropeptides activate human mast cell degranulation and chemokine production. *Immunology* **2008**, *123*, 398–410.
(159) Theoharides, T. C.; Donelan, J. M.; Papadopoulou, N.; Cao, J.; Kempuraj, D.; Conti, P. Mast cells as targets of corticotropin-releasing factor and related peptides. *Trends Pharmacol. Sci.* **2004**, *25*, 563–568.